To the Graduate Council:

I am submitting herewith a thesis written by Todd Richard Downey entitled "Gold-Island Thin Film Surface Plasmon Excitation on an Optical Fiber". I have examined the final copy of this thesis for form and content and recommend that it be accepted in partial fulfillment of the requirements for the degree of Master of Science, with a major in Physics.

Dr. Thomas L. Ferrell, Major Professor

We have read this thesis
and recommend its acceptance:

Accepted for the Council:

Associate Vice Chancellor and
Dean of The Graduate School

Gold-Island Thin Film Surface Plasmon Excitation on an Optical Fiber

A Thesis

Presented for the

Master of Science Degree

The University of Tennessee, Knoxville

Todd R. Downey

May 1998

Acknowledgments

I would like to thank Dr. Tom Callcott, Dr. Tom Ferrell, and Dr. John J. Quinn for their advice and support. I would also like to thank the staff, students, and PostDocs at Oak Ridge National Laboratory that assisted me in this work. I would especially like to thank Stephen Bonte, Gregory Crosnier, Dr. Fabrice Meriaudeau, Ali Passian, Andrew Wig, Dr. Milan Buncick and Dr. Patrick Oden. A special thanks goes to my Father, Robert, who attracted me to science at an early age.

Abstract

The absorbance of light passing through an optical fiber that is coated with a thin film of gold islands on a section stripped of cladding is investigated. Optical absorption by the excitation of surface plasmons on the gold islands has been measured. The position of the resonance peak of the absorbance curve was shown to be shifted to a higher wavelength by surrounding the gold with a refractive index liquid. Comparisons with theoretical predictions for the amount of the resonance peak shift versus the applied index are presented.

Table of Contents

List of Tables

List of Figures

Chapter I

Introduction

The evaporation of less than 120 (angstroms) of a metal onto an optically flat substrate has been shown[1] to produce electrically discontinuous islands. Heating of the metal-island films forces the small islands to anneal into larger islands that have a characteristic shape of oblate spheroids. Measurements[2] of the absorbance of light passing through samples of gold-island films evaporated onto optically flat substrates have shown changes in the absorbance with the angle of incidence of the light, annealing temperature and time, and polarization rotation of the incident light. A similar study[3] presented the measurements for silver-island films.

A theoretical model[4,5,6] that was successfully used in studies of electron bombardment causing the radiative decay of surface plasmons[7] on the islands was used to accurately describe these absorbance changes in the above experimental studies. This model is based on the results of a theoretical procedure[8] that characterizes surface plasmons in various geometrical situations.

This model assumes the metal-islands formed are small compared to the wavelength of the incident light. Therefore, since the electric field does not vary considerably over the whole size of an individual island, this justifies the use of non-retarded electrodynamics.

In this model, the absorbance is caused by the excitation of surface plasmons on the islands, which are modeled as oblate spheroidal particles. A dipole approximation is used and only the first few terms of the dielectric response function obtained are used with experimentally obtained values to produce a dispersion relation for actual islands. Laplace's equation is solved in oblate spheroidal coordinates for the potential function and the electric field is found from the potential. The components of the polarization vector are obtained and, using the volume of the spheroid, the dipole moments are found and used to find the polarizability components as a function of the dielectric response function. Finally, the total, scattering and absorbance cross sections are

evaluated, and the optical absorbance is found in terms of the number of particles per unit area and the total cross section.

The investigation presented here uses gold as the metal and an optical fiber as the substrate. We removed a portion of the cladding on the fiber and deposited the required amount of gold to form the islands. Techniques similar to ours have been used to coat an optical fiber with a silver metal-island thin film[9], and measure the absorption and peak shifts. Our sample preparation technique, described in Chapter II, allows for the creation of an evanescent field during total internal reflection of the light traveling in the core of the optical fiber. The escaping evanescent field will interact with the electrons in the gold islands and 'create' surface plasmons.

A simple diagram of the fiber with the island coating on the decladded region is shown in **Figure I.1.** In this figure, the size of the islands and the diameter of the core are exaggerated. E_{inc} is the incident light launched into the entrance face of the fiber, E_{leak} is the portion of the light propagating through the fiber that escapes because the core is exposed, and E_{tr} is the light that propagates out of the exit face of the fiber.

Figure I.2. shows the assumed orientation of the islands on the substrate. In this case, the light that is used to excite the surface plasmons is traveling through the cylindrical waveguide created by the core and cladding layers in the fiber, and exits the waveguide in the region of the fiber that has been decladded.

Snells law is valid at all interfaces of two different medium, specifically at the exit and entrance faces of the fiber and at the exposed core/surrounding medium area. It is easy to see that when the cladding has an index less then the core, for a range of angles greater than the critical angle θ_c, where

$$\sin \theta_c = n_s/n_{cr},$$

total internal reflection of the propagating light will occur. For a typical optical fiber, θ_2 is less than 25 degrees. When the cladding is removed and the index of the surrounding medium, n_s, is greater than the index of the fiber core, n_{cr}, E_{leak} will increase with increasing θ_2.

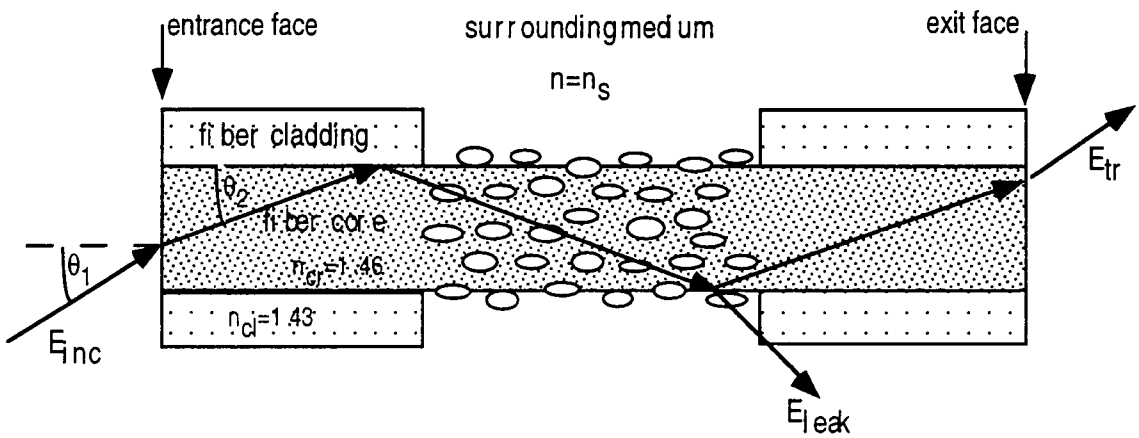

Figure I.1. Island coated fiber diagram.

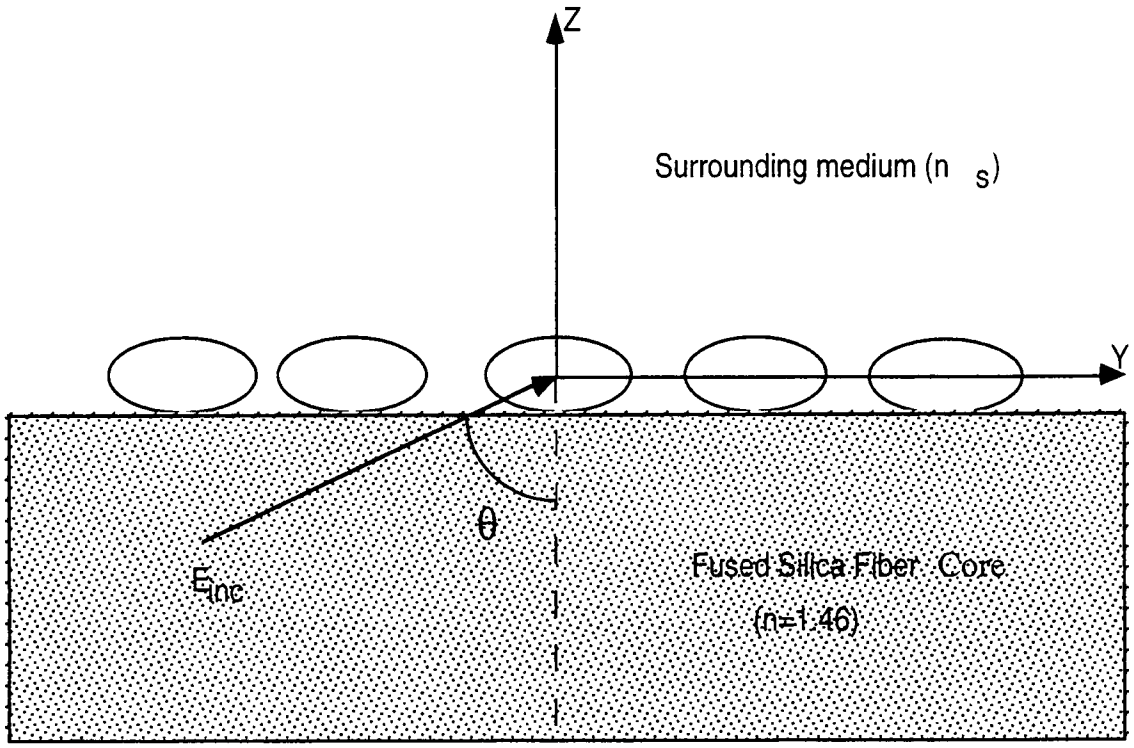

Figure I.2. **Orientation of the islands on the surface of the fiber.**

When the cladding is not completely removed, and for angles of incidence greater than the critical angle, total internal reflection (TIR) of the traveling light will occur. This greatly reduces the light available to interact with the exterior gold-islands, as compared with a sample that has all of the cladding removed. However, it is possible for the evanescent field created by the TIR light to interact with the islands and excite surface plasmons, just as in the case of a continuous film over a prism[10,11,12]. This is also the case when n_S is less than n_{cr}. The evanescent field contains an amplitude term that decays exponentially with z in **Figure I.2.**, and has a wavenumber k in the x,y plane of **Figure I.2.**

The absorbance of the light by the creation of the surface plasmons is defined as:

$$ABS=Log_{10}(I/I_0),$$

where I is the intensity of the light measured with a gold-island film, and I_0 is the intensity without the gold. For each set of data for gold coated samples the above absorbance number was found at each increment of wavelength.

A previous experiment[13] showed that the position and strength of the absorption maximum can be changed by increasing the amount of a solid dielectric material that is evaporated on the substrate, which is then covered with annealed silver islands. In this case the medium used was xylene. The substrate was silicon and it was the effects of this substrate that were of primary concern.

Furthermore, the use of the excitation of surface plasmons on thin film coatings, both continuous[14,15,16,17] and metal-islands[18,19], has proven useful, particularly in biosensing, for detecting changes in the index of refraction of the medium surrounding the thin film. The immersion of a metal-island sample into liquid solvent has shown[20,21] that the absorption resonance is shifted to higher wavelengths when the index of refraction of the liquid is increased.

Earlier experiments[22,23,24] have shown the usefulness of a continuous thin metal film on an optical fiber in biosensing.

In our experiments, the exposed core area of samples coated with the gold-islands that showed an absorption peak were then coated with an overlaying optical liquid[25]. These optical liquids have a known index of refraction (n), and the variation of n with respect to temperature and wavelength are small. The absorption peak was seen to shift to a higher wavelength. This shift of the resonance can be easily explained by examining the correct electromagnetic boundary conditions.

Chapter II will present the theoretical calculations for the absorbance and the expected absorbance peak shifts.

Chapter III discusses the details of the experimental procedure including sample preparation and the experimental setup, along with microscope pictures of the sample islands.

Chapter IV presents the experimental data results and analysis, with graphs of ABS versus wavelength and a tabulation of the results for the samples.

Concluding remarks are given in chapter V, with an important graph of ABS peak shift versus the index of the applied optical liquid, and a discussion of future work on this topic. **Appendix A.** introduces prototype designs for a useful implementation of our fiber optic sensor.

Chapter II

Theory

A. Introduction

We used the results summarized elsewhere[26] for the dependence of the absorbance on incident angle and the ratio R of the minor to major axis of the spheroid as a basis for our work. The usual boundary condition are that the normal component of the electric displacement vector inside and outside of a spheroid is continous, and that the tangential component of the electric field is continous. Laplace's equation is satisfied inside and outside the gold spheroid,

$$\nabla^2 \Phi_{in} = 0 \quad \text{and} \quad \nabla^2 \Phi_{out} = 0 .$$

The boundary conditions at the surface of the gold-outside material interface are also satisfied

$$\Phi_{in}|\text{surface} = \Phi_{out}|\text{surface}$$

and

$$\varepsilon(\omega)\, \vec{n} \cdot \vec{\nabla} \Phi_{in}|_{surface} = \varepsilon_{out}\, \vec{n} \cdot \vec{\nabla} \Phi_{out}|_{surface},$$

where $\vec{n}$ is the unit vector that is normal to the surface of the spheroid, $\varepsilon(\omega)$ is the frequency dependent dielectric function of gold, and ε_{out} is the dielectric function of the medium. We need to solve for the case $\varepsilon_{out} \neq 1$.

To solve Laplace's equation, the potential function is assumed to be the product of three functions, each of which is dependent on only one of the three coordinates in the spheroidal coordinate system (η, θ, ϕ)

$$\Phi = F(\eta)G(\theta)H(\phi).$$

Laplace's equation is solved by the separation of variables. The solutions to the equation for $F(\eta)$ are Legendre polynomials with

imaginary arguments. The solutions to the equation for $G(\theta)$ are Legendre polynomials with real arguments. The solutions to the equation for $H(\phi)$ are cosine and sine functions of real arguments. When the condition that the potential must be finite is imposed on the solutions obtained, the simplified product of $G(\theta)H(\phi)$ forms the real spherical harmonics. The final boundary condition that the potential is continuous at $\eta = \eta_0$ is then applied and the general solutions are

$$\Phi_{in} = \sum_{l,m,p} A_{l,m,p} Q_{l,m}(i\eta_0) P_{l,m}(i\eta) Y^p_{l,m}(\theta,\phi),$$

$$\Phi_{out} = \sum_{l,m,p} A_{l,m,p} P_{l,m}(i\eta_0) Q_{l,m}(i\eta) Y^p_{l,m}(\theta,\phi),$$

where l=0,1,2,..., m=0,1,2,...l and p is either +1 or -1.

Solving Laplace's equation with the boundary conditions leads to the resonant condition for $\varepsilon(\omega)$

$$\frac{\varepsilon_{lm}}{\varepsilon_{out}} = \frac{P_{l,m}(i\eta_0)\left[dQ_{l,m}(i\eta)/d\eta\right]|\eta=\eta_0}{Q_{l,m}(i\eta_0)\left[dP_{l,m}(i\eta)/d\eta\right]|\eta=\eta_0},$$

where η_0 is related to the ratio of the minor axis of the spheroid to the major axis by

$$\eta_0 = \frac{R}{\sqrt{(1-R^2)}},$$

and where $P_{l,m}$ and $Q_{l,m}$ are the associated Legendre polynomials.

Since we are assuming the dipole approximation, only the l=1, m=0 and l=1, m=1 terms are considered. These l=1 terms for $\varepsilon(\omega)$ are

$$\varepsilon_{1,0} = \varepsilon_{out}\left\{1 + \frac{1}{(1+\eta_0^2)(\eta_0 \cot^{-1}\eta_0 - 1)}\right\},$$

and

$$\varepsilon_{1,1} = \varepsilon_{out}\left\{1 - \frac{2}{\left(1+\eta_0^2\right)\left(\eta_0 \cot^{-1}\eta_0 - \eta_0^2\right)}\right\}.$$

Utilizing these relations, we now continue by stating the final results that have been given elsewhere[27].

The Fourier transform of the x, y and z components of the dipole moment that are induced on the island are found to be

$$p_x = \frac{2\,a^3\sqrt{\left(1+\eta_0^2\right)}\left(\varepsilon(\omega)-1\right)}{3\,Q_{1,1}(i\,\eta_0)\left(\varepsilon(\omega)-\varepsilon_{1,1}(i\,\eta_0)\right)}E_x(\omega),$$

$$p_y = \frac{2\,a^3\sqrt{\left(1+\eta_0^2\right)}\left(\varepsilon(\omega)-1\right)}{3\,Q_{1,1}(i\,\eta_0)\left(\varepsilon(\omega)-\varepsilon_{1,1}(i\,\eta_0)\right)}E_y(\omega),$$

$$p_z = \frac{-a^3\eta_0\left(\varepsilon(\omega)-1\right)}{3\,Q_{1,0}(i\,\eta_0)\left(\varepsilon(\omega)-\varepsilon_{1,0}(i\,\eta_0)\right)}E_z(\omega),$$

where a is the focal length of the spheroid.

The general expression for the electric field that will be at large distances from the islands is

$$\vec{E} = \frac{\omega^2 e^{ikr}}{c^2 r}\left(\vec{n}\times\vec{p}\right)\times\vec{n},$$

with $\vec{n}$ being the vector of unit length that points in the direction of the observation point and r is the length from an island to this point.

Finally, we must distinguish from the separate effects of the incident light that has its electric field either perpendicular, *s* polarized, or parallel, *p* polarized, to the plane that the islands are positioned upon. This gives the total cross sections

$$\sigma_{tot,s} = \frac{4\pi\omega}{c}\mathrm{Im}\left(\frac{2\,a^3\sqrt{\left(1+\eta_0^2\right)}\left(\varepsilon(\omega)-1\right)}{3\,Q_{1,1}(i\,\eta_0)\left(\varepsilon(\omega)-\varepsilon_{1,1}(i\,\eta_0)\right)}\right),$$

and

$$\sigma_{tot,p} = \frac{4\pi\omega}{c}\mathrm{Im}\left(\begin{array}{l}\dfrac{2\,a^3\sqrt{\left(1+\eta_0^2\right)}\left(\varepsilon(\omega)-1\right)\cos^2(\theta)}{3\,Q_{1,1}(i\,\eta_0)\left(\varepsilon(\omega)-\varepsilon_{1,1}(i\,\eta_0)\right)}+ \\ \qquad\qquad \dfrac{-a^3\eta_0\left(\varepsilon(\omega)-1\right)\sin^2(\theta)}{3\,Q_{1,0}(i\,\eta_0)\left(\varepsilon(\omega)-\varepsilon_{1,0}(i\,\eta_0)\right)}\end{array}\right).$$

From these expressions, the absorbance is

$$ABS = \log_{10}\left(\frac{1}{1-N\sigma}\right),$$

where N is approximately the density of islands in a unit of surface area.

The data points for the real and imaginary parts of the dielectric function, ε_1 and ε_2, of gold were calculated by a basic program[28] that used a spline fit of experimental data published elsewhere.[29] These values were used to determine the index n and wavenumber k for each point using a Kramers-Kronig calculation. If the effect of the substrate is to be included, an approximation is to modify the dispersion relation in quadratic form in the same manner as in the case of a continuous thin film.

B. Theoretical Peak Shift Curves

MathCad worksheets were written to utilize the above mentioned calculation procedure to obtain graphs for the shift of the absorbance curve for the surrounding medium having indices of refraction of 1.300 and 1.700 for three different angles of propagation, (90^o - θ_2) in **Figure I.1.**. Graphs were produced to show these results. **Figure II.1.** through **Figure II.6.** show these graphs.

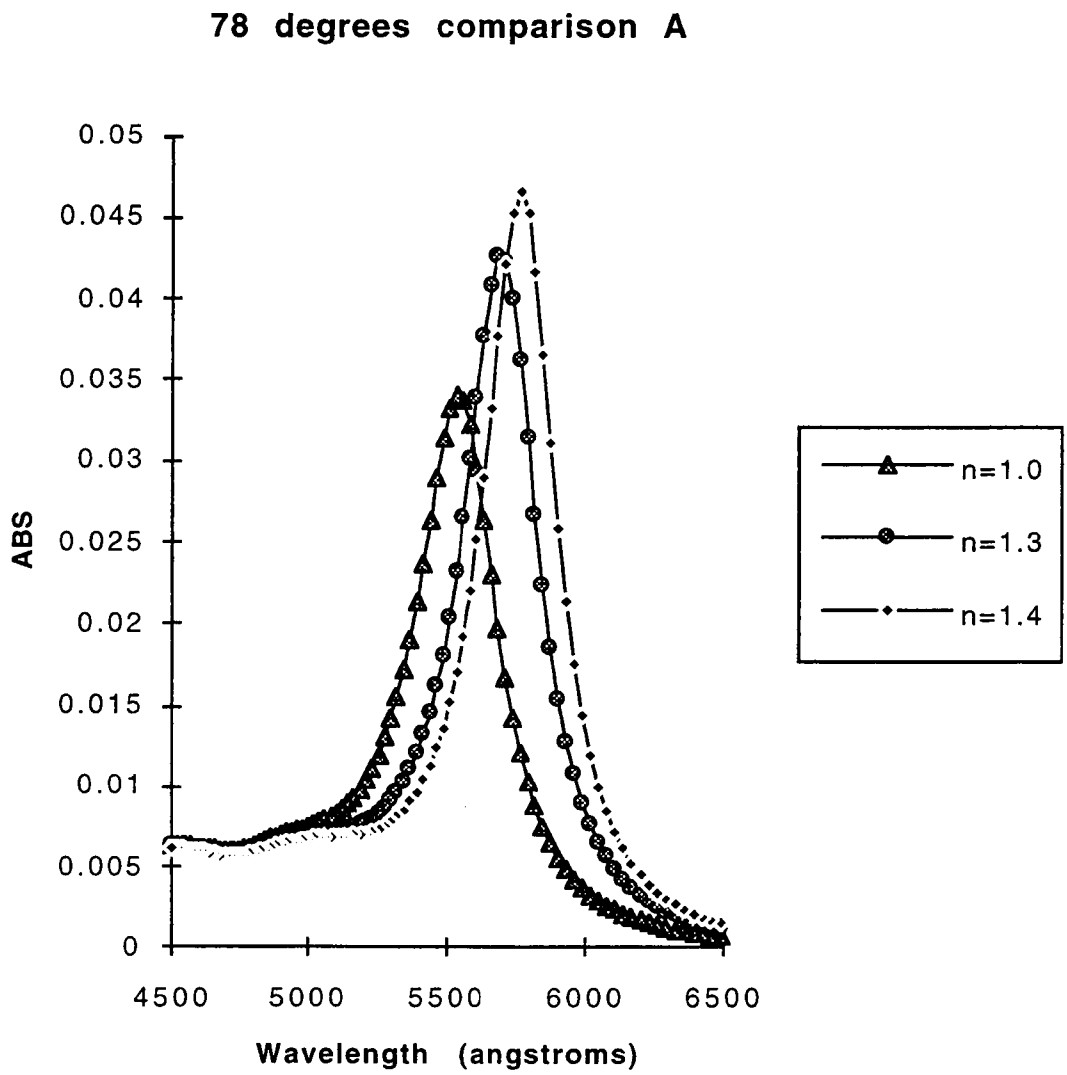

Figure II.1. Theoretical absorbance for 78 degrees A. Gold spheroids with R=0.45, N=0.1, for an angle of incidence of 78 degrees.

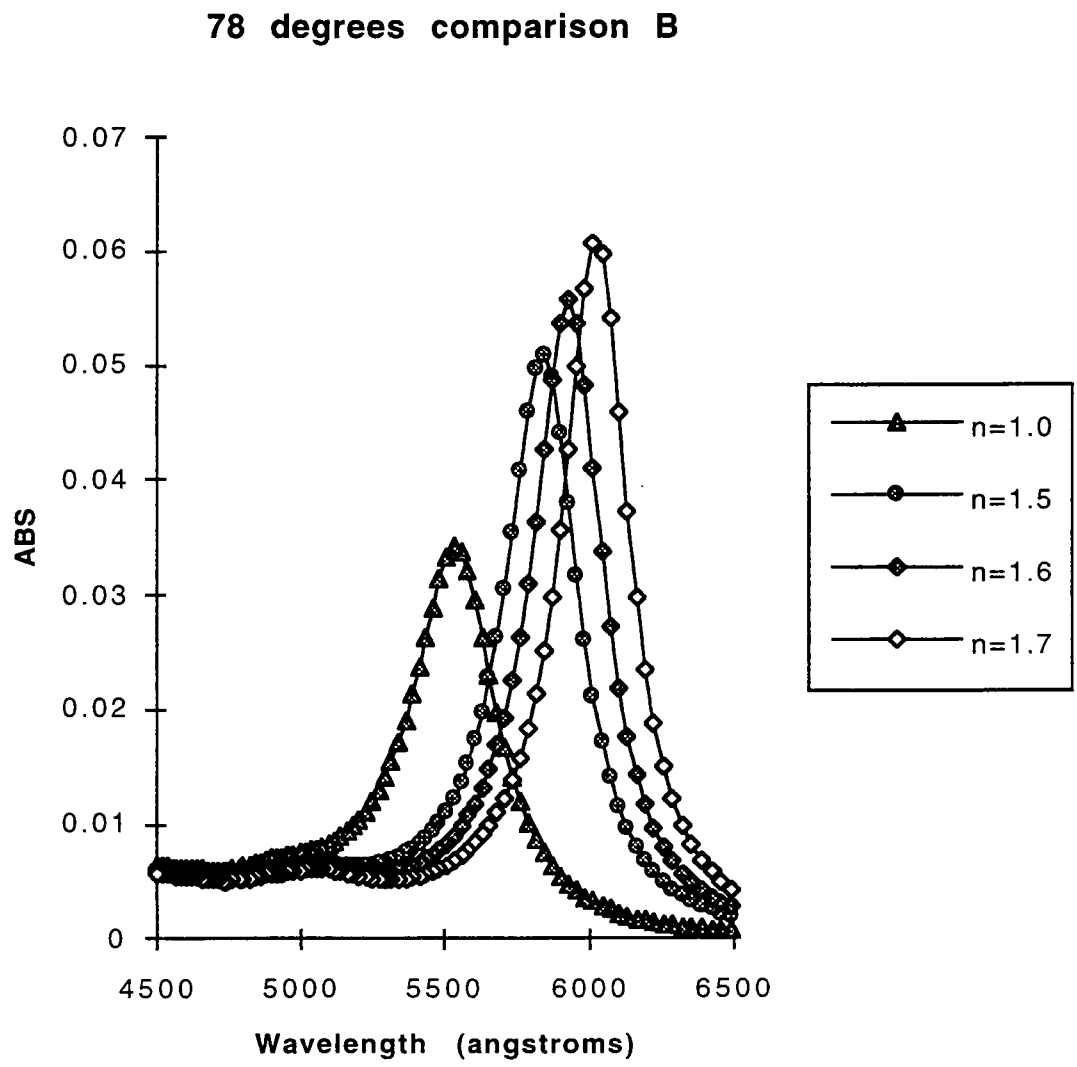

Figure II.2. Theoretical absorbance for 78 degrees B. Gold spheroids with R=0.45, N=0.1, for an angle of incidence of 78 degrees.

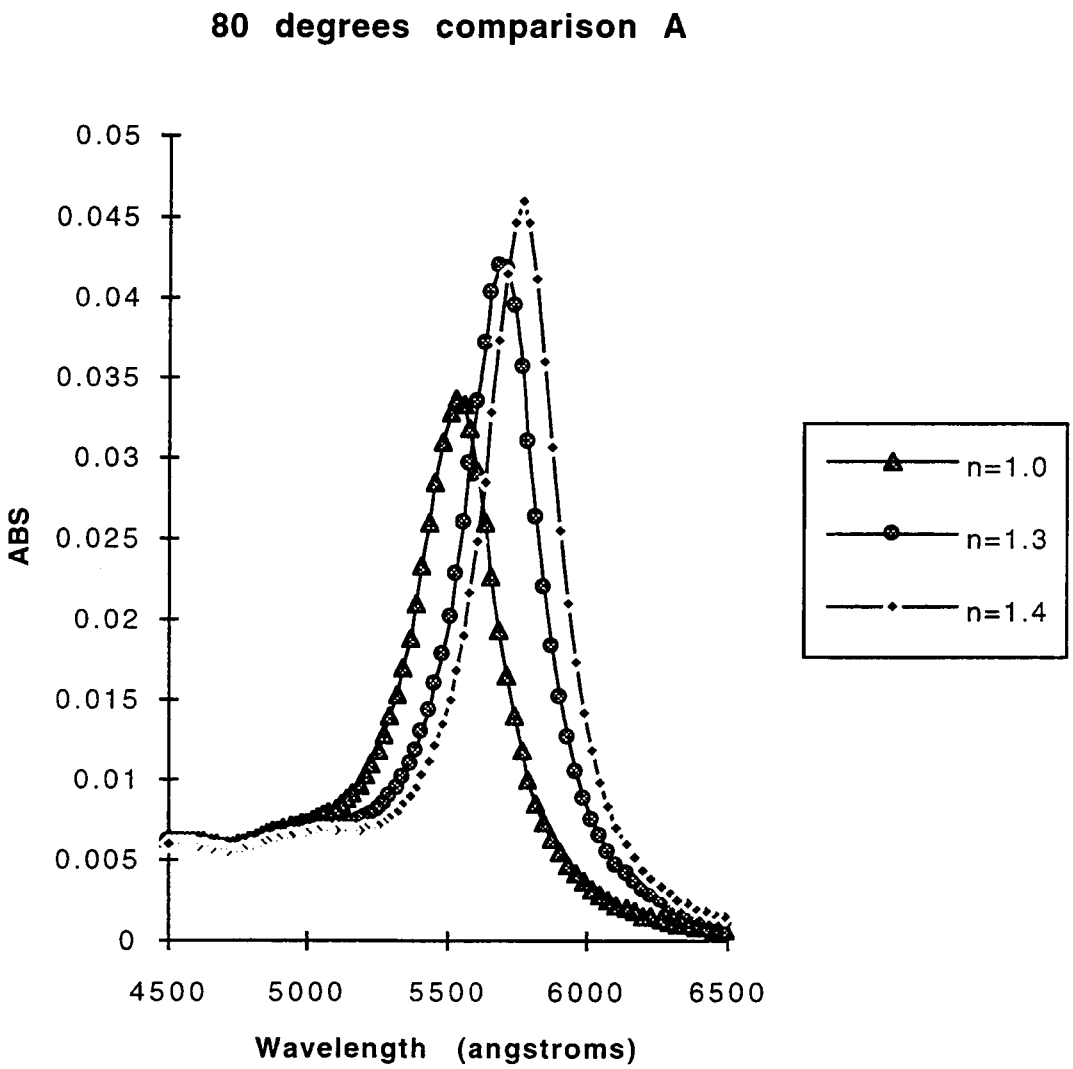

Figure II.3. Theoretical absorbance for 80 degrees A. Gold spheroids with R= 0.45, N=0.1, for an angle of incidence of 80 degrees.

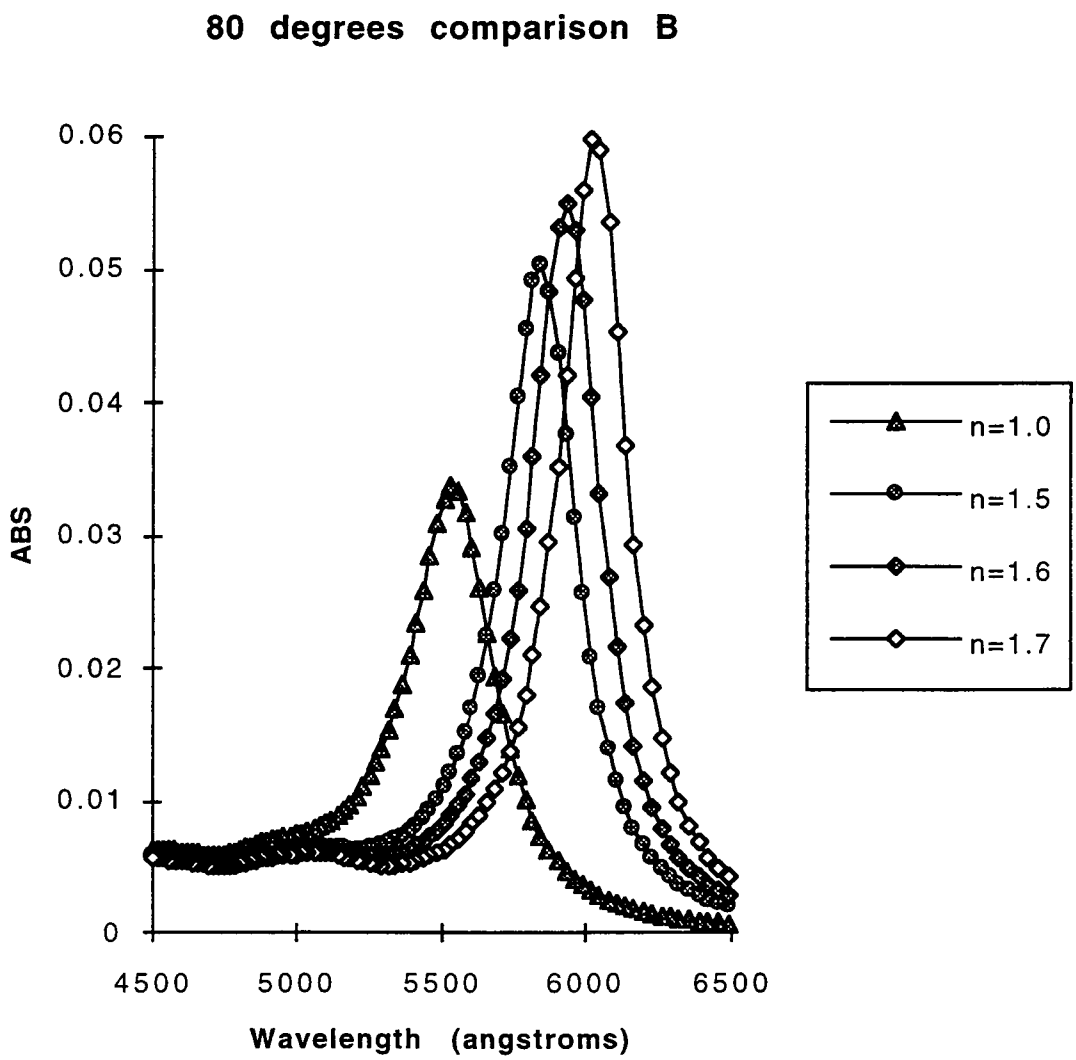

Figure II.4. Theoretical absorbance for 80 degrees B. Gold spheroids with R= 0.45, N=0.1, for an angle of incidence of 80 degrees.

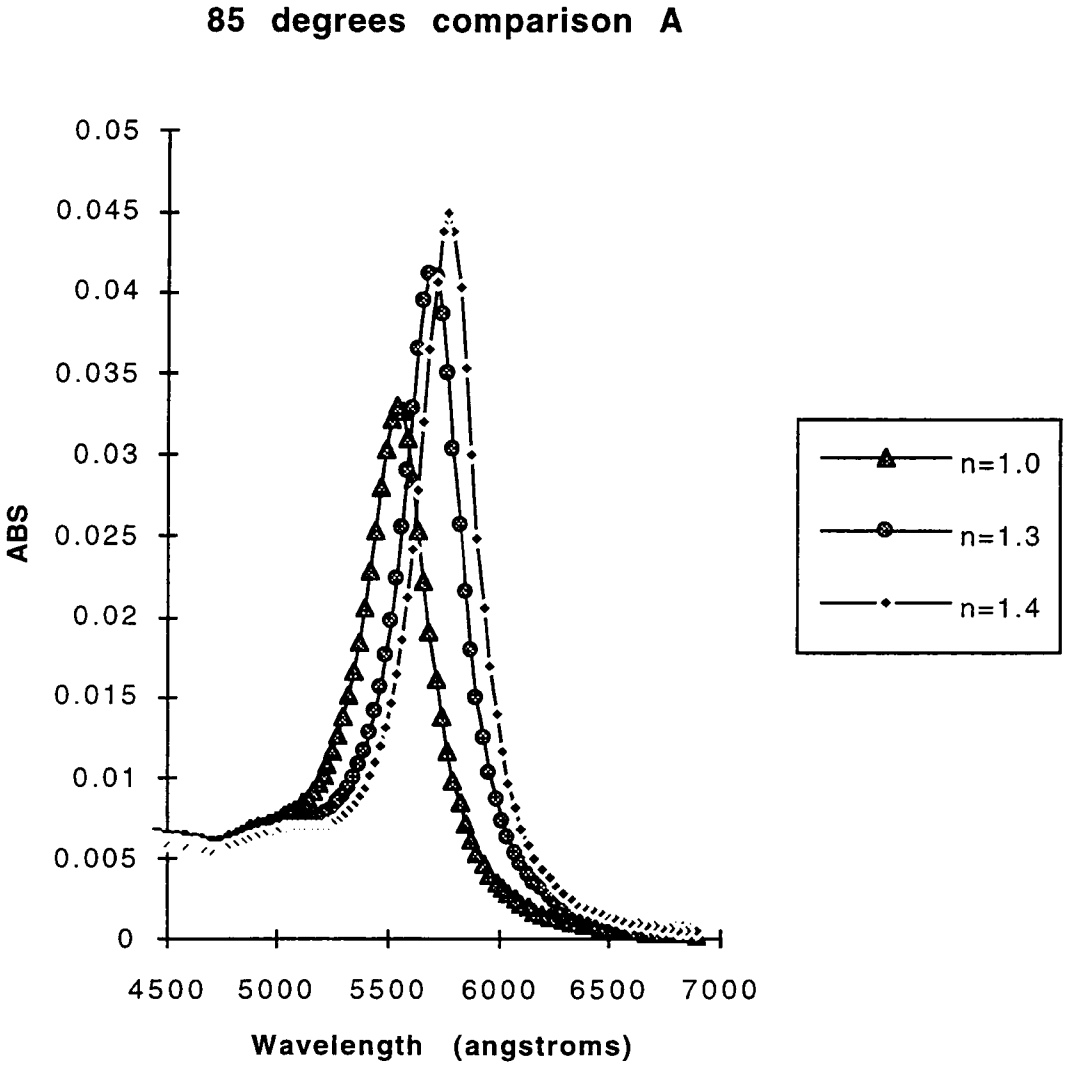

Figure II.5. Theoretical absorbance for 85 degrees A. Gold spheroids with R=0.45, N=0.1, for an angle of incidence of 85 degrees.

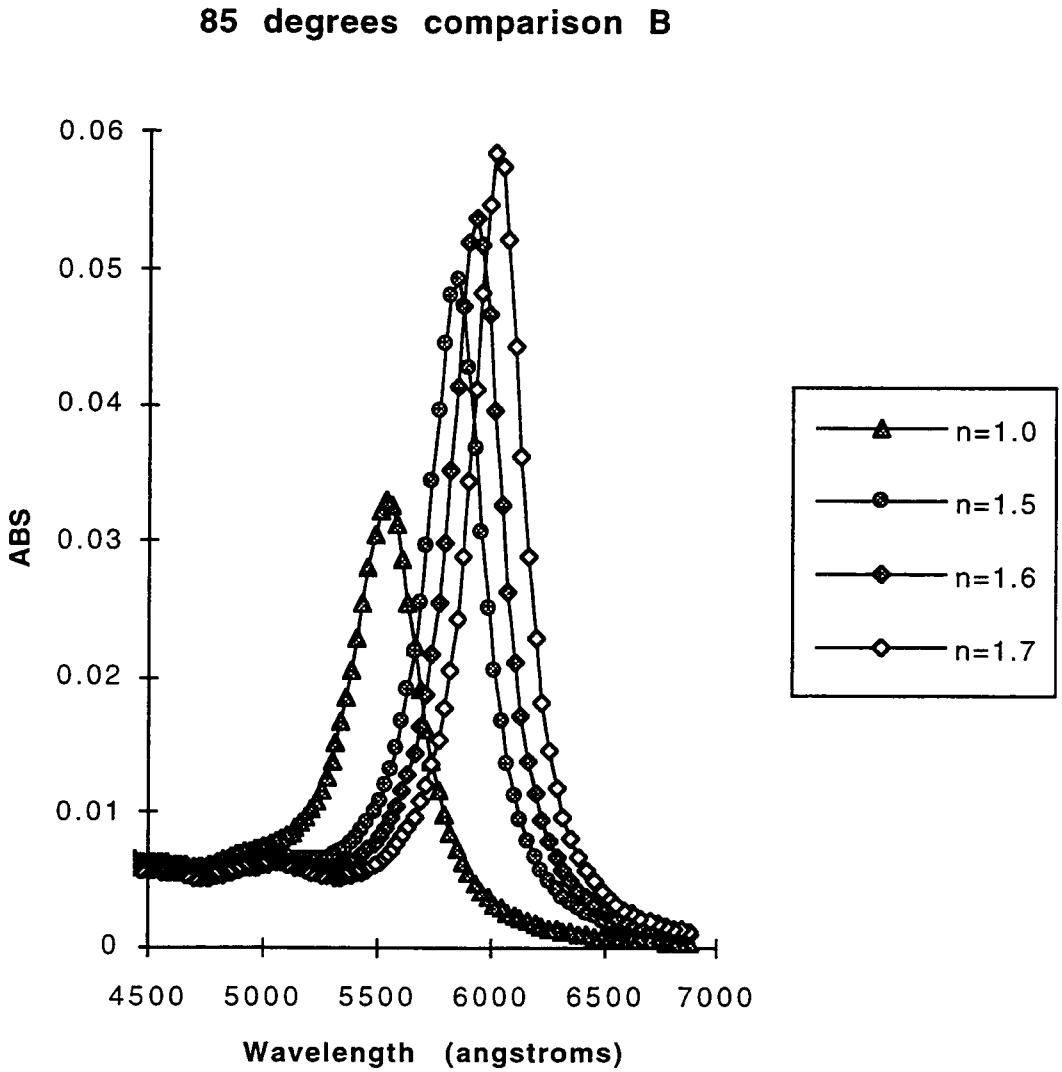

Figure II.6. Theoretical absorbance for 85 degrees B. Gold spheroids with R=0.45, N=0.1, for an angle of incidence of 85 degrees.

Figure II.1. through **Figure II.6.** are all for the same single value of R=0.45. However, the components of $\varepsilon_{1,1}$ and $\varepsilon_{0,1}$ are dependant on the shape of the spheroid. A change in R leads to a change in the position of the resonances. This is clearly seen in **Figure II.7.**, where we used R=0.29 in our calculations and the shift amounts for n=1.3 and n=1.7 increased. This lower R value corresponds to a spheroid that has a greater difference between the minor and major axis, and it is this increased difference that increased the shift amount.

From **Figure II.1.** through **Figure II.7.**, we see that the maximum ABS will decrease with increasing angle of incidence. More importantly, we found the theoretical shift of peak ABS for the index changing from n=1.0 to n=1.3, 1.4, 1.5, 1.6 and 1.7 from these calculations.

When the complete range from 0^{o} to 90^{o} is investigated in this manner, we see a slight decrease in shift amount with increasing angle of incidence because the peak height position will be at a lower wavelength. However, since the critical angle for the optical fiber that we used in our experiments is 78^{o}, angles less than this are of no interest. **Figure II.8.** shows that the position of the ABS peak does not change with the values of incident angle that we are interested in.

We can summarize these calculations, and refer to the particular core and cladding indices that we utilize in our experimental samples, with **Table II.1.** It shows the theoretical shift amount for each of the R values, for an angle of incidence of 78^{o}, from n=1.0 to one of the 5 different indices.

The above calculations show that the position of the absorbance peak shifts to a higher wavelength when the surrounding index is increased. An important limitation on this analysis is the relatively inaccurate experimental optical data for gold. These inaccuracies, and the procedure in the spline fit program, led to a wavelength increment that was not constant and just less than 30Å.

It is also very important to remember that we have used a single value for the ratio R in each of our calculations presented above. A more realistic approach should include a Gaussian distribution of ratios[30, 31], and would lead to a broadening of the ABS curve. In this case the

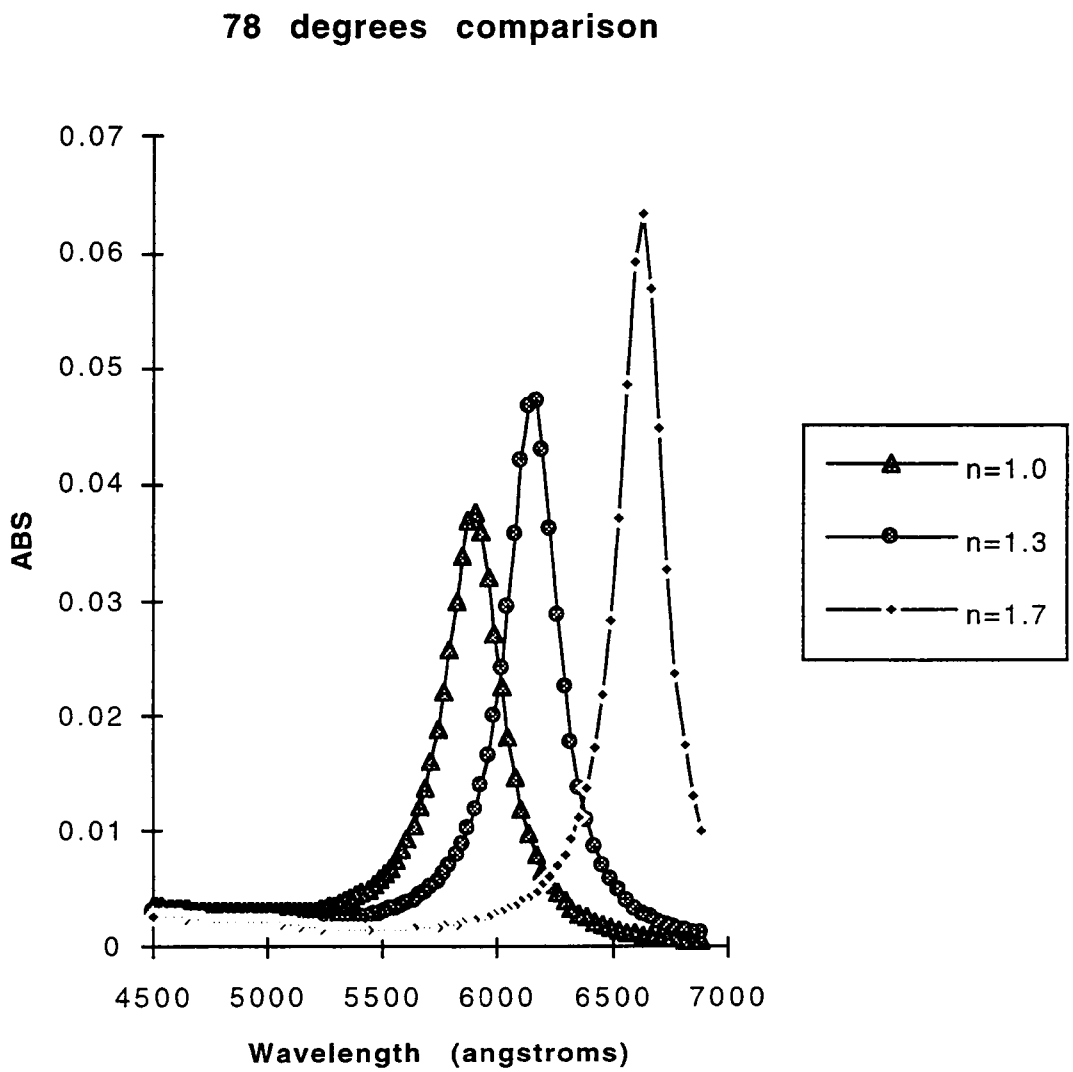

Figure II.7. Theoretical absorbance for 78 degrees C. Gold spheroids with R=0.29, N=0.1, for an angle of incidence of 78 degrees.

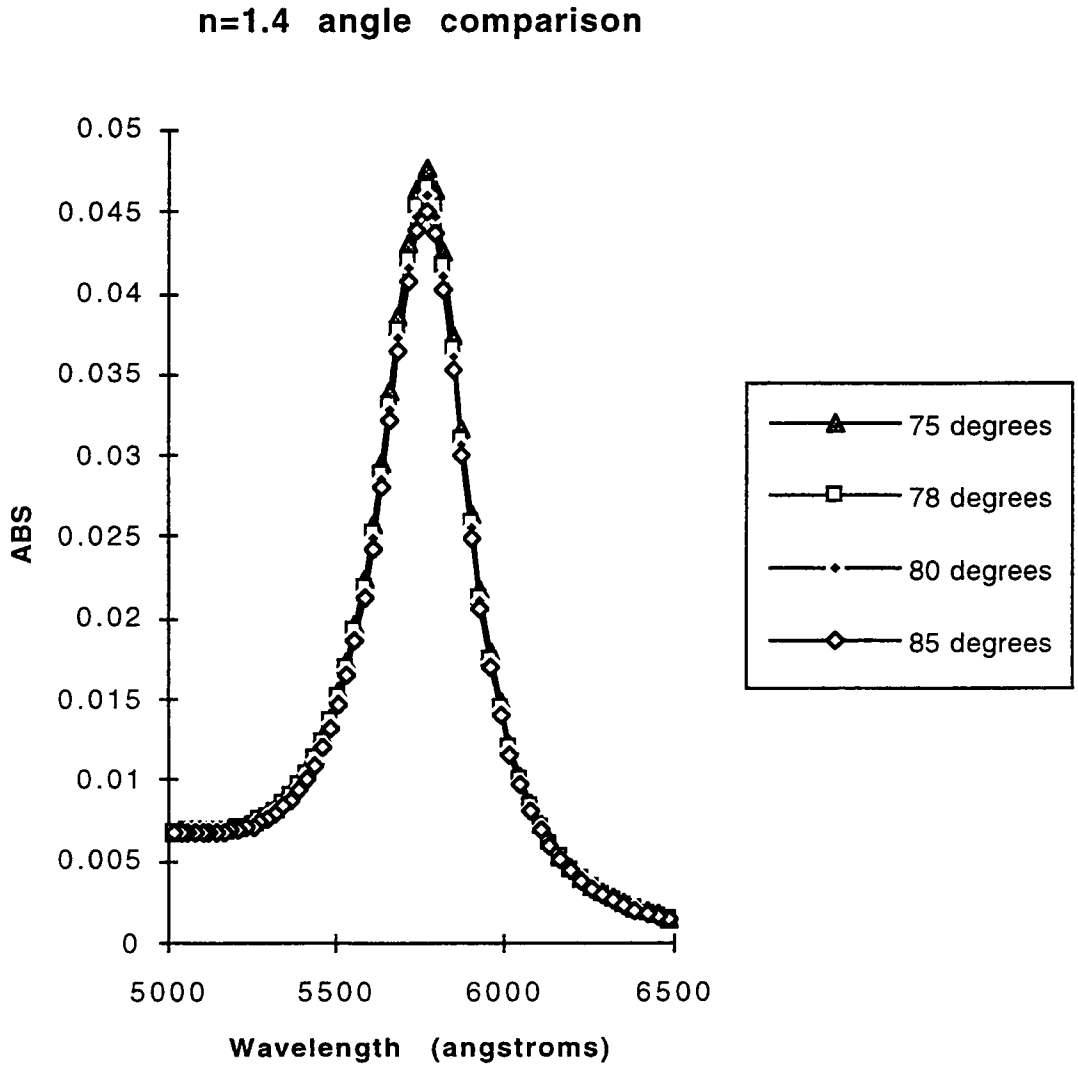

Figure II.8. Theoretical absorbance for n=1.400. Gold spheroids with R=0.45 an N=0.1.

Table II.1. Theoretical peak shift with respect to index. Shift 1 is for R=0.45, shift 2 is for R=0.29. Both shifts are for an angle of incidence of 78°.

Index n	Shift 1 (nm)	Shift 2 (nm)
1.300	15.2	26.4
1.400	23.2	35.8
1.500	31.3	45.4
1.600	39.7	58.7
1.700	48.4	72.6

absorbance formula becomes

$$ABS = -\sum_{R=0}^{1} \log_{10}\left[1 - \frac{N_0\left(f\left(R\right)\right)^2}{\cos(\theta)}\right],$$

where

$$f\left(R\right) = \frac{\exp\left[\frac{-\left(R_0 - R\right)^2}{2R_s^2}\right]}{\sum_{R=0}^{1} f(R)},$$

R_0 is the center of the distribution and R_s is the width. We note here that the position of the maximum of the peak will not be changed by the inclusion of the Gaussian distribution.

We have attempted to implement the Gaussian distribution in our calculations, but the results are not available at the time of this writing.

In our experiments we used five different refractive index liquids (n=1.300, 1.400, 1.500, 1.600 and 1.700), and we will compare the theoretical and experimental results for two indices in Chapter V.

Chapter III

Experimental Procedure

A. Sample preparation

The optical fiber[32] used in our experiments had a fused-silica core and cladding, protected by a plastic buffer coating. A 15-17 cm. length of fiber was cut from the roll of fiber. The plastic coating was removed by a mechanical stripper[33] for the first 35 fiber samples. This led to many samples being broken at this initial stage of preparation. Immersing the fiber in methylene chloride for 10 minutes was used in succeeding samples to remove the coating. The methylene chloride softened the plastic coating and a clean, lint-free kimwipe easily and completely removed the coating. This reduced breaking dramatically.

The temperature of the annealing process, described below, affects the coating removal process. When the fiber was to be heated above 300 ^{o}C, all of the coating along the whole length of the sample was removed in order to protect against both the plastic coating burning in the oven and melting plastic covering some of the nearby gold. When a room temperature annealing was to be used, only the ends of the fiber and the middle section that was to be etched had the coating removed.

After the coating was removed, the cladding in the center portion 2.5 cm of the sample was removed by etching with a solution of hydrofluoric acid (HF, 48%). The area to be etched was immersed in HF for 8 minutes. A piece of hard plastic contained the HF, while an adjustable alligator-clip holder was used to position the area to be etched in the HF correctly. This etching time was utilized after tests looking at the effect of as much as 5 hours of etching were investigated under an optical microscope. Since the ratio of core diameter to cladding+core diameter was known, these tests showed that eight minutes of etching time removed all of the cladding and did not allow the HF to start to attack the core. A final etch with a weak solution of 5-10% HF for 30 seconds was also tested on four samples to check if the surface of the core was smoother than a sample without this weak etch. Scanning Electron

Microscope (SEM) investigations at magnifications of up to 50 KX did not show any difference between fiber samples with and without the extra smoothing etch.

A fiber cleaver[34] was now used on both ends of the sample fiber to assure that the entrance and exit ends of the sample were flat and signal loss due to non-normal incidence would be minimized.

The sample was connected to a five cm. length of one mm. diameter steel rod by covering part of the sample with a three cm. long piece of plastic electrical wire sheathing.

The stripped and etched fiber sample mounted in this holder was then cleaned in a shallow Pyrex container with a solution of 10% Microwash that was placed in an ultrasonic cleaner[35] for 15 minutes. The fiber was then rinsed in hot tap water to remove all of the microwash and then cleaned in ethanol followed by isopropanol, both with ultrasonic cleaning for 15 minutes. Any residual solvents remaining on the sample were then dried with nitrogen gas.

After the last cleaning step, the end of the cleaned sample mount was quickly connected to a small electrical rotator that was inside the evaporation chamber created by a bell-jar. The orientation of the sample was horizontal so that the etched part of the sample was at the same height as a quartz crystal that was used by a thickness monitor, and would remain at this same height while rotated. The bell jar was placed back onto the evaporator and a dry, oil-free rough pump was then used to reduce the chamber pressure from one atmosphere less to than 200 torr. After this vacuum was attained, the valve to atmosphere was closed and the rough pump was turned off. The valve to an adsorption pump that was cooled by liquid nitrogen was opened and the pressure was lowered to below 10 microns of mercury. Then the valve to the adsorption pump was closed and a high vacuum valve was opened to allow a cryopump to reduce the pressure to as low as was needed. This cryopump and the compressor that pumped its helium supply were started before this evaporation process started and the internal temperature inside the cryopump was at 15 ^{o}K. The pressure for the evaporation of metal-island thin films that showed good adsorption results was below 2×10^{-6} Torr; the

absolute lowest pressure attained with the cryopump used in this work was 2.1×10^{-7} Torr.

The pure Gold used was placed in a vitreous carbon crucible and this crucible was inserted in the crucible dimple at the electron-gun target point. A movable metal separator was positioned so that the sample and thickness monitor crystal were blocked from the gold filled crucible, so that the sample would not be coated with any gold at a low rate of deposition during the time when the gold was being heated from a solid state to a liquid state.

When the pressure desired was reached, the electron-beam/crystal detector cooling water supply was opened. The electron beam power supply was then turned on and the uncalibrated current control meter was turned to 40 on its dials scale. Staying at this setting for one minute allowed for the crucible and gold to slowly heat.

The voltage supply for the sample rotation motor was then turned on and the sample started rotating at approximately two revolutions per second.

The current control was then moved to 50 for one minute and the crucible started to glow a deep orange color. The gold also started to liquefy at this setting. Finally, the current control was moved to 55-57.

This setting range provided a peak rate of gold deposition from 4-6 Å/second that allowed for two important considerations. This setting was fast enough to reliably form the needed metal-islands on each sample. It is possible that with a higher evaporation rate, the size of the islands formed will be dramatically larger than lower evaporation rates. A published work[36] has stated that much faster deposition rates would lead to a homogenous film when depositing a similar amount of silver. We are unsure of these claims, but our interest is to utilize the above mentioned assumption that the particles are much smaller than the wavelength of the interacting light, so we used the intermediate rate stated above. We have observed that the annealing processes may be much more critical in terms of the size, shape and variations of these important measures.

This setting also allowed preparation of samples with exactly the same amount of gold deposited, within the accuracy of the thickness monitor; whereas higher deposition rates lead to lack of control, on the

part of the sample preparer, and fluctuations of more than +/- 1 Å in the total amount of gold deposited.

The metal shield was rotated to one side of the chamber to allow a free path for the evaporated gold to travel upwards towards the crystal and sample, and deposition started. The evaporation of 100 Å or less was easily completed in less then one minute. After evaporation, the high vacuum valve was closed and the crucible was allowed to cool for ten minutes. After this time, a supply of nitrogen gas was connected to the vent-to-atmosphere valve and opened. The nitrogen was allowed to enter the chamber until atmospheric pressure was attained. The bell jar was then removed and the sample was extracted.

The annealing process now occurred. Two methods of annealing the sample were used in this work: 24 hour room temperature annealing while the sample was mounted in the experimental set-up described in section 2 of this chapter, and annealing at a high temperature for a short amount of time in an oven. The fiber samples were not rotated during heating because the particles are small enough so the gravitational force acting on their mass is negligible in comparison to surface tension. After the oven annealing process the sample was mounted in the experimental setup.

The color of the gold-island on the fiber samples changed from dark green, just before heating, to purple after 4 minutes at 200°C and finally to pink, after heating at 600°C or higher. **Figure III.1.** shows these differences for annealed quartz slide samples. The same color changes occured on our fiber samples.

B. Sample Pictures

In order to be sure that the gold-islands were being produced we used two different microscopes to take images of flat substrate samples that we prepared. Images of islands on fiber samples have not been obtained.

Figure III.2. through **Figure III.11.** show pictures of metal-island films that were taken using an atomic force microscope (AFM) in

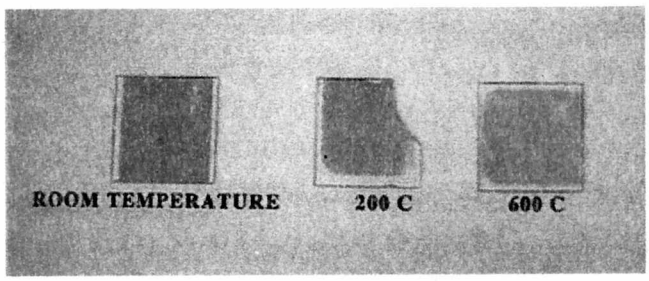

Figure III.1. Color differences of annealed slide samples. Quartz slides onto which a 4 nm gold film has been evaporated. Thereafter the slides were annealed during 4 minutes at different temperatures. The slides tend to redish with high temperature, which corresponds to a shift to a higher wavelength for the plasmon.

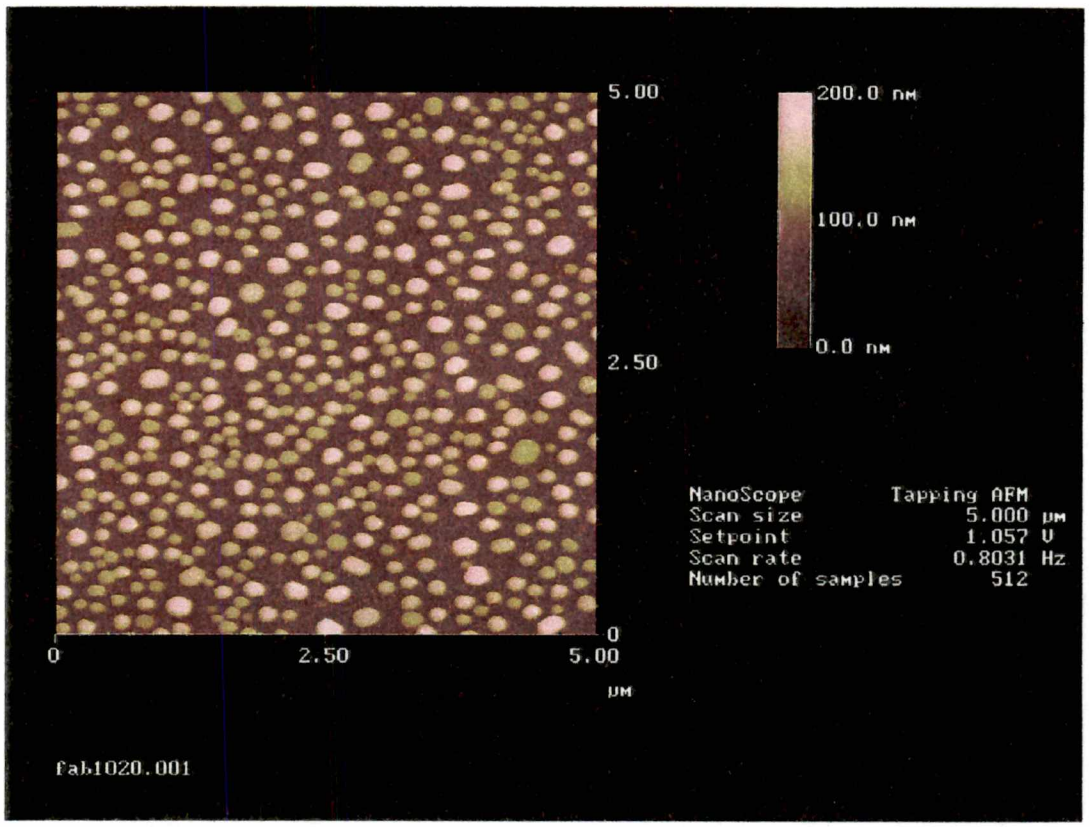

Figure III.2. Magnification of gold islands annealed at 800°C. Annealing time was 4 minutes. AFM tapping mode used.

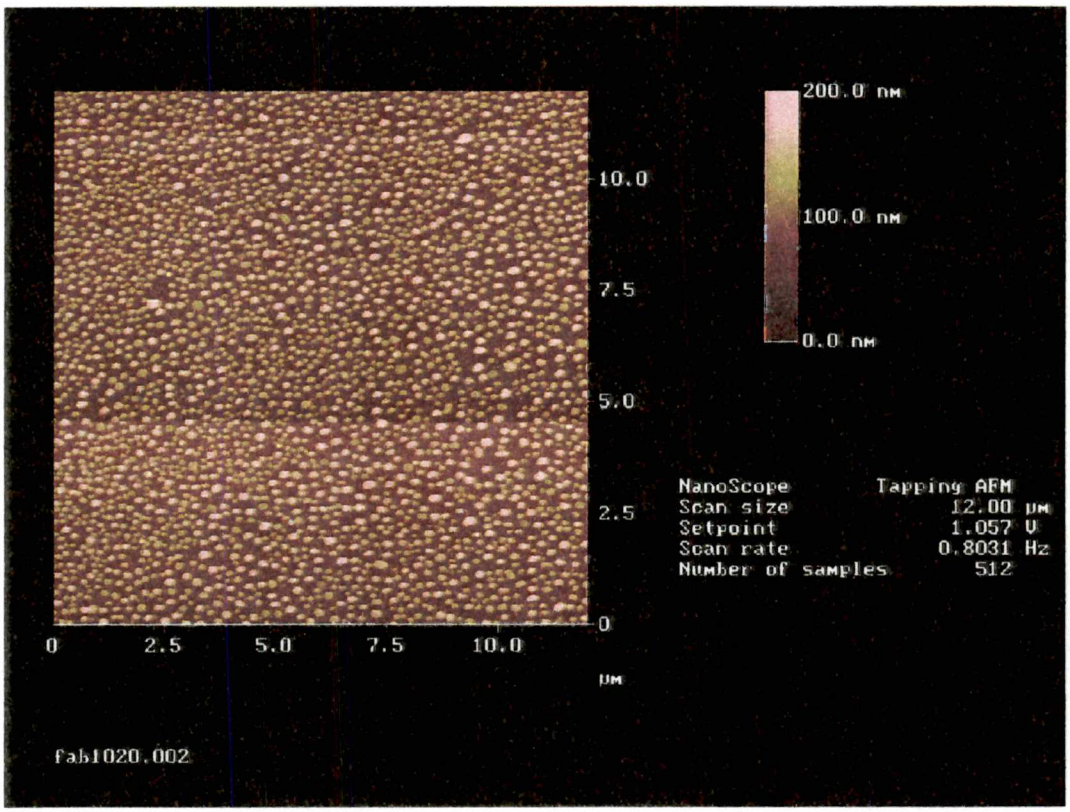

Figure III.3. Gold islands annealed at 800°C. Annealing time was 4 minutes. AFM tapping mode used.

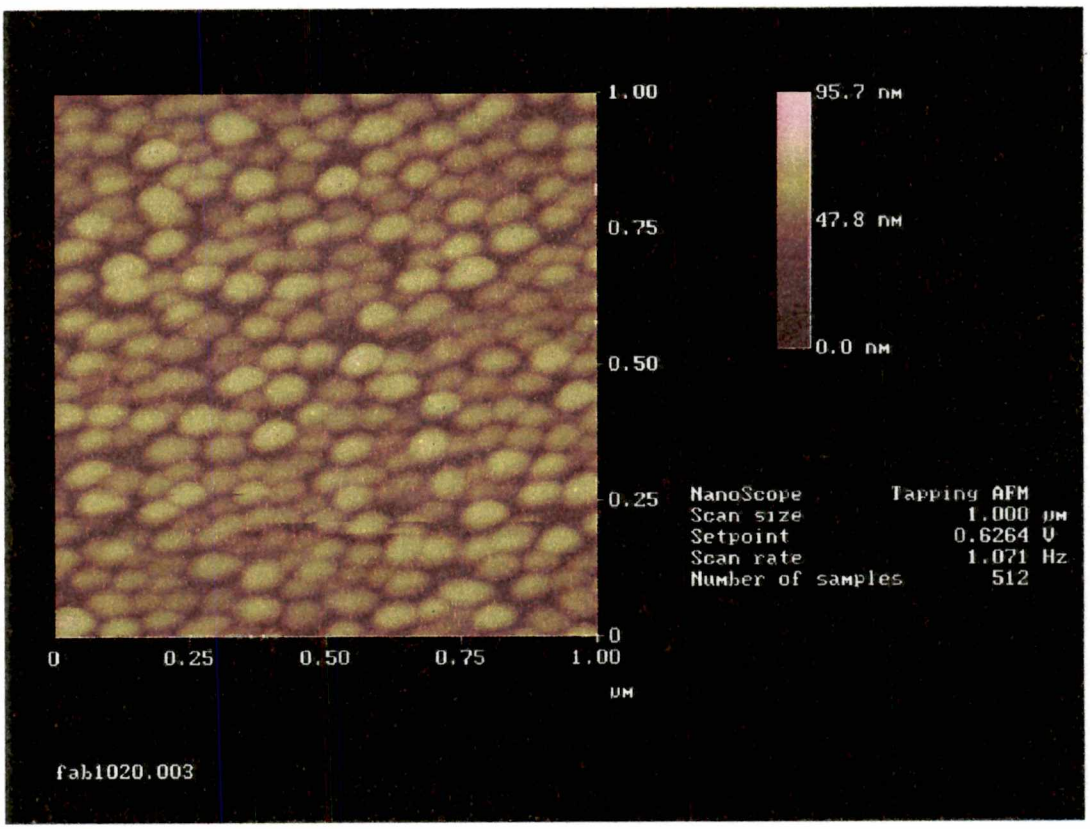

Figure III.4. Magnification of gold islands annealed at 110°C. Annealing time was 4 minutes. AFM tapping mode used.

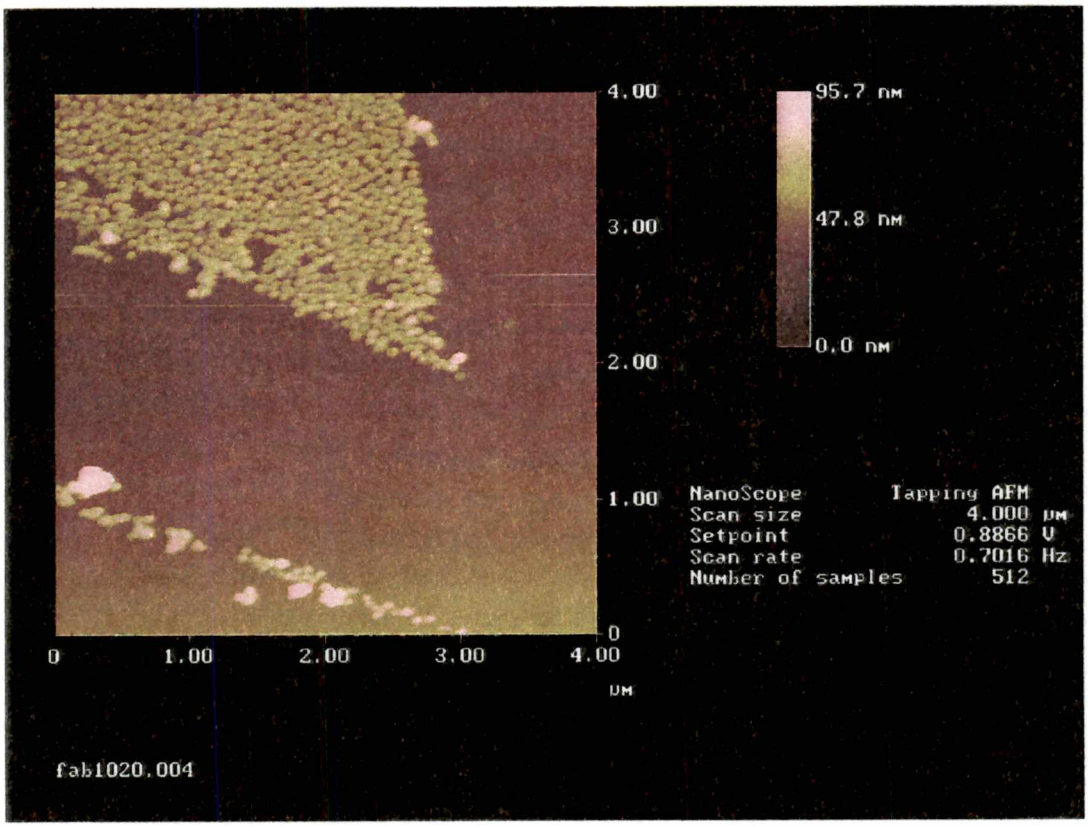

Figure III.5. Gold islands annealed at 110°C. Annealing time was 4 minutes. AFM tapping mode used.

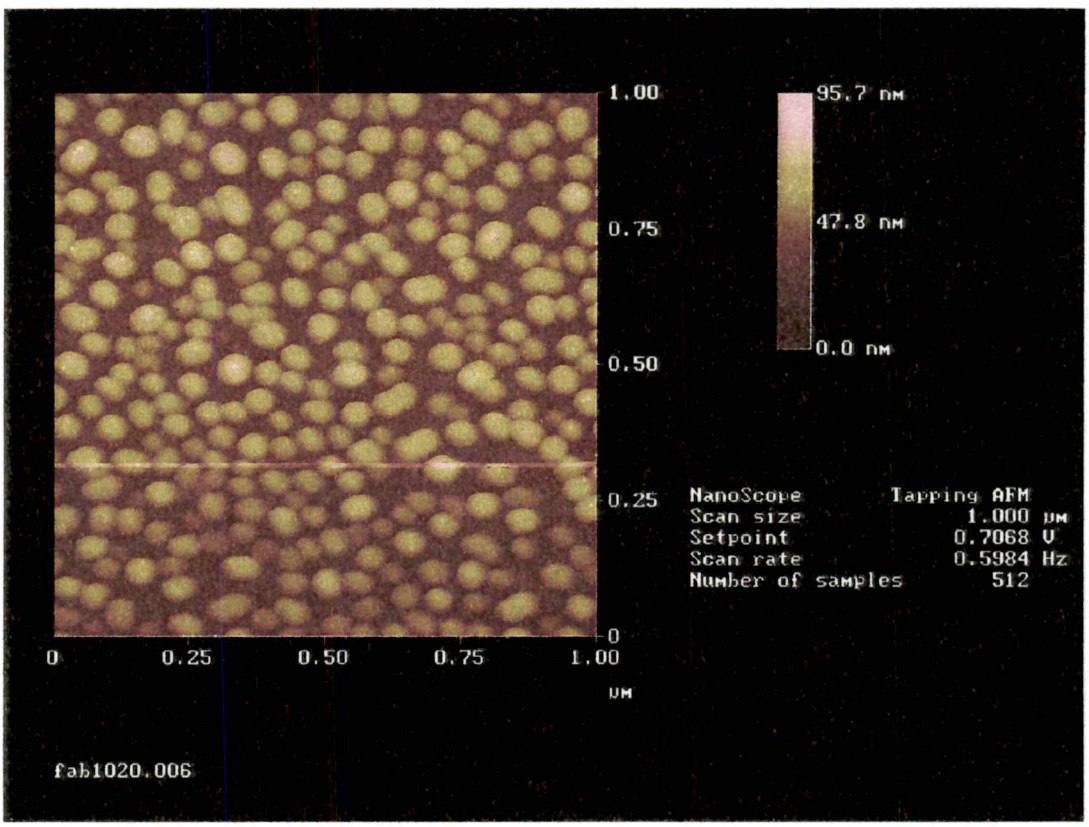

Figure III.6. Magnification of gold islands annealed at 110°C. Annealing time was 4 minutes. AFM tapping mode used.

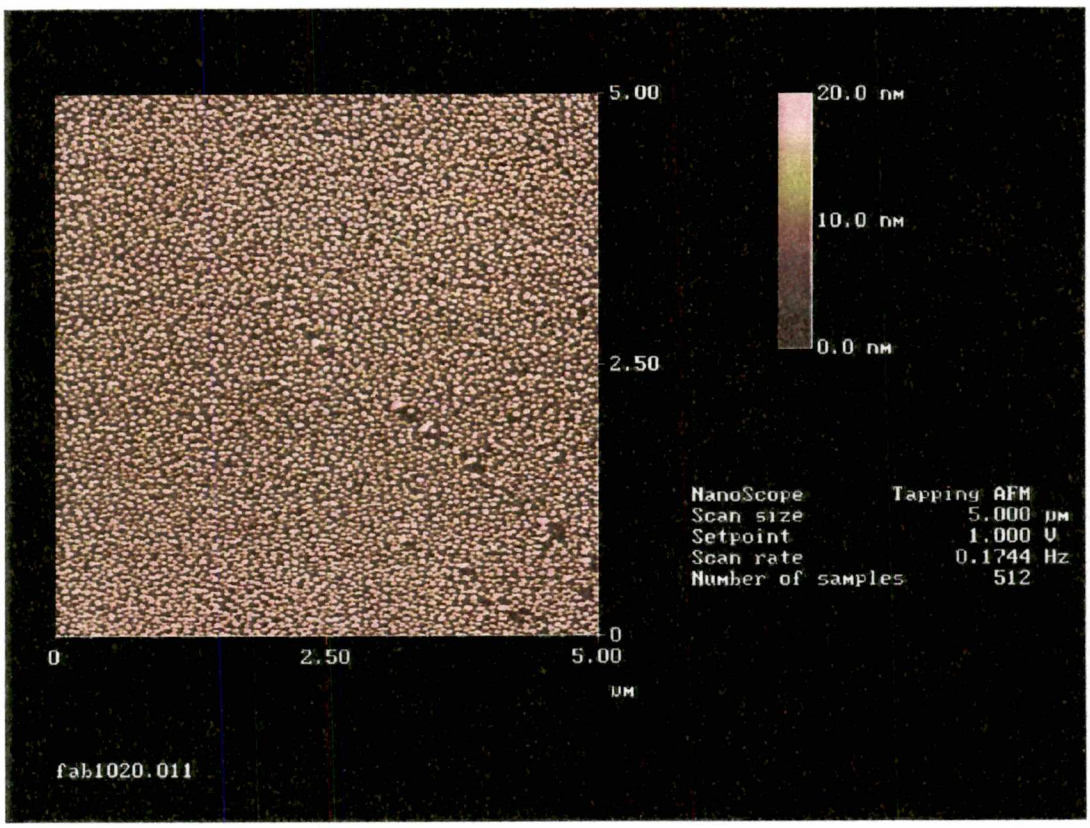

Figure III.7. Gold islands annealed at 20°C. Annealing time was 3 hours. AFM tapping mode used.

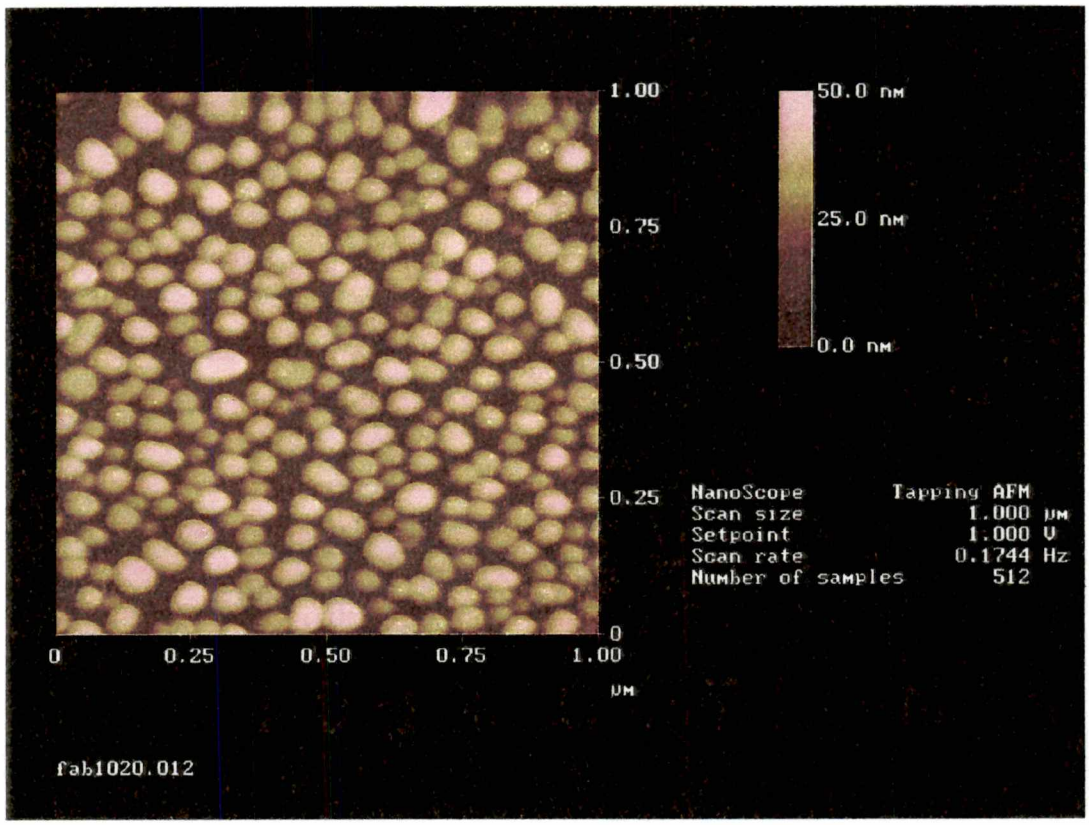

Figure III.8. Magnification of gold islands annealed at 20°C. Annealing time was 3 hours. AFM tapping mode used.

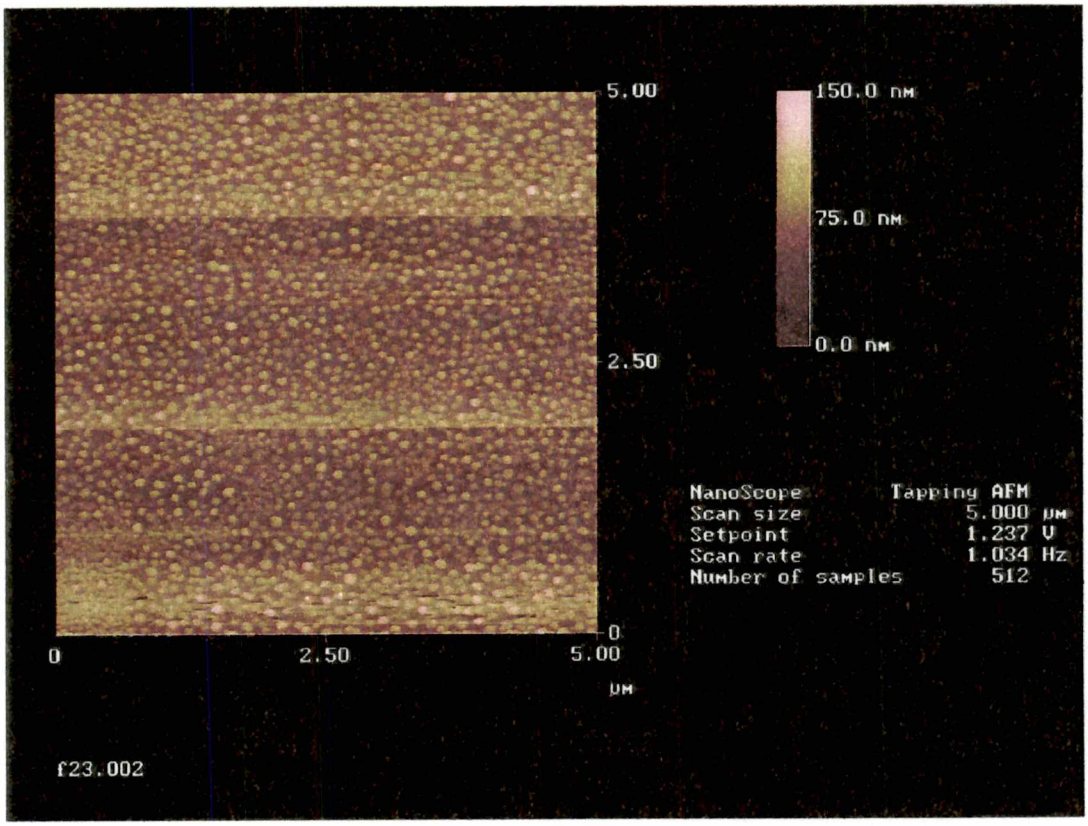

Figure III.9. Gold islands annealed at 600°C. Annealing time was 3 minutes. AFM tapping mode used.

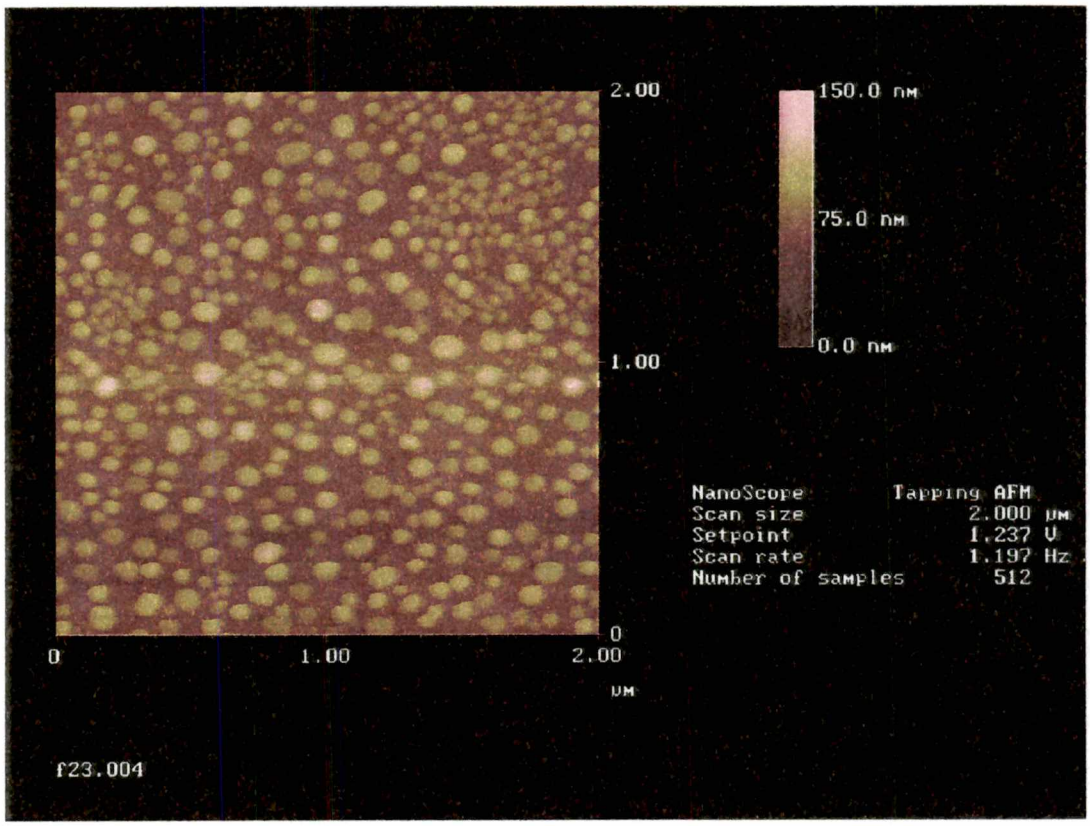

Figure III.10. Magnification of gold islands annealed at 600°C. Annealing time was 3 minutes. AFM tapping mode used.

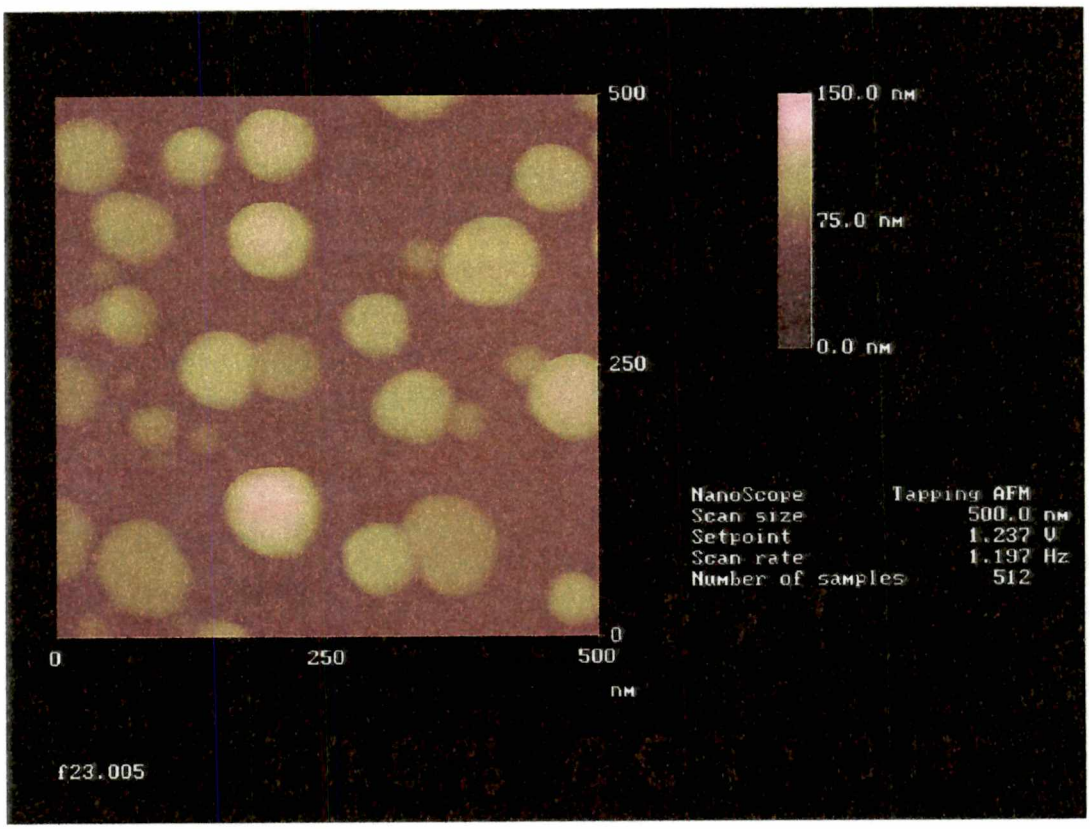

Figure III.11. High magnification of islands annealed at 600°C. Annealing time was 3 minutes. AFM tapping mode used.

tapping mode. The substrate used in these pictures were flat quartz slides. These samples were evaporated at the same time as fiber samples #139 and 140, and were mounted directly next to the fiber samples.

As we will show in Chapter III, fiber samples #139 and 140 did show good absorption when annealed at 800°C for four minutes, the same annealing process as this AFM slide.

Figure III.2. and **Figure III.3.** are both pictures of the same sample slide that was annealed at 800°C for 4 minutes. **Figure III.2.** is a magnified scan of the lower left corner (0 to 5 μm by 0 to 5 μm) of **Figure III.3.** The size of the islands in this sample are distributed about an approximate average diameter of 165 nm.

Figure III.4., **Figure III.5.** and **Figure III.6.** are all pictures of the same sample that was annealed at 110°C for 4 minutes. The size of the islands in this sample are distributed about an approximate average diameter of 52 nm. A slightly larger average separation between islands and a more spherical shape of the islands exists in **Figure III.6.**, as compared to the region pictured in **Figure III.4.** Some very large voids between clusters of islands are present in **Figure III.5.**

Figure III.6. and **Figure III.8.** are both pictures of a sample that annealed in room temperature for 3 hours. The size of the islands in this sample are distributed about an approximate average diameter of 53 nm. The similarities of the islands in **Figure III.6.** and those in **Figure III.8.** show that room temperature annealing, for a number of hours effects the size distribution in a manner similar to the 110°C for 4 minutes annealing process.

Figure III.9. through **Figure III.11.** are all pictures of a sample that was annealed at 600°C for 3 minutes. The size of the islands in this sample are distributed about an approximate average diameter of 90 nm.

In these figures, the coalescing of the small islands into larger islands after high temperature heating is evident. Variations in the size and shape of the islands are also noticeable, and thus justifies the use of the Gaussian distribution for the shape of the particles in the theoretical development. It is interesting to notice the increase in the separation between the larger particles and any neighbors, as compared to the

smaller particle separation. This shows how the annealing process causes neighboring smaller particles to collect into larger particles. In several of these figures, some of the islands almost have a hexagonal shape. The annealing process may have forced this partial crystallization of the islands. This effect can also be seen in SEM pictures of annealed silver islands in a previously published paper[37].

Images were also taken of the same quartz slide samples with a SEM. **Figure III.12.** and **Figure III.13.** show these pictures. The use of a quartz substrate gives inherent difficulties in imaging the metal-island because of excess electron collection on the dielectric quartz. Even with these difficulties, it is quite evident that most of the larger particles do not have a spherical shape, and that a wide variation in the sizes exist. The size, shape, separation and distribution of the sizes of the particles in these images are similar to the AFM images of a sample annealed at 800°C for 4 minutes.

These pictures are similar to those found by others for silver[38] and gold[39], where silicon, a semiconductor, was used as a substrate, and much clearer images were obtained. This previous gold islands work included a SEM picture of 20Å deposited on silicon that was annealed at 800°C for 4 minutes. Comparing this sample with our sample shown in **Figure III.2.** and **Figure III.3.**, which was prepared in similarly, we see a greater size variation in the sample prepared on silicon. We believe that the size variation is reduced with increased deposition amount, and is not greatly affected by the substrate differences. Our SEM pictures also show less size variation. Size variation was also stated[40] to be reduced by lower annealing temperatures, but we wished to maximize the amount of absorption and utilized the higher temperatures.

Using NIH Image software, we were able to characterize the lengths of the magor axis of the spheroids in these images. This software could be used to measure the minor axis of the particles, however the AFM tip gives incorrect measurements of the heights of particles due to the diameter of the tip being close to the height. **Figure III.14.** provides a histogram prepared with major axis measurements of 155 of the particles in the magnified center portion of **Figure III.1.**, which was annealed at 800°C for 4 minutes. Calibration was performed by

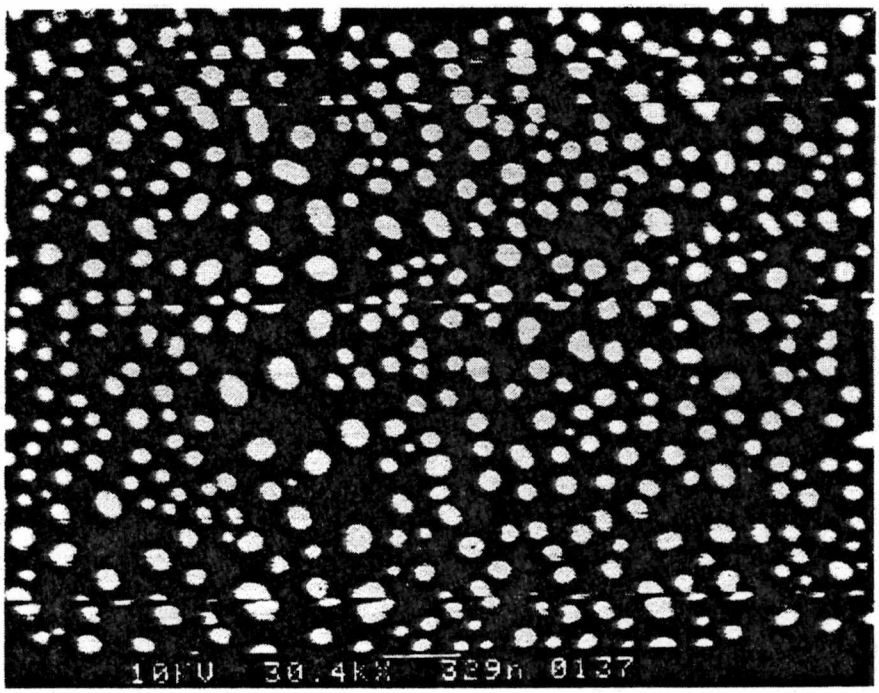

Figure III.12. SEM Gold islands annealed at 800°C. Annealing time was 4 minutes. An SEM was used to take this photograph. The horizontal bar indicates a length of 329 nm.

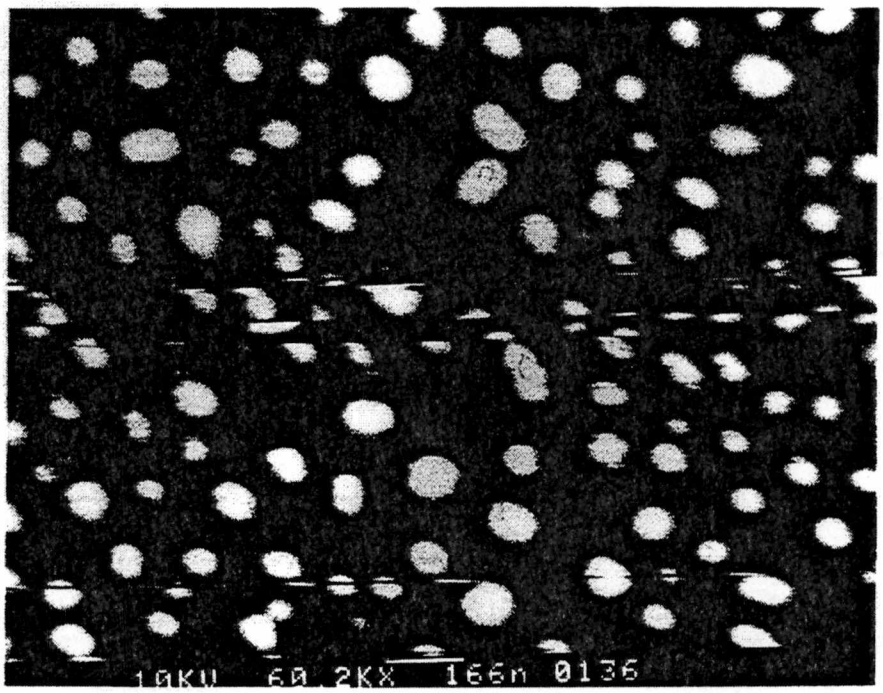

Figure III.13. SEM Magnification of Gold islands annealed at 800°C. Annealing time was 4 minutes. SEM used to take this photograph.

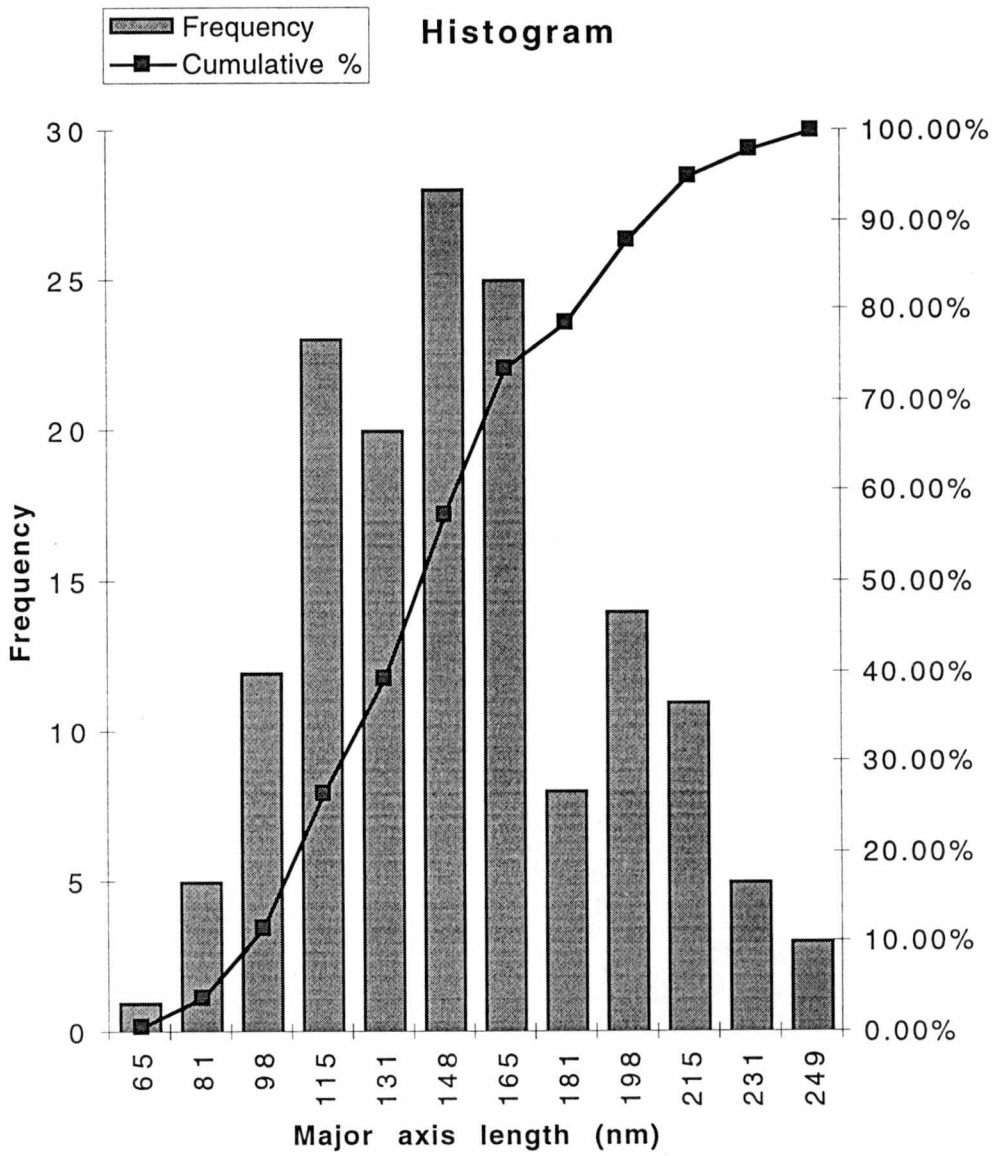

Figure III.14. Histogram of major axis lengths for 800°C sample.

measuring the scale at the bottom of the image, from 0 to 2.5 microns, under the same image magnification. The average major axis of these particles is approximately 165 nm. **Figure III.14.** shows that just above 60 percent of the particles have major axis lengths between 115 nm and 165 nm, and the smallest are 65 nm while the largest are 250 nm.

Figure III.15. provides a histogram prepared with major axis measurements of 265 of the particles in **Figure III.5.**, which was annealed at 110°C for 4 minutes. Calibration was performed by measuring the scale at the bottom of the image, from 0 to 1.0 microns. The average major axis of these particles is approximately 52 nm. **Figure III.15.** shows that just above 70 percent of the particles have major axis lengths between 37 nm and

Our results[41] for the absorbance and peak shift of gold-islands on quartz slides were obtained by the use of a double-monochromator, scanning spectrophotometer[42]. The absorbance data were very similar to an earlier paper[43]. We compared these slide-only results to the absorbance and shift measurements using the same equipment for our combination slide/fiber samples and found similar results. The absorption results for the slide/fiber samples will be given in Chapter IV, along with a few representative quartz slide ABS results for comparison.
55 nm. Both by examining **Figure III.15.**, and comparing it to **Figure III.14.**, and by comparing the cooresponding pictures, we see that the major axis length distribution does vary much more for the high temperature annealed sample.

Figure III.16. provides a histogram prepared with major axis measurements of 265 of the particles **Figure III.7.**, which was annealed at 20°C. Calibration was performed by measuring the scale at the bottom of the image, from 0 to 1.0 microns. The average major axis of these particles is approximately 53 nm. **Figure III.16.** shows that just below 50 percent of the particles have major axis lengths between 40 nm and 55 nm. We see again that the major axis length distribution varies much more for the high temperature annealed sample. Comparison of **Figure III.15.** and **Figure III.16.** shows that the effect of room temperature annealing is similar, in terms of the size and distribution of the islands created.

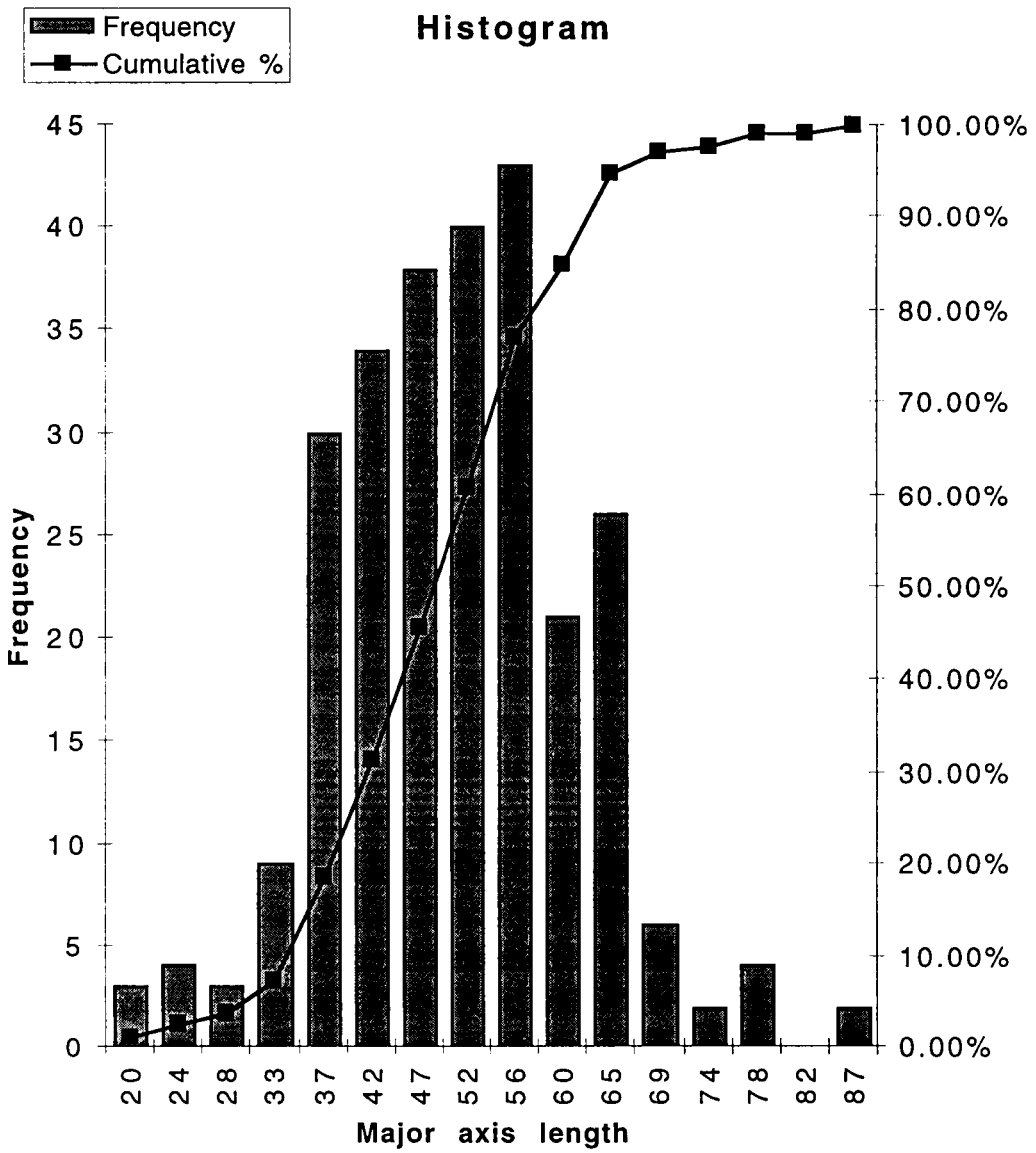

Figure III.15. Histogram of major axis lengths for 110°C sample.

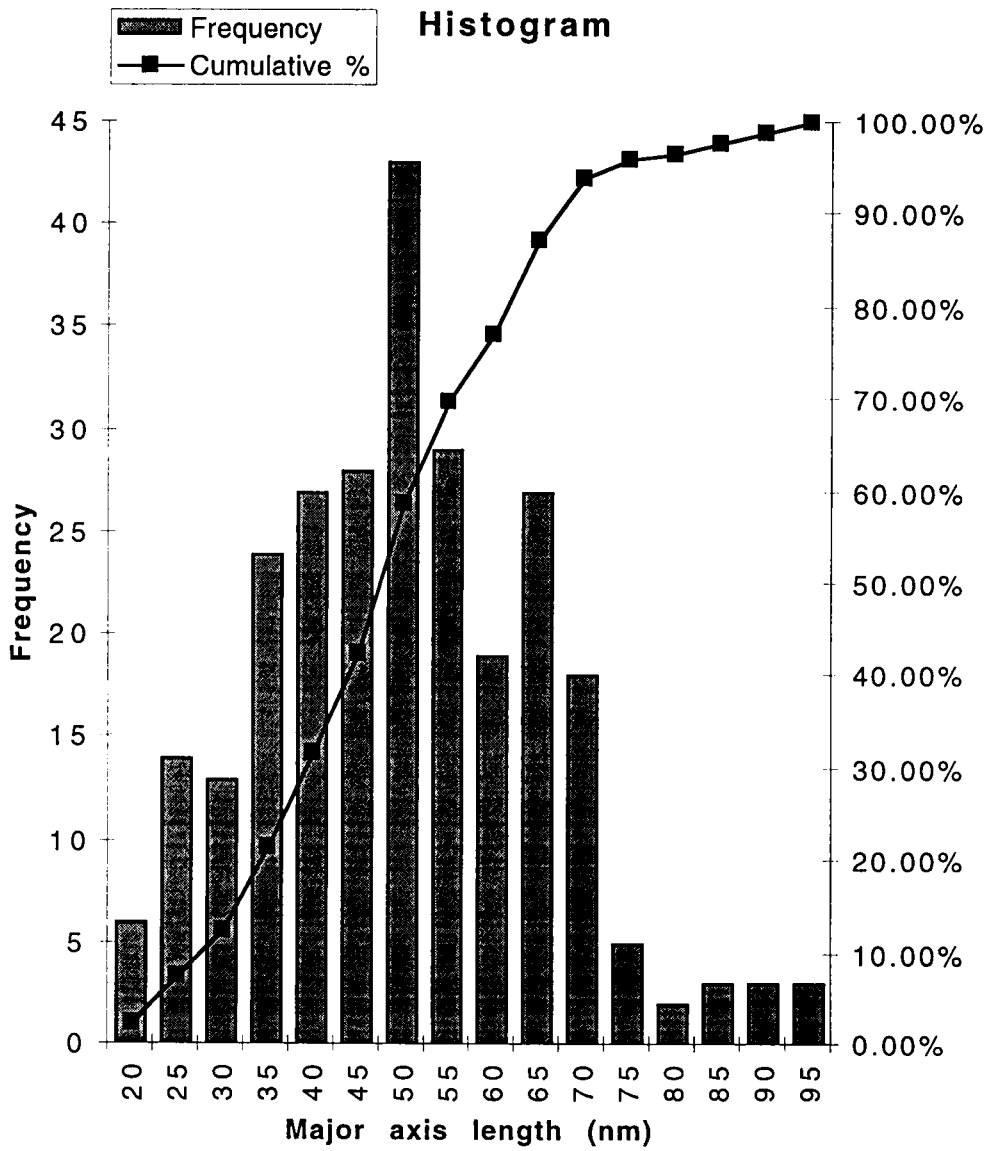

Figure III.16. Histogram of major axis lengths for 20°C sample.

As a second check for the reproducible formation of gold-islands, several samples were prepared in a procedure different from that described above. These samples were cleaned and then attached, in pairs, to clean quartz slides with two drops of epoxy away from the etched portion of the sample. The slide-fiber combination samples were then mounted in the evaporation chamber and approximately 40 Å of gold was deposited. These samples were not rotated, and gold was deposited onto only the portion of the fiber that was facing away from the slide.

C. Experimental setup

The light from a high-pressure xenon (Xe) arc lamp[44] was focused into the entrance slit of a monochromator[45]. The Xe arc lamp produces a characteristic spectrum. A graph[46] of the spectral irradiance of a Xe arc lamp for wavelengths between 200 nm and 1500 nm is shown in **Figure III.17.** The arc lamp had a power supply[47] that could vary the current supplied to the lamp and was contained in a protective housing[48]. During all experiments, the current was set to the maximum recommended for the arc lamp. A different power supply[49] and lamp housing[50] were used in later experimental runs, in order to increase the intensity of the light launched into the fiber sample. This housing was vertically mounted, and used a concave mirror mounted at 45 degrees to focus the light onto the initial entrance mirror of the monochromator. Both of the lamp housings had ultraviolet grade windows or condenser lens assemblies.

At the exit slit of the monochromator, a microscope objective[51] was used to focus the exiting light into the prepositioned entrance end of the fiber sample. A silicon photodiode[52] with a SMA connector[53] attached to its SMA mounting bracket was used to produce a voltage proportional to the intensity of the light that passed through the sample. The monochromator was scanned over the spectral range of 300 nm to 900 nm with an increment of 1 nm during the experiment, and the voltage readings from the photodiode were recorded and stored in a text file.

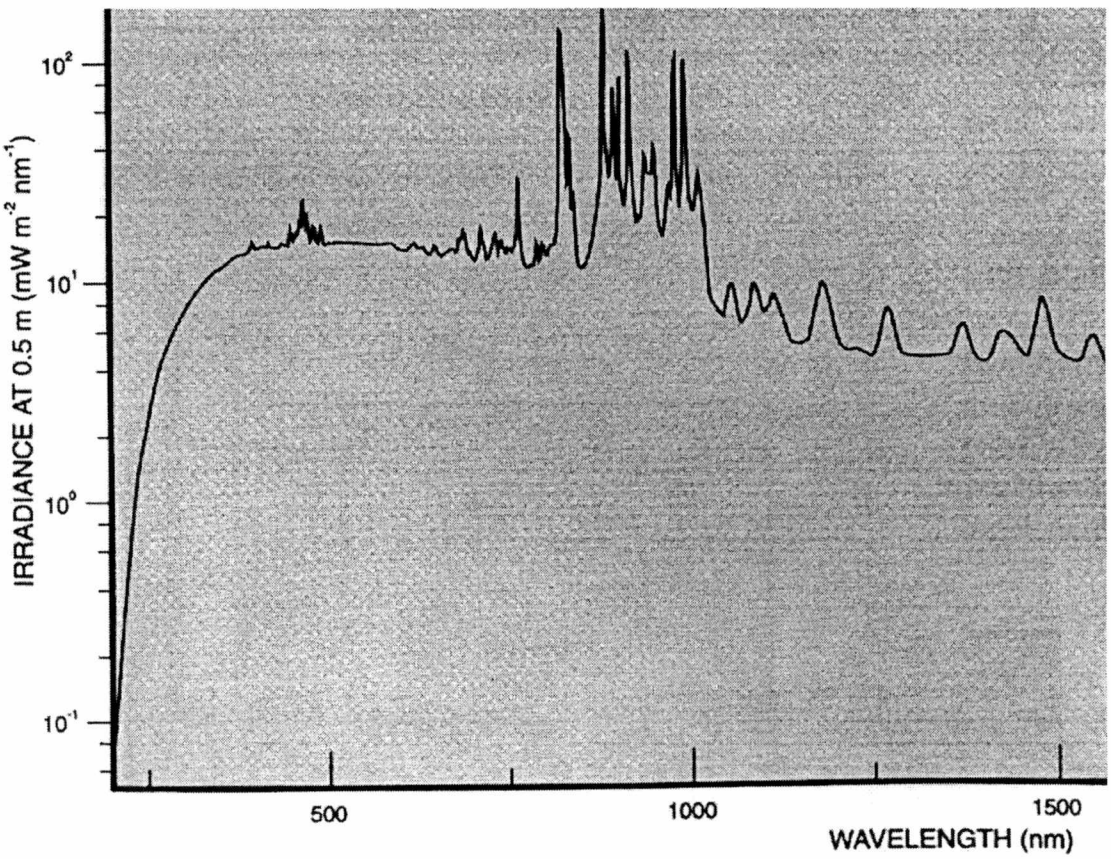

Figure III.17. Xenon arc lamp irradiance versus wavelength.

A graph[54] of signal versus wavelength for a typical silicon photodiode is given in **Figure III.18.** The same measurements were taken for stripped, etched and cleaned fiber samples that were not coated with any gold. These measurements were used as baseline fiber data, and formed the I_0 values in the ABS formula above. Three separately performed measurements of different baseline fibers from the same spool of cable were compared and did not show any significant variation. A set of voltage data points were taken from one of these tests and was used as a baseline for the samples that used fiber from the same spool.

The monochromator has a asymmetric Czerny-Turner optical mount, and a 640 m. focal length. The 1200 gr/mm. ruled grating mounted inside the monochromator allowed for a useful spectral range from 165 nm to 5000 nm, a precision of +/- 0.5 Å within this entire range, and repeatability of +/- 0.2 Å. The wavelength motor of the monochromator was powered by an interface box[55] that was controlled by ASCII codes set by the serial communications port of a personal computer. The monochromator was found to be calibrated well by testing with 632.8 nm red and 543 nm green helium-neon lasers. The recorded data used with the Xe source also had peaks of intensity at wavelengths that correlated with the known Xe spectrum.

The microscope objective used was composed of glass optics. This greatly reduced the ultraviolet part of the Xe spectrum and caused low signals in the 300 nm - 400 nm range. A collimator[56] composed of quartz optics that focused light into a SMA connector, that was the same as the connector on the photodiode, was used to try to increase the signal. The combination of SMA connectors at both ends of the sample caused low signal at all wavelengths between 300 nm through 900 nm and, therefore, was not used. SMA connectors which would normally be used with optical fiber of much higher outer diameters of 500 microns and 1050 microns were tested for use with the collimator, but were also found to not significantly increase the signal.

A fiber positioning system[57] provided fine adjustments on the x, y and z axis to assure an efficient launch of the light into the fiber. Since the focal length of the microscope objective was less than a millimeter,

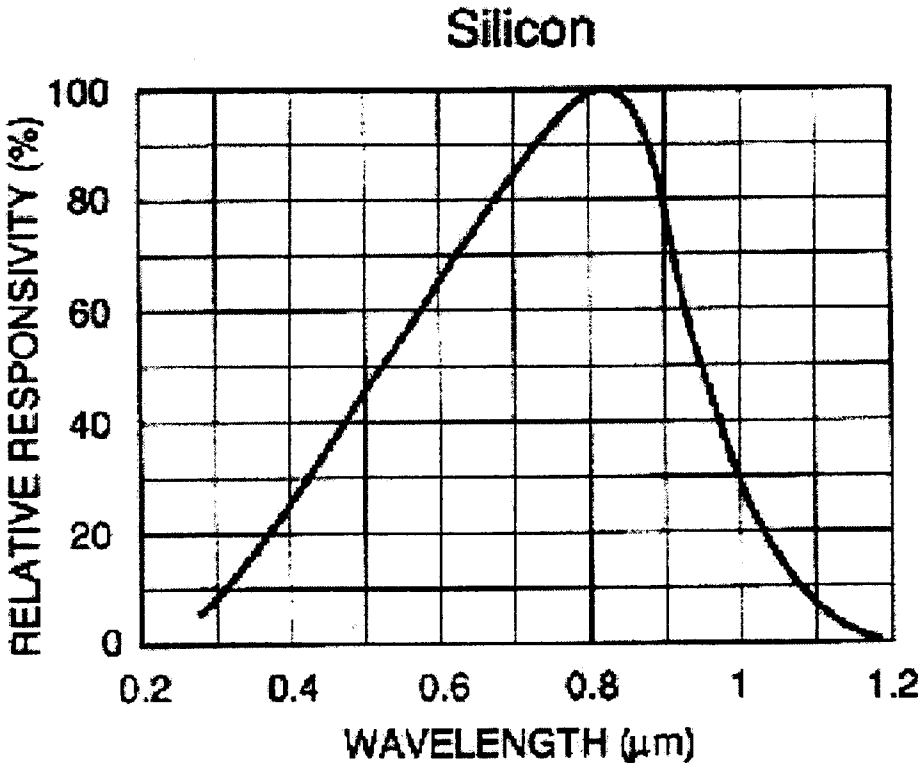

Figure III.18. Silicon photodiode response versus wavelength. The relative responsivity of the photodiode increases linearly from 25% at our low wavelength (400nm) to 100% at 825 nm, then decreases to 80% at our maximum wavelength of 900 nm.

the entrance end of the fiber was almost touching the end of the microscope objective.

A system of two individual single axis positioners[58] with total travel of 2.5 centimeters were cross mounted and the fiber positioning system was mounted onto the top of this system. A vertically adjustable optical mount[59] inserted into a magnetic optical base[60] was used to support the above mentioned system and optical table connection. This whole system provided very flexible fine and coarse adjustments and made signal maximization easier.

A fiber chuck with a flexible four point clamping end that tightened around the fiber was shortened and used to hold the fiber sample in the positioning system.

The silicon photodiode with the attached SMA connector was mounted onto a combination of two cross-mounted single axis positioners and a magnetic base. This system enabled signal maximization by having the transmitted light coming out of the exit face of the fiber hitting the most sensitive part of the surface of the photodiodes active area. The wire leads of the photodiode were attached to a voltage measurement device.

For the first samples tested, a hand held digital multimeter[61] (DMM) was used to measure the voltage. An ASCII code was sent to the DMM by the computer program controlling the experiment through the computers second serial communications port (COM2). The measurement was sent back to the computer and stored in a text file. For later samples, a data acquisition board[62] was mounted in the computer and was used to directly measure the voltage and record it in a text file. This board was also controlled by the modified computer program. The A/D board was found to be more accurate than the multimeter, but this caused the noisy xenon arc lamp output to be visible in the data collected.

At the end of writing this thesis, we have inserted a simple averaging routine in the experiment control program. This collects 100 voltages at each wavelength and calculates the average that is used as the voltage data point for that single wavelength. The initial testing of this scheme seems to have reduced the noise. Most of our experimental runs did not use this averaging technique, and the voltage data was smoothed using a moving average with a smoothing width of usually 10 nm. We

feel that future use of this system with the averaging will not require data smoothing.

Figure III.19. shows a simplified, overhead view of the complete experimental setup.

Upon completion of this experimental run with n=air surrounding the gold-islands, the quotient I/I_0 was calculated in an Excel spreadsheet. A fiber sample that showed a quotient graph with absorption for n=air was then tested with one of the five optical liquids surrounding the islands. The samples that were treated with the high temperature annealing showed good absorption from simply looking at the raw detector voltage data and comparing it to the baseline data. An excellent example of this is shown in **Figure III.20.**, where the n=air solid line clearly shows a reduction in the relative amount of detector voltage at wavelengths centered around a small neighborhood about 520 nm. The calculated ABS for this sample will be shown in Chapter IV.

Several configurations for using the liquids were used. Initially, the liquid was simply dropped onto the fiber from above and surrounded the islands before dropping further below the fiber. The lowest index liquid, n=1.3000, which also has the lowest density, seemed to evaporate quickly in this configuration. In order to protect from excess evaporation, a one axis positioner was used to vertically raise and lower a horizontal platform that held a clean glass slide. Several drops of the liquid to be used was dropped onto the slide, and the slide was raised until the fiber was completely immersed in the liquid. This area was then covered with a plastic cover.

Another attempt to cover the liquid during testing used a glass tube with an inside diameter of 0.5 mm. that was inserted into one end of the fiber chuck and completely covered the active portion of the sample. This tube was positioned horizontally so as not to have any of the fiber touching the inside glass, but to allow for capillary action to pull and hold the index dropped onto the free end. This configuration worked well if the fiber chuck was washed after each use to avoid mixing different index liquids for following experiments.

Each optical liquid used has a tolerance of 0.0002 from it's index of refraction that was specified only at 25 ^{o}C and a wavelength of 5893 Å.

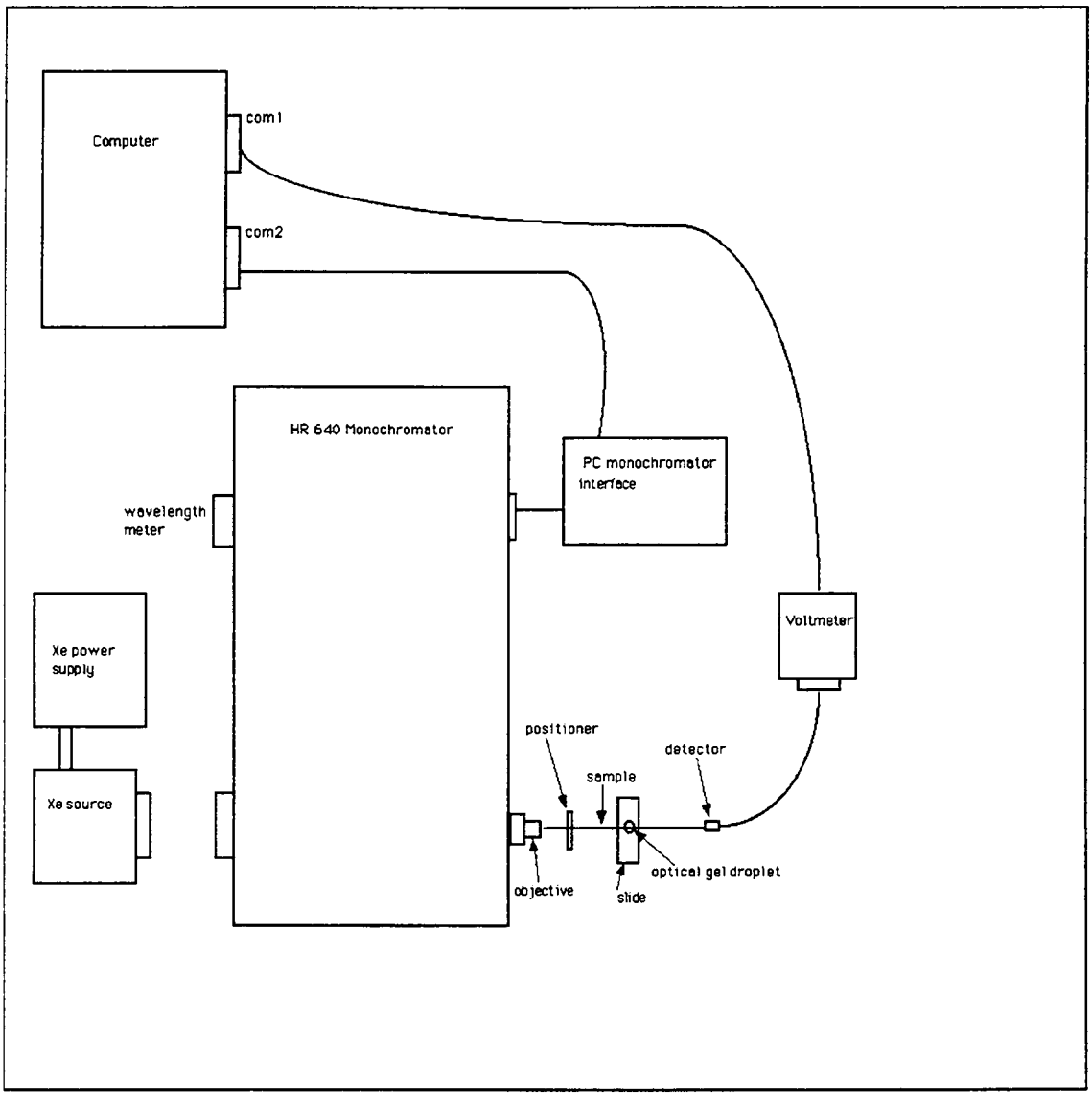

Figure III.19. Experimental equipment.

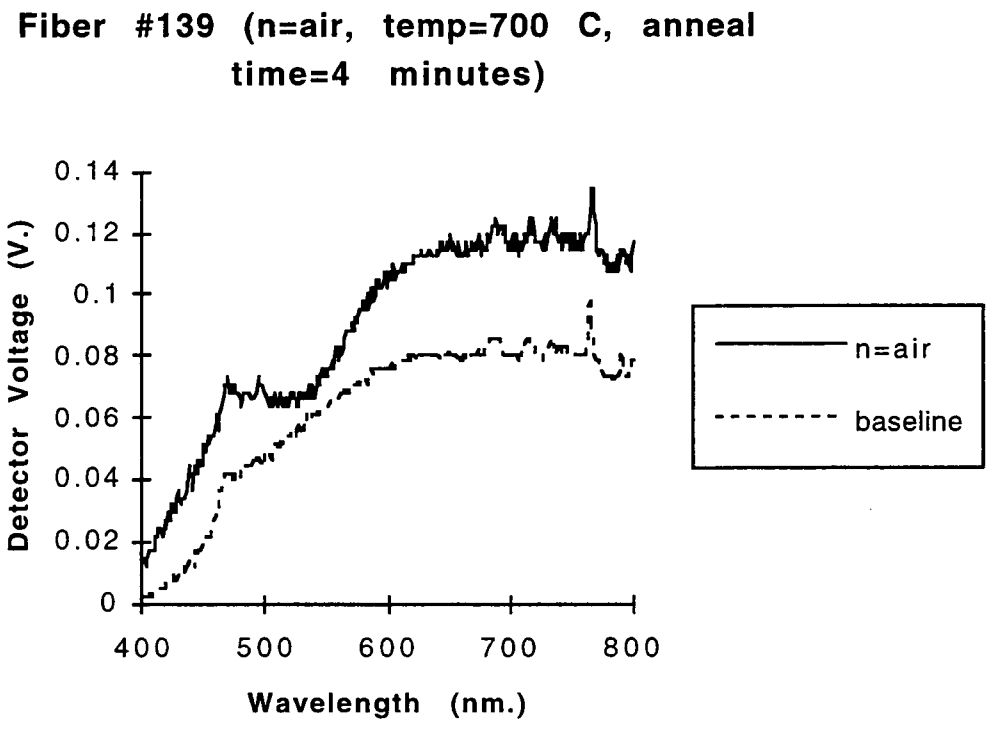

Figure III.20. Example voltage data showing absorption. The data have not been normalized in order to clearly show the reduction of the voltage with the n=air, gold island coated sample.

The variation with temperature can be characterized by the manufacturer supplied temperature coefficient dn_D/dt and F-C difference between the Fahrenheit and Celsius values, $n_F - n_C$. The Abbe number was also given as

$$v_d = (n_D - 1)/(n_F - n_C).$$

Another consideration for the optical liquids is the change of the index of refraction over the range of wavelengths that we used in our experiments. The Cauchy equation given with the optical liquids for determining the actual refractive index as a function of wavelength at 25 ^oC is:

$$n(\omega) = C(1) + C(2)/(\omega^2) + C(4)/(\omega^4),$$

where C(1), C(2) and C(4) are the supplied Cauchy numbers for a specific optical liquid. These numbers allowed us to note a variation of less than +/- 1% from the specified index over the wavelength range we were using.

The temperature parameters and the Cauchy numbers for the five refractive index fluids used in this work are tabulated in **Table III.1.**, and **Table III.2.** An example of the variation of the n=1.400 index liquid with respect to wavelengths within the range that we used is given in **Table III.3.**

Table III.1. Parameters for the optical liquids.

Series number	Index	F-C diff	Abbe v_d	Temp. coef
AST433 AAA	1.3000	0.0031	97.9	-0.000337
AST S1050 AA	1.4000	0.0077	51.7	-0.000412
AST 5050 A	1.5000	0.0120	41.7	-0.000401
AST 40BN A	1.6000	0.0234	25.6	-0.000438
AST BNDN B	1.7000	0.0371	18.9	-0.000480

Table III.2. Cauchy numbers for the optical liquids.

Index of refraction	C(1)	C(2)	C(4)
1.3000	1.294756	198560.5	-5.809673E+11
1.4000	1.387868	434180.6	-4.474685E+11
1.5000	1.483347	538728.8	1.3696E+12
1.6000	1.570218	883391.4	5.238595E+12
1.7000	1.655743	1217813	1.108288E+13

Table III.3. Example of n=1.400 wavelength variation.

Wavelength (Å)	Refractive index at 25°C
2900	1.43
3650	1.418
4861	1.4054
5461	1.4019
5893	1.4000
6328	1.3984
6563	1.3977
6943	1.3967
8400	1.3939

Chapter IV

Data Analysis and Results

The measurements of the voltage across the wire leads of the silicon photo detector that were created by the light that is transmitted through the fiber sample were analyzed to show two important effects.

The absorbance of the light by the excitation of surface plasmons on the gold-islands was calculated from these voltage measurements.

Our experiments included tests of fiber samples that were rotated while evaporation occured, combination fiber samples mounted to flat fused silica slides that were not rotated, and slide-only samples. The slide-only were used to compare our data with previous work.

A. Absorption and shift results for rotated samples

These samples were prepared exactly as described in chapter III. All of the following graphs of ABS versus wavelength are for fiber samples that showed absorption of the incident light and were rotated during the gold evaporation step.

One of the first samples that successfully showed absorption when a n=1.7 liquid was applied to it was used to see the affect of aging of the absorption. **Figure IV.1.** shows the ABS for the sample just after the liquid was applied, and, for the same sample that was not moved in the experimental set-up seven days later. The sample was covered from debris falling from above by a clear plastic dish, but was not protected in any other way. The widely varying quotient for wavelengths less than 500 nm was caused by both noise of the Xe source and low signals for both I and I_0.

The following **Figure IV.2.** through **Figure IV.3.** show examples of the absorption peak was being removed with the application of the n=1.600 liquid. These two samples were prepared together.

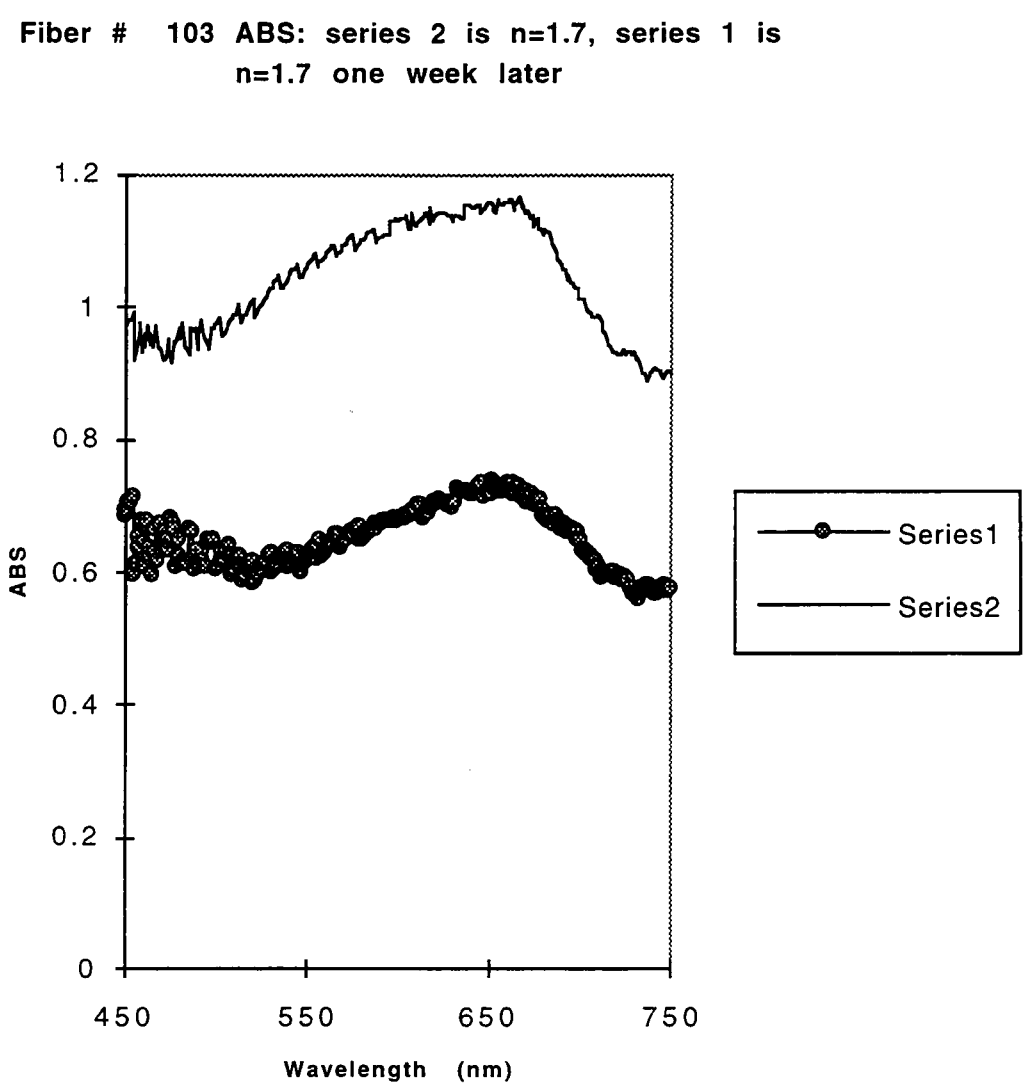

Figure IV.1. Change over time of ABS for n_S=1.700. The absorption peak, centered at 660 nm, is weakened after a week of exposure to the room environment. Sample was annealed at room temperature for 24 hours.

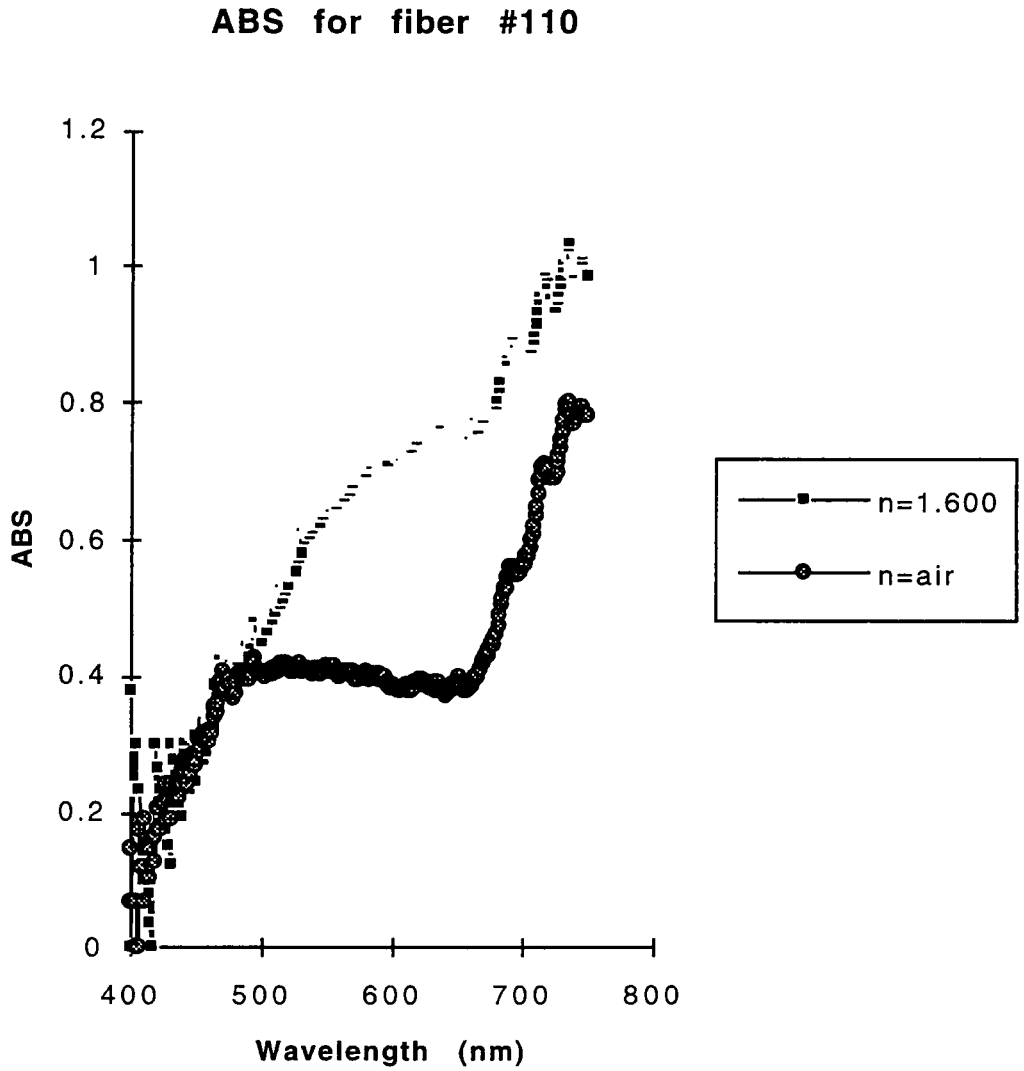

Figure IV.2. ABS for n_S=1.600 A. Data was normalized at 650 nm. This sample shows a very broad absorption peak, centered at about 490 nm, and shows the complete disappearance of the absorption with the applied n=1.6 liquid. Sample was annealed at room temperature for approximately an hour.

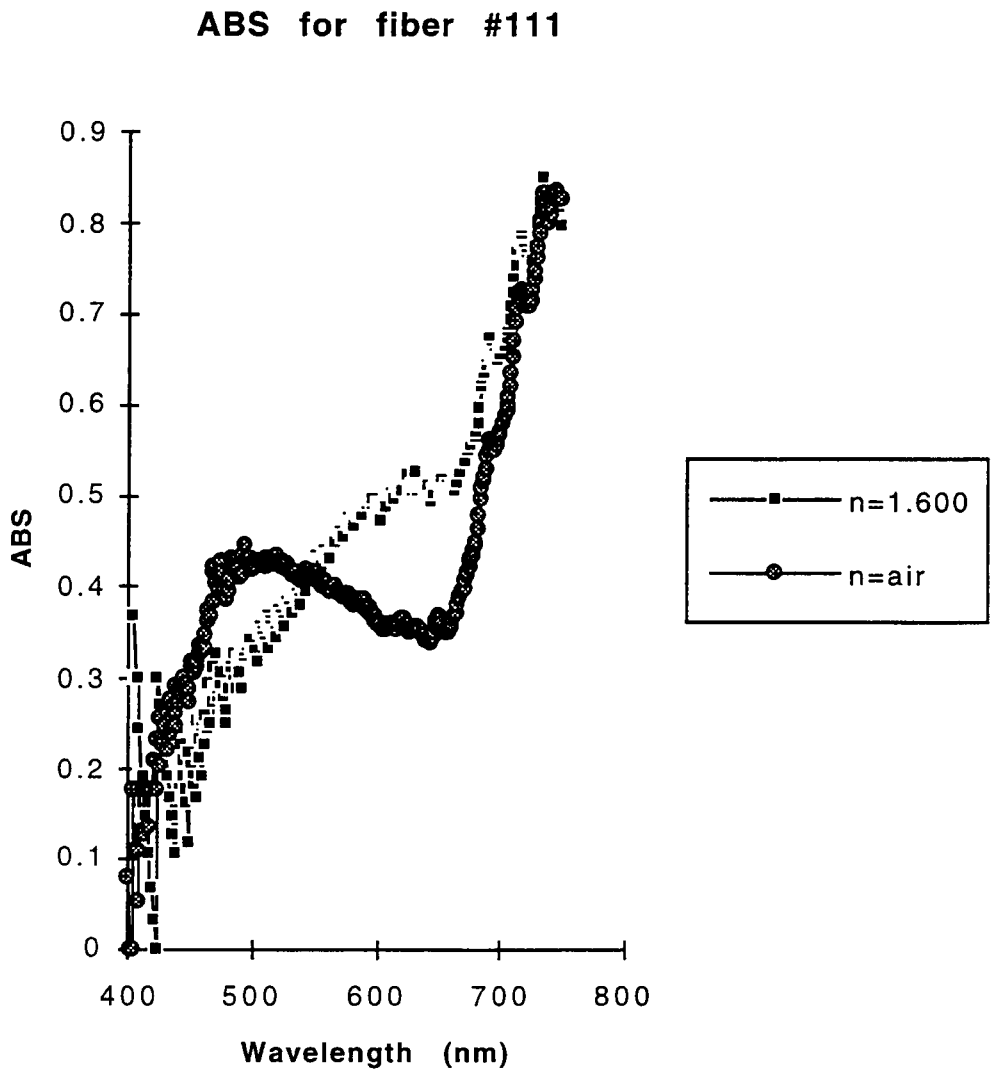

Figure IV.3. ABS for n_S=1.600 B. Data was normalized at 655 nm. This sample shows a very broad absorption peak, centered at about 490 nm, and shows the complete disappearance of the absorption with the applied n=1.6 liquid. Sample was annealed at room temperature for approximately an hour.

Figure IV.4. shows a slight absorption peak at approximately 500 nm that is reduced but not shifted with the application of the n=1.300 optical liquid. All three of these samples were annealed in room temperature for approximately an hour.

The following **Figures IV.5.** through **Figure IV.12.** show the absorbance shift results for samples that exhibited the expected behavior, as determined in Chapter II. Since we are interested in the amount of shift in the absorption peak we have not used a consistent wavelength at which we normalized the data. In some cases, wavelengths beyond 800 nm seemed to present a better point of normalization; whereas some datasets did not include wavelengths beyond 800 nm, and a different point was used. Obviously, an inconsistent normalization point would not affect the measured amount of resonant peak shift.

The room temperature annealed samples have n=air peak positions at a mean wavelength of 575 nm. This corresponds to the theory with a value of R at the center of the distribution of approximately R=0.33. The high temperature annealed samples have n=air peak positions at a mean value of 535 nm. The approximate value of R here is R=0.67.

We note here that almost every high temperature annealed sample that showed a good absorption peak with n=air also showed the disappearance of the absorption when an optical liquid of index greater than the fiber core index (n_C=1.457) was applied. We found several good peak shifts for low or room temperature annealed samples when these high index liquids were applied. Our conclusion is that the gaps between the islands, which increase with higher annealing temperature, allow two important effects to occur.

When these gaps are filled with an optical liquid having an index higher than the core, Snell's law dictates that TIR may no longer occur for the angles that are utilized in our samples. Therefore, the evanescent field no longer exists, and a transmitted component that exits the fiber through the gaps between the islands is created. This greatly reduces the amount of light that is transmitted to the detector and thus reduces our ability to measure the absorption.

The second effect of the gaps between the islands is the possibility of the applied high index liquid forcing a mode change in the fiber[63].

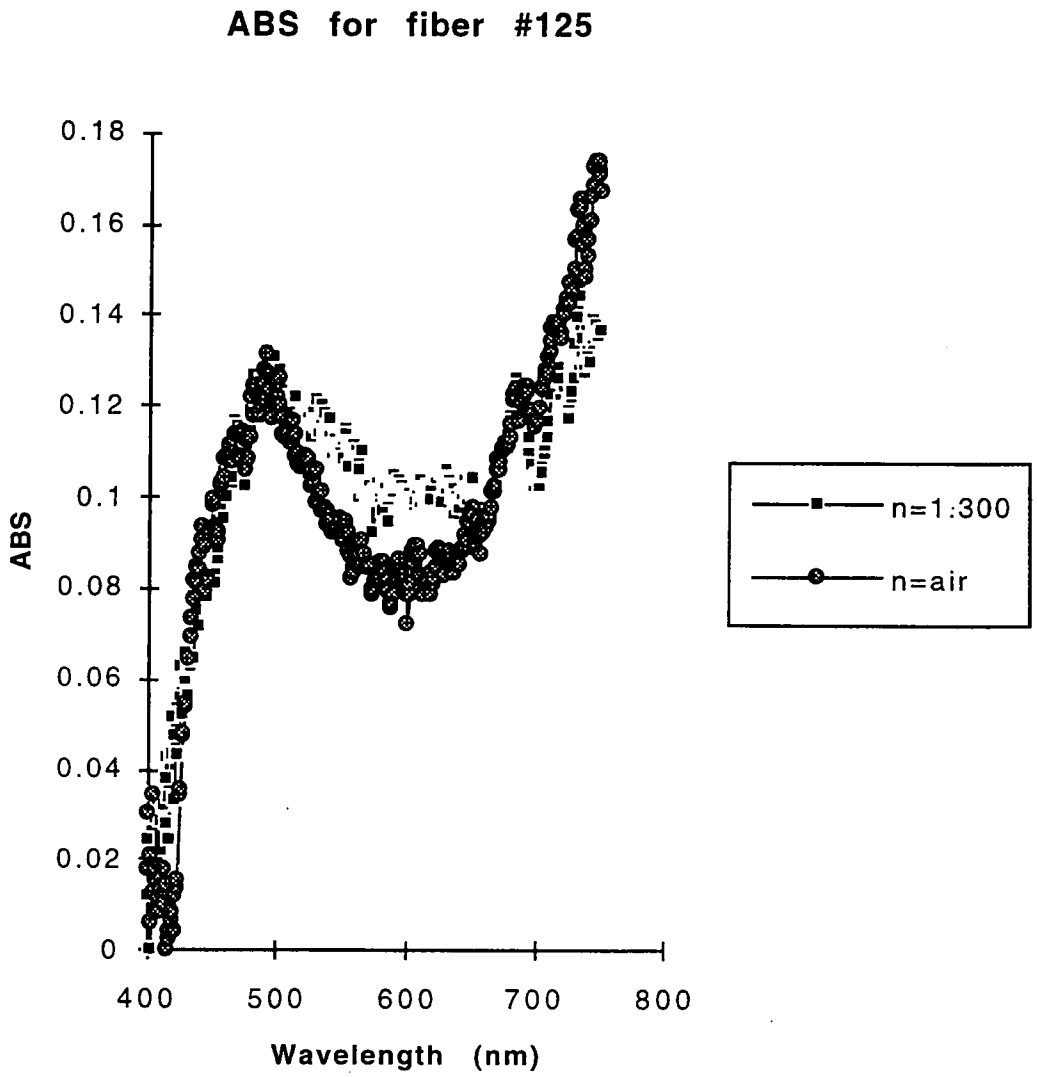

Figure IV.4. ABS for n_S=1.300. Data was normalized at 600 nm. This sample shows a very broad absorption peak, centered at about 500 nm, and shows a completely unshifted reduction of the absorption with the applied n=1.3 liquid. Sample was annealed at room temperature for approximately an hour.

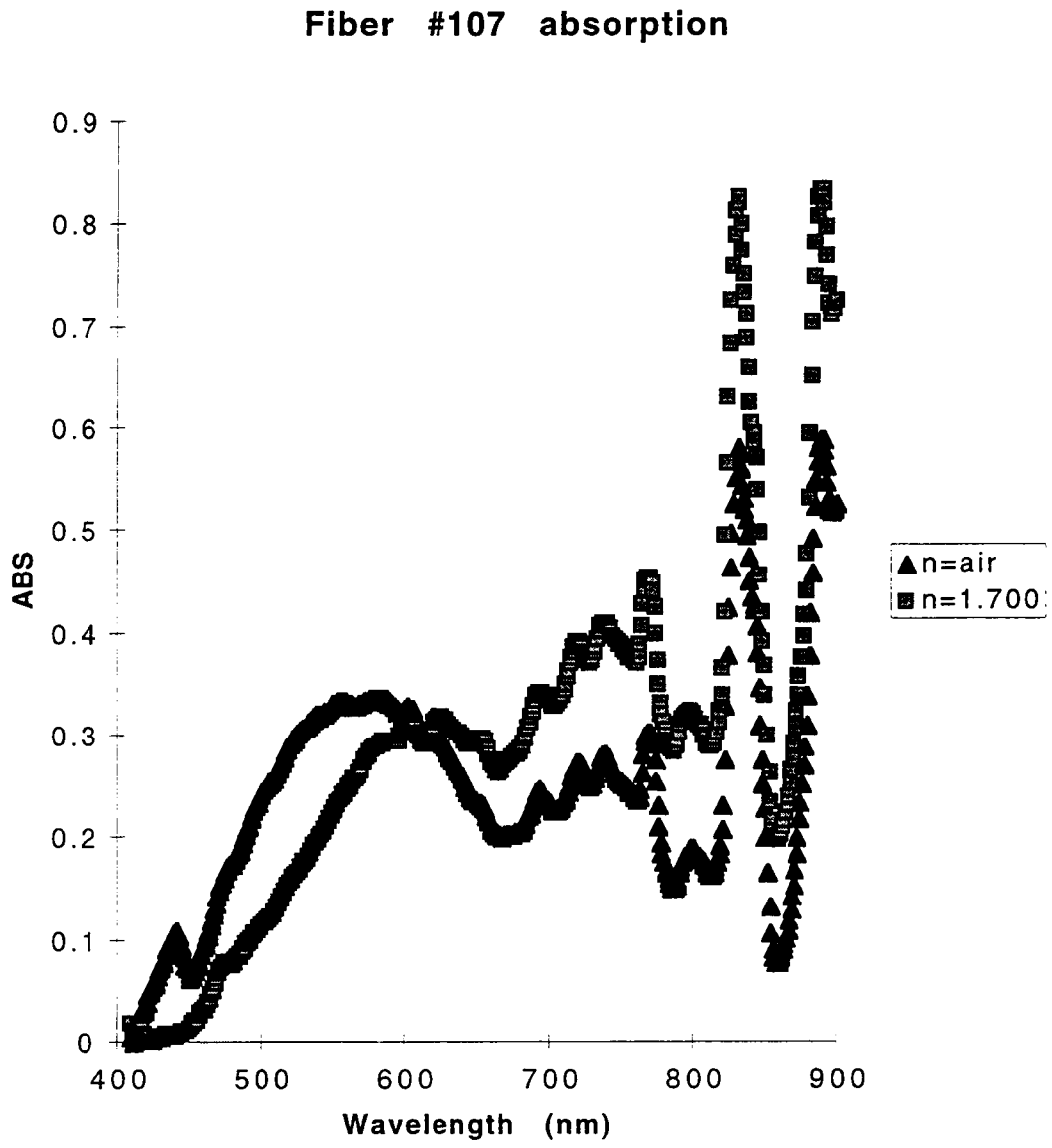

Figure IV.5. Calculated ABS for n_S=1.700 A. This sample shows a shift of 25 nm, from 570 nm to 595 nm with a n=1.7 liquid. The n=1.7 ABS is very weak. Data was normalized at 660 nm. Sample was annealed at room temperature for approximately 2 hours.

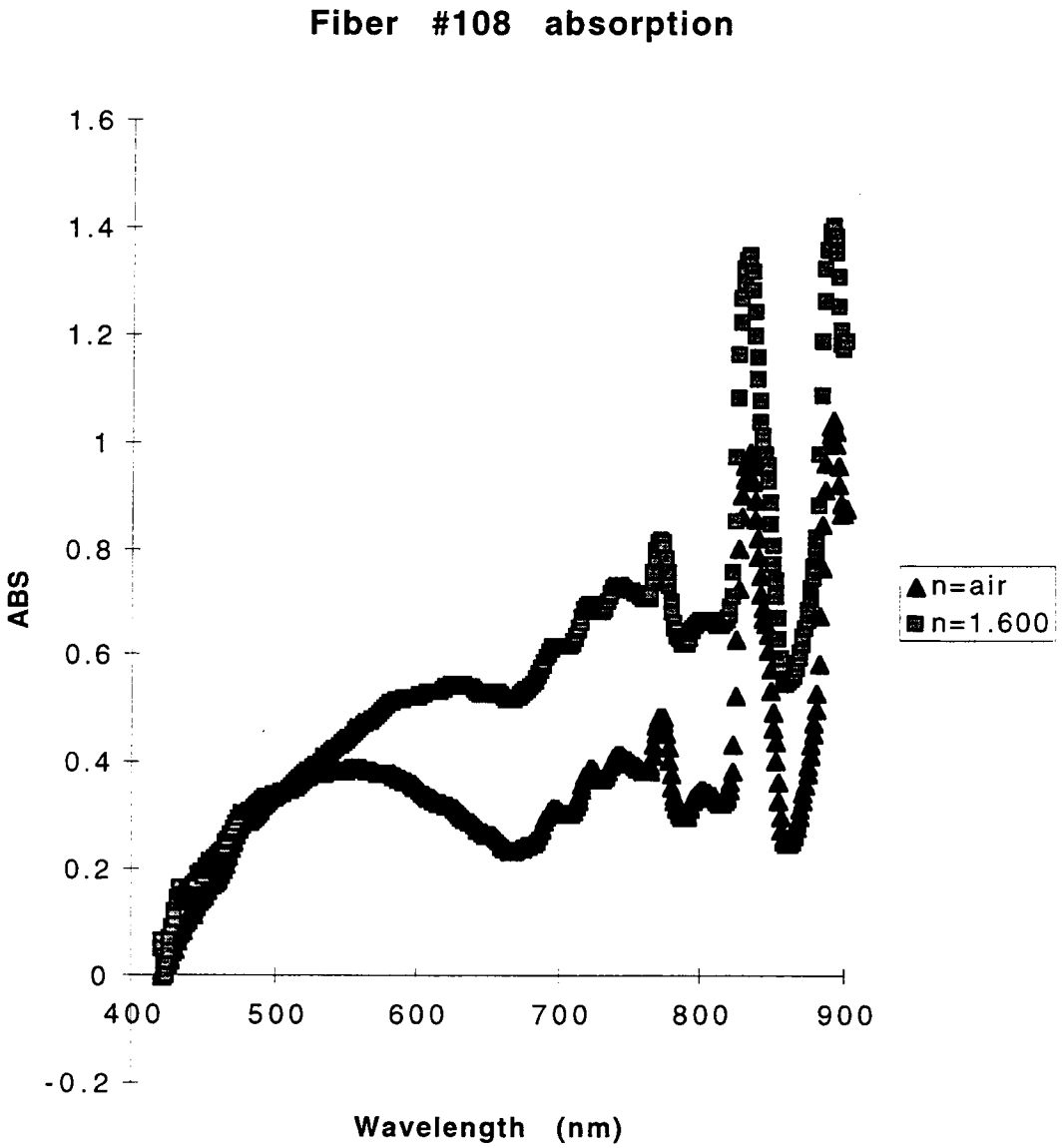

Figure IV.6. Calculated ABS for n_S=1.600 A. This sample shows a very broad absorption peak, centered at about 550 nm, and a shift of the absorption of almost 70 nm with the applied n=1.6 liquid. The n=1.6 peak is very weak. Data was normalized at 660 nm. Sample was annealed at room temperature for approximately an hour.

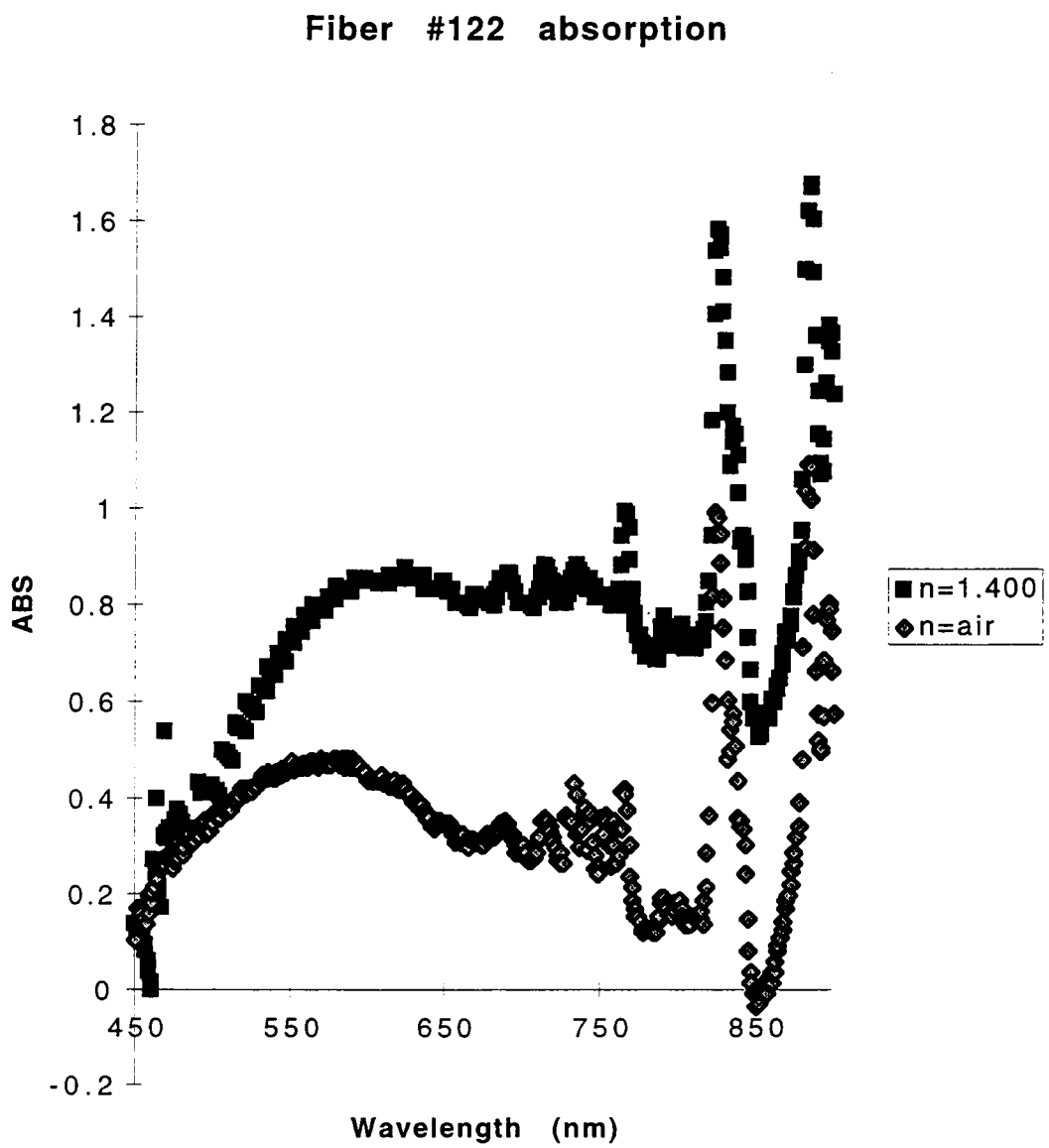

Figure IV.7. Calculated ABS for n_S=1.400. The data was normalized at 850 nm and was not smoothed. Room temperature anneal was used, with a 24 hour duration. An absorption peak shift of approximately 45 nm, from 580 nm to 625 nm, occurred with the application of the n=1.400 liquid.

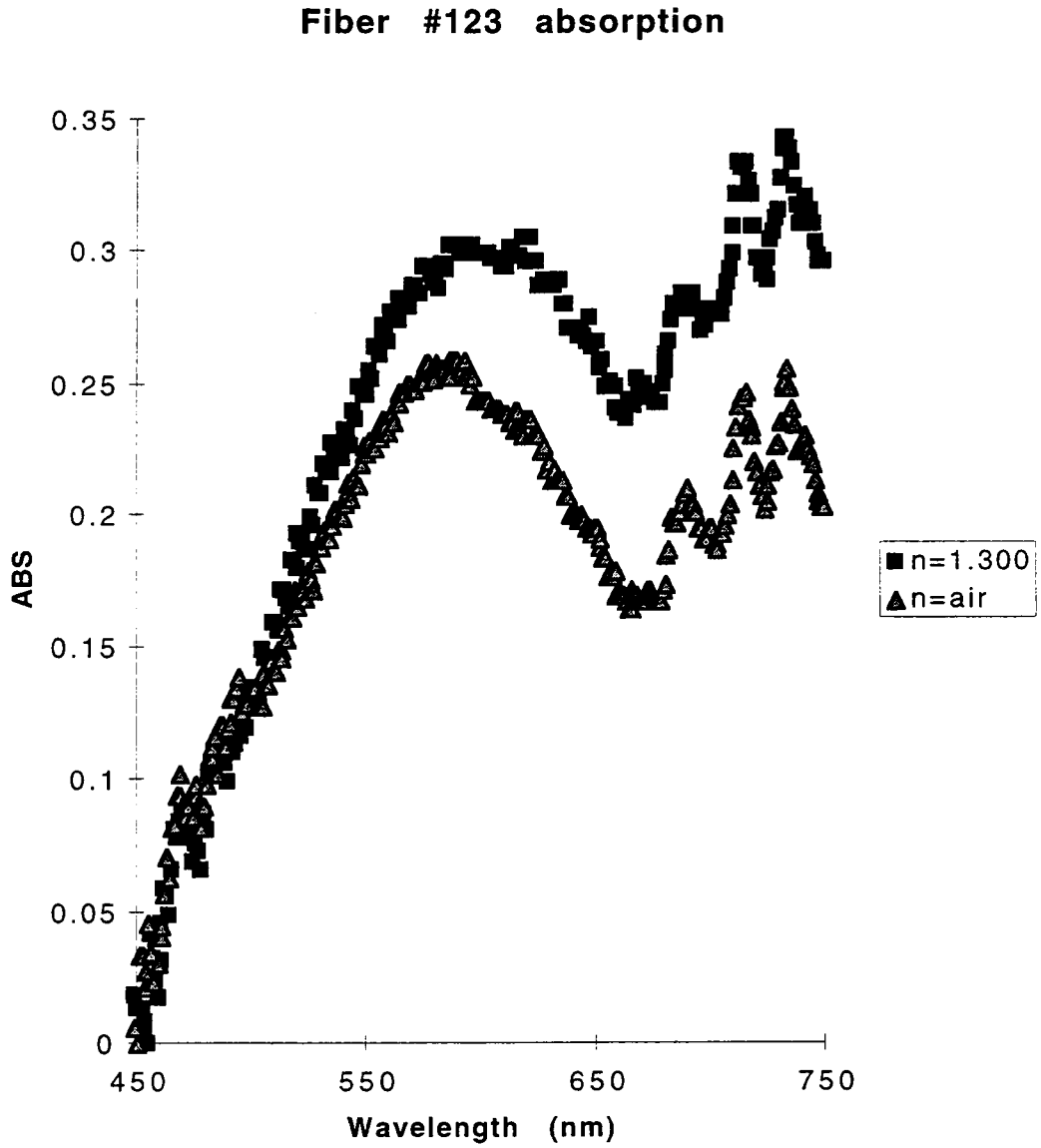

Figure IV.8. Calculated ABS for n_S=1.300 A. The data was normalized at 650 nm and smoothed using a moving average with a width of 10 nm. Room temperature anneal was used, with a 24 hour duration. An absorption peak shift of approximately 10 nm, from 580 nm to 590 nm, occurred with the application of the n=1.300 liquid.

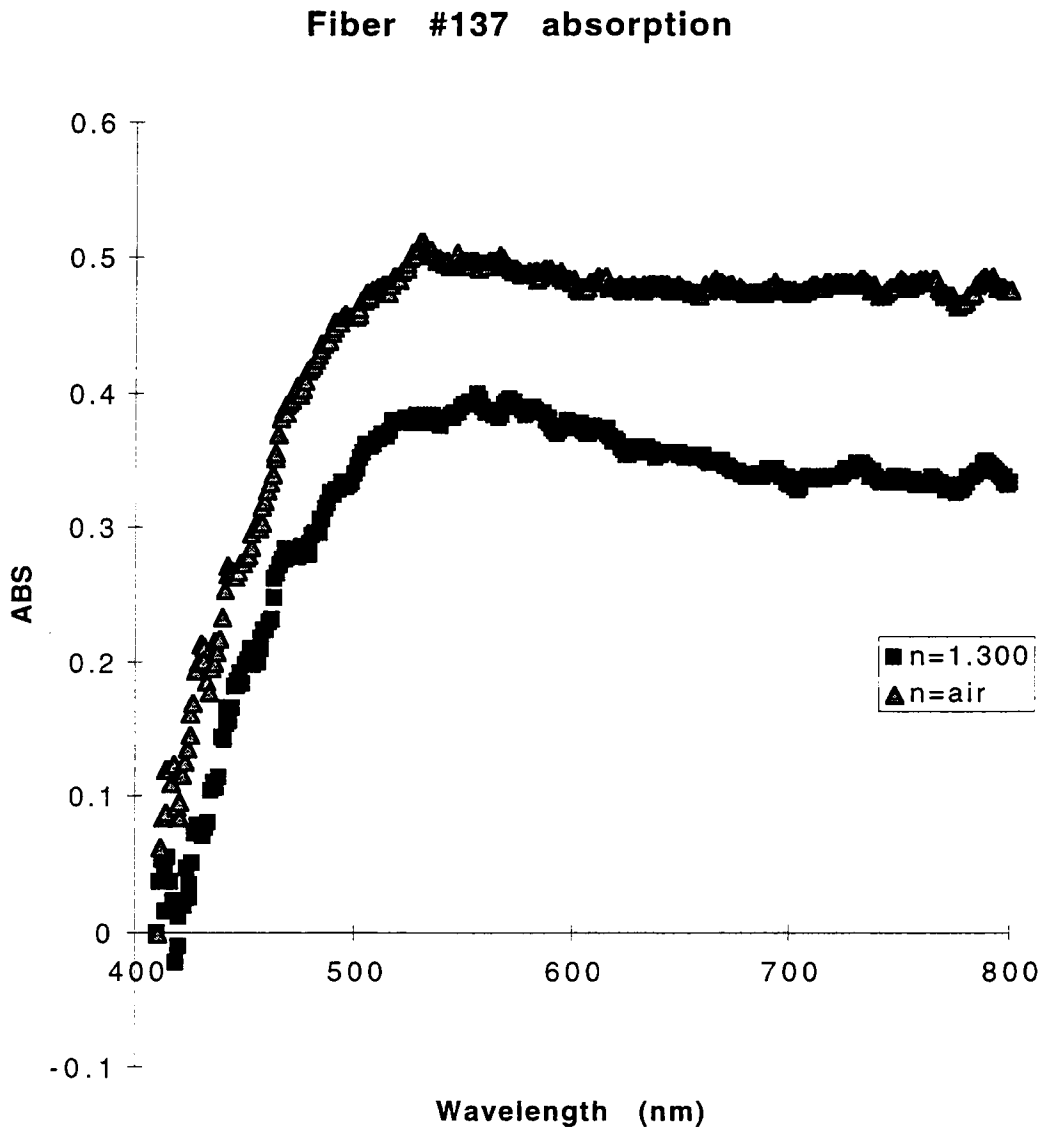

Figure IV.9. Calculated ABS for n_S=1.300 B. The data was not normalized but was smoothed using a moving average with a width of 10 nm. Annealing temperature of 600°C was used, with a 4 minute duration. An absorption peak shift of approximately 30 nm, from 530 nm to 560 nm, upon applying the n=1.300 liquid, is shown.

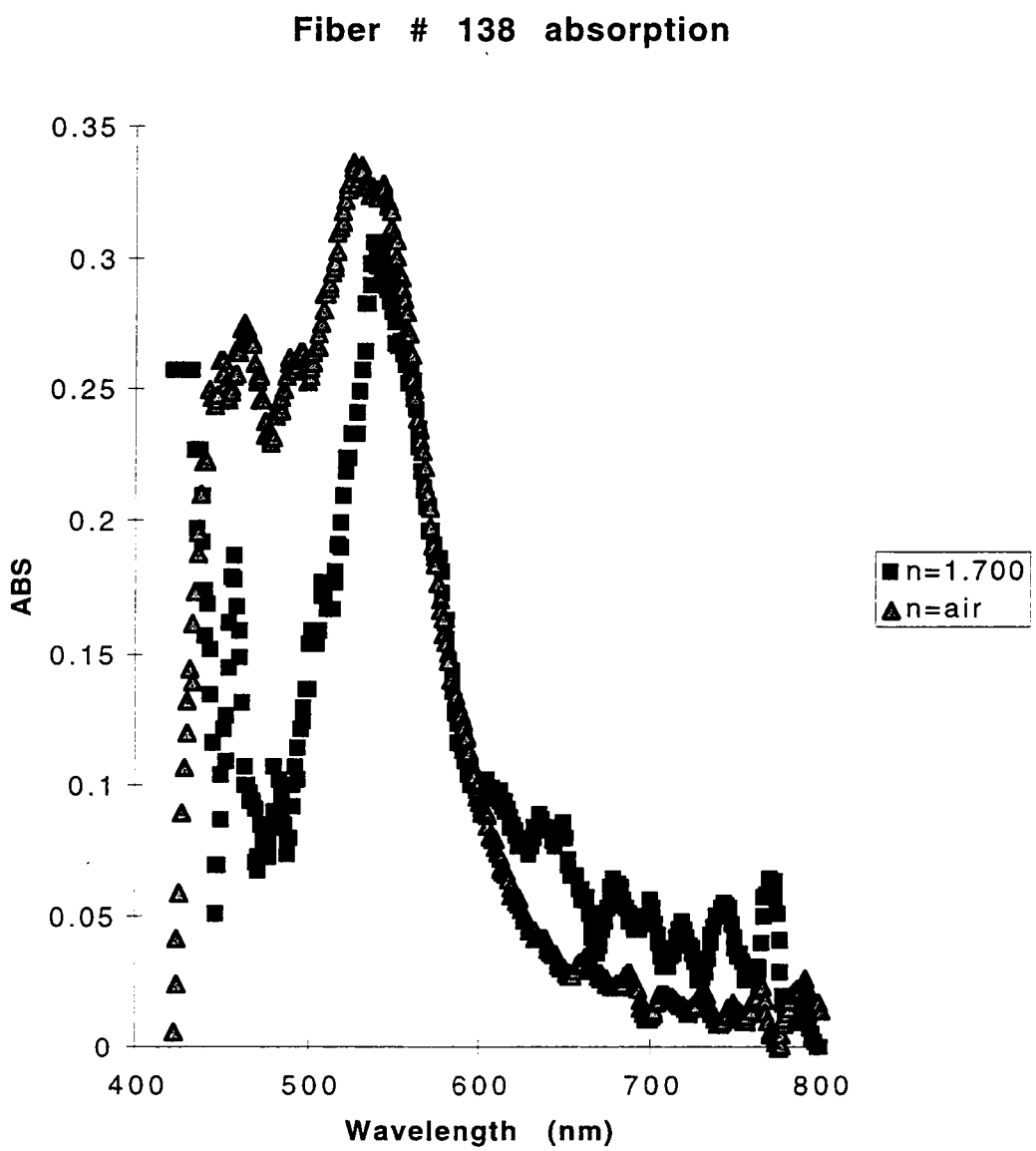

Figure IV.10. Calculated ABS for n_S=1.700 B. The data was normalized at 775 nm and smoothed using a moving average with a width of 10 nm. Annealing temperature of 830°C was used, with a 4 minute duration. An absorption peak shift of approximately 15 nm, from 525 n m to 540 nm, upon applying the n=1.700 liquid, is evident.

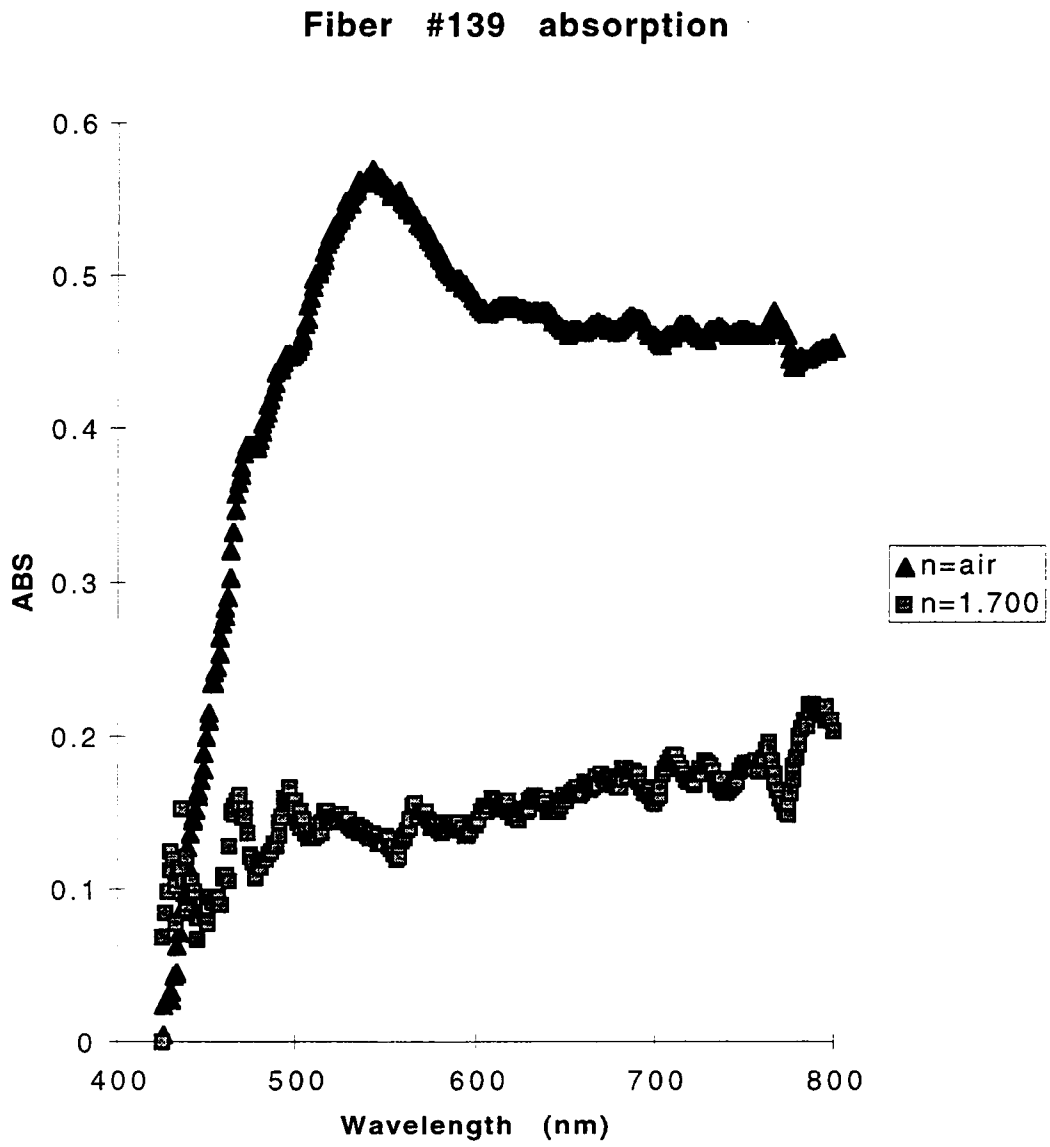

Figure IV.11. Calculated ABS for n_S=1.700 C. The data was normalized at 775 nm and smoothed using a moving average with a width of 10 nm. Annealing temperature of 700°C was used, with a 4 minute duration. Absorption is evidently gone with the application of the n=1.700 liquid.

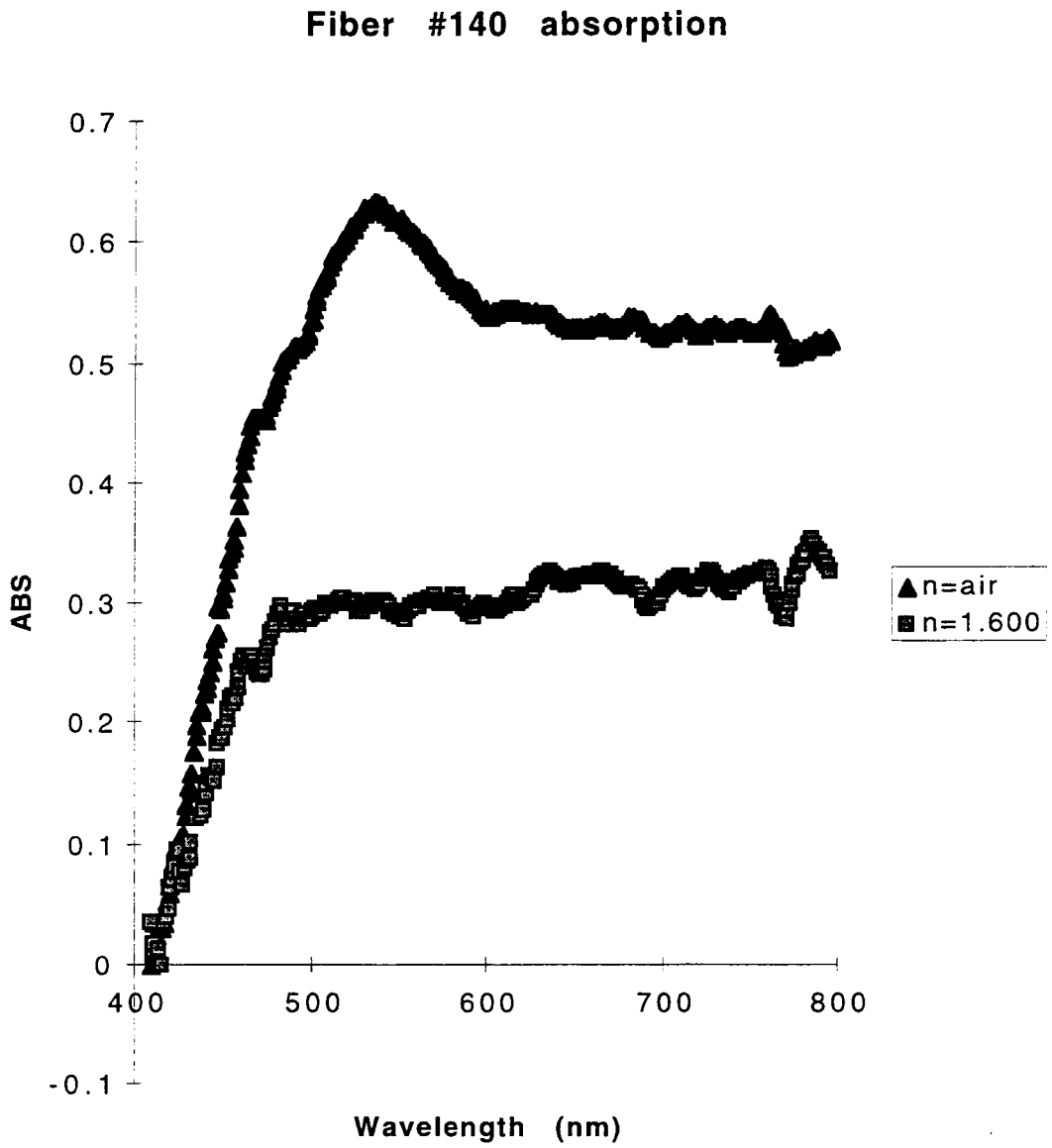

Figure IV.12. Calculated ABS for n_S=1.600 B. The data was normalized at 775 nm and smoothed using a moving average with a width of 10 nm. Annealing temperature of 700°C was used, with a 4 minute duration. Absorption is evidently gone with the application of the n=1.600 liquid. Fiber samples #139 and #140 were prepared adjacent to each other, at the same time.

A multimode fiber can support a finite number of propagation modes, specified by a pair of integers l and m. For propagation on the z axis, these modes are are the well known transverse electric (TE, E_Z=0) and magnetic (TM, B_Z=0) modes, and the so-called skewed ray modes (HE and HM). Skewed ray modes do not have light rays that pass through the center axis of the fiber.

The scalar wave equation for either E or B in the cylindrical waveguide is

$$\frac{d^2\psi}{dr^2}+\frac{1}{r^2}\frac{d\psi}{dr}+\frac{1}{r^2}\frac{d^2\psi}{d\phi^2}+\left(n^2k^2-\beta^2\right)\psi=0,$$

where n is the index of the fiber core, k is the in-vacuum propagation constant for the light, r and ϕ are the cylindrical coordinates, and β is the allowable propagation constants for the modes, with $n_2k<\beta<nk$, n_2 being the cladding index.

Separating variables gives the form of the solutions for ψ:

$$\psi=E(r)\left\{\frac{\cos(l\phi)}{\sin(l\phi)}e^{(\omega t-\beta z)}\right\}$$

Upon inserting this form into scalar wave equation, the equation for the electic field is, as expected, Bessel's equation. Matching the correct boundary conditions at the core/cladding interface, r=0 and infinity gives the electric field in the core as proportional to Bessel's functions J_l, and inside the cladding involving the modified Bessel's functions K_l:

$$E\left(r\right)=G\,J_l\left(UR\right),\ \text{in the core}$$

and

$$E\left(r\right)=G\,J_l\left(U\right)\frac{K_l\left(WR\right)}{K_l\left(W\right)},\ \text{in the cladding,}$$

where G is a constant that determines the amplitude of E(r), R=r/a, a being the radius of the core, and U and W are the eigenvalues of a given mode for the core and cladding such that:

$$U = a\sqrt{\left(n^2 k^2 - \beta^2\right)},$$

and

$$W = a\sqrt{\left(\beta^2 - n_2^2 k^2\right)}.$$

The number of modes M is found to be approximately $M=V^2/2$, where V is called the normalized frequency and

$$V = \sqrt{\left(U^2 + W^2\right)} = \frac{2\pi}{\lambda} aNA,$$

NA being the numerical aperature of the fiber with

$$NA = \sqrt{n^2 - n_2^2}.$$

Figure IV.13. graphs the change in the number of modes. Since we are changing n_2, we are obviously changing the number of modes and the eigenmode U and W values. When n_2 approaches n, the number of modes approaches zero. Since we are using step-index, multimode fiber, this mode change can occur, and the resonance peak may be reduced dramatically enough to become unmeasurable.

We believe that both of these effects are occurring when high temperature samples have high index liquids applied, and do not allow us to measure the peak shift. When low temperature annealed samples are used, we have seen less impact of these effects, assume this is because the islands are separated by smaller gaps, and have measured peak shifts. However, we were unable to find a sample that had a resonable peak shift for n=1.500. We have, therefore, used these low temperature annealed sample results for the values in **Table IV.1.**, shown below, which tabulates our resonance peak shift results.

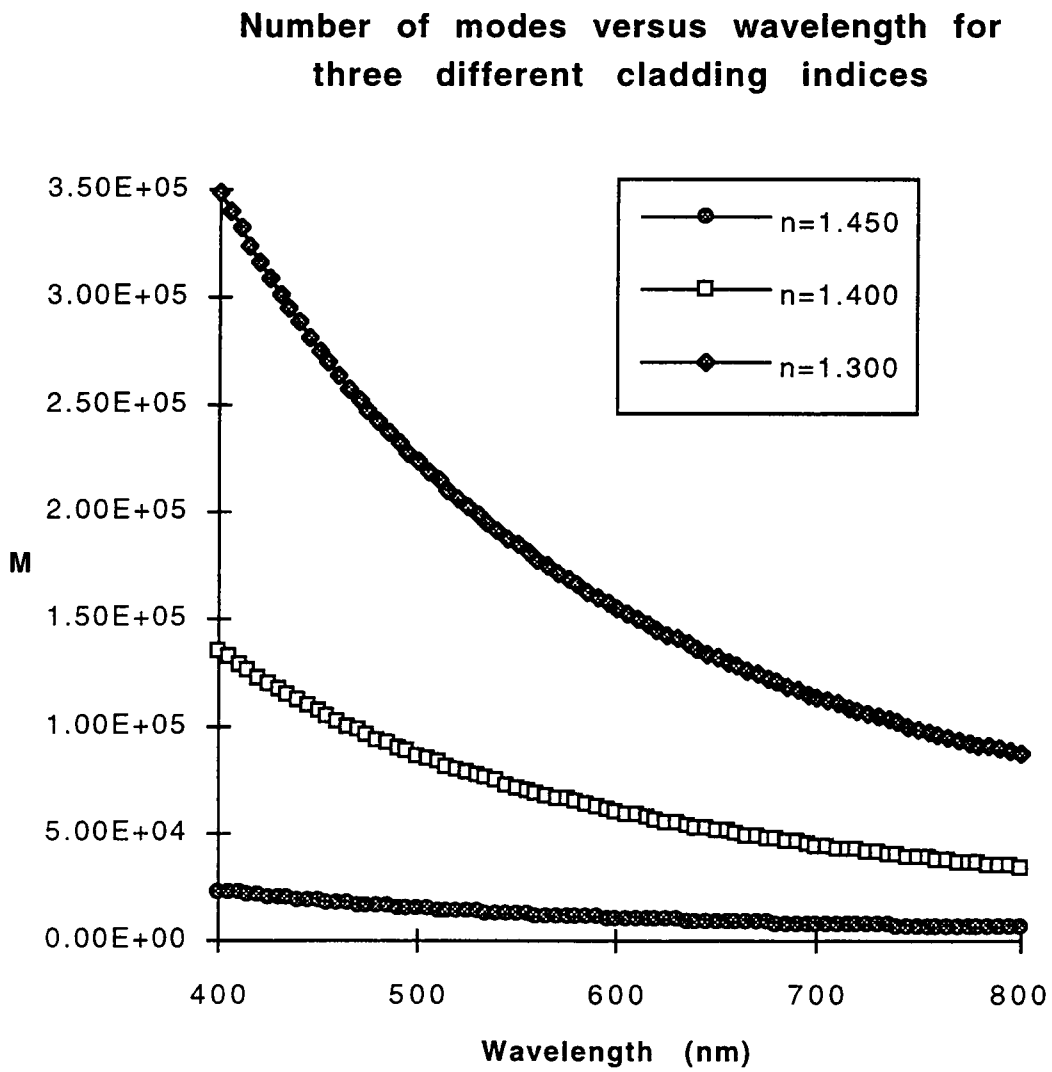

Figure IV.13. Changes in the number of propagation modes. The number of modes (M) reduces dramatically as the cladding index approaches the core index. The number of modes will be zero when the cladding index is equal to the core index.

Table IV.1. Shift changes with an applied optical liquid. The peak shift is the wavelength for the resonance peak maximum with the liquid minus the wavelength for the maximum in air (a=room temperature annealing, b=high temperature annealing)

index applied (n_{ap})	peak shift (nm)
1.3(a)	10
1.3 (b)	30
1.4(a)	45
1.5	n a
1.6(a)	70
1.7(a)	25
1.7(b)	15

We have made every attempt to achieve reproducible data. However, even with two fibers that were prepared, evaporated, annealed and tested identically, differences in the measured peak shift were noticed. This inability to find reproducibility was also found in our slide-only tests, to be discussed later in this chapter. The primary cause of not attaining reproduceability should be the creation of different R distributions on samples

B. Absorption and shift results for non-rotated samples

It was suggested that more reproducible data could be produced if 2 or 3 samples were completely still and mounted very close to each other on the surface of a fused silica slide during evaporation and testing. This also let us test the absorption and peak shift characteristics of the islands on the slides, which is a valuable tool to make sure that our sample preparation steps were producing the islands on the fiber samples that are required.

Here, we are assuming that the mobility of gold on the surface of the quartz slide is approximately the same as the mobility on the silica core of the fiber. This would allow for the creation of the same distribution of island sizes and shapes on both the fiber and slide surfaces.

The steps used to testing the slides, and the results that we obtained, are given in the next section. We restrict ourselves here with the absorbance data obtained for the fibers.

Approximately 7.5 cm of the middle length of the non-rotated fiber samples was etched in 48% HF for 8 minutes. This allows for approximately the same amount of decladded fiber surface area to come into contact with the islands, as in the case of our rotated samples. All other sample preparation steps were the same as described above, but these samples were not rotated during evaporation. The samples were attached on a cleaned slide by two drops of a gel-epoxy. This epoxy was chosen for its low viscosity, thus removing the possibility of surface tension attracting the epoxy towards, and possibly covering, the etched area where the islands would be deposited.

Initial attempts at using high temperature annealing led to the scorching and vaporization of the epoxy. This caused fibers to drop off the slides. We reduced the annealing temperature to 300^{o}C, to remove this unwelcome effect. We also attempted to hold the fibers to the slides with wire, and use the high temperature annealing. This process did not hold the fiber samples securely, and led to several samples dropping off in the oven and being heated for two long of a period.

We have tried this procedure and have found preliminary results. In **Figure IV.14.**, we have a n=air absorption peak centered at approximately 620 nm, a center point which was not seen in any other sample. The application of the n=1.7 index resulted in a shift of the resonance to 665 nm, a difference of 45 nm, a shift amout that agrees with the theory for islands that have an approximate ratio of R=0.45.

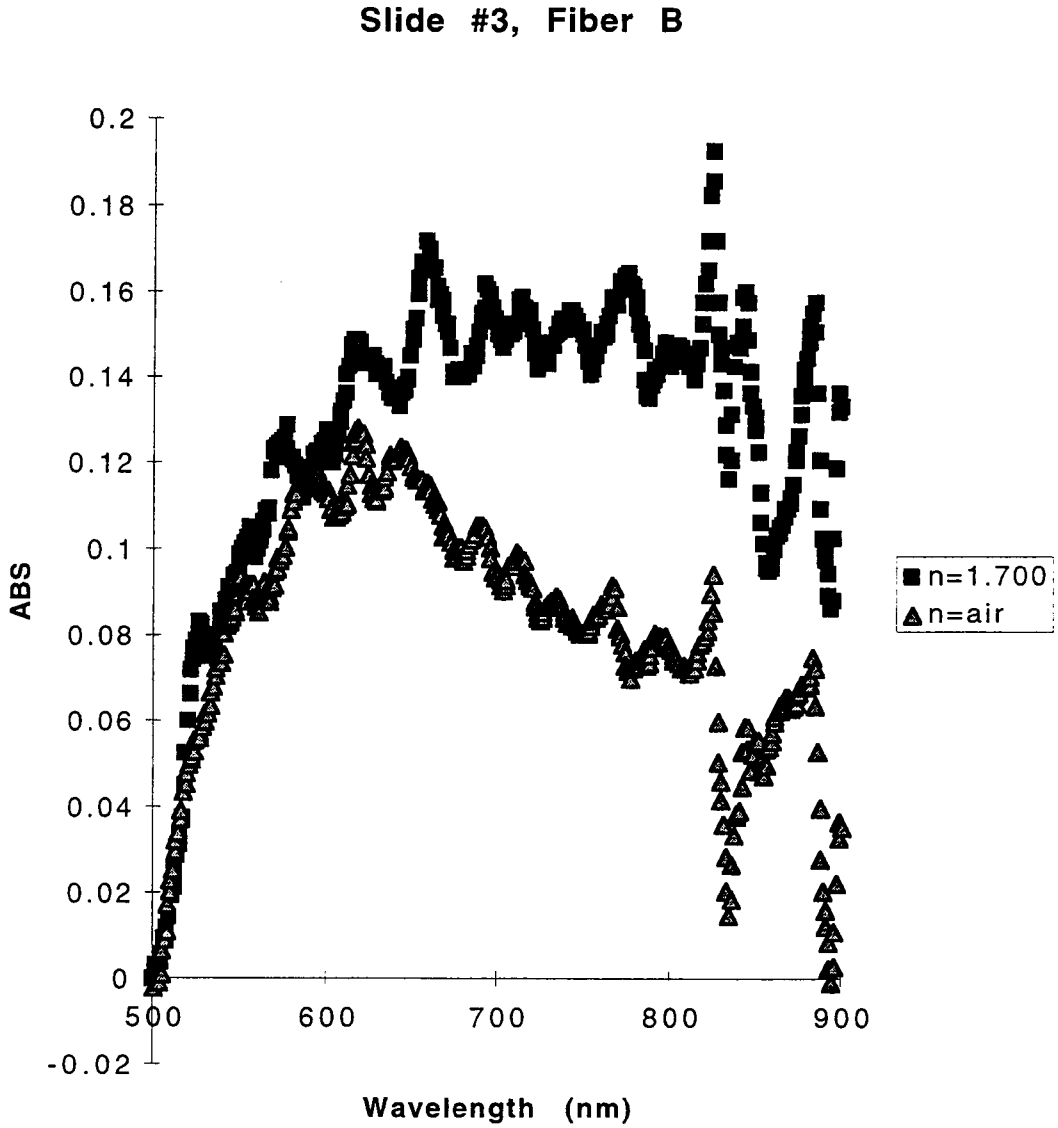

Figure IV.14. Calculated ABS for n_S=1.700 D. The data was normalized at 895 nm, and smoothed with a width of 10 nm. Annealed at 275 °C for 4 minutes. An absorption peak for n=air exists at 610 nm, and at 655 nm for the n=1.700 data, giving a shift of 45 nm.

C. Absorption and shift results for large-core samples

Additional rotated and non-rotated samples were made from a large-core optical fiber[64]. The etching time was increased to 2 hours in order to find good absorption data, because of the increased cladding thickness on this fiber. A larger SMA connector[65] was used with these samples. Much more signal was available for data collection, and the surface area of the decladded area was increased by a factor of five. Most of these samples were tested with a 5 nm increment between sequential wavelength positions. The following **Figure IV.15.** and **Figure IV.16.** show the ABS data calculations for the large-core samples. **Figure IV.16.** shows data for a non-silica cladded, large-core fiber[66], which used an acetone bath to remove the cladding.

D. Slide results

As stated above, we performed evaporations of gold onto fiber samples, combination fiber attached to slide samples, and slide only samples. In this section we provide the results for the ABS data for the slide samples, in order to provide a comparison to the fiber sample ABS results.

Each quartz slide[67] sample was cleaned using the above mentioned fiber cleaning method. Slide samples were mounted just beside fiber samples during evaporation. All samples had 40Å of gold deposited and were annealed at 800°C for 4 minutes. Testing of the slide samples was performed on a dual monochromator, scanning spectrophotometer. The samples to be tested were positioned for normal incidence on a vertical mounting system in the sample section of the spectrophotometer. A clean quartz slide was placed in the reference section.

A scan of wavelengths within the region of interest, approximately 400 nm to 800 nm, was performed, and the ABS data was graphed on the spectrophotometer's chart recorder.

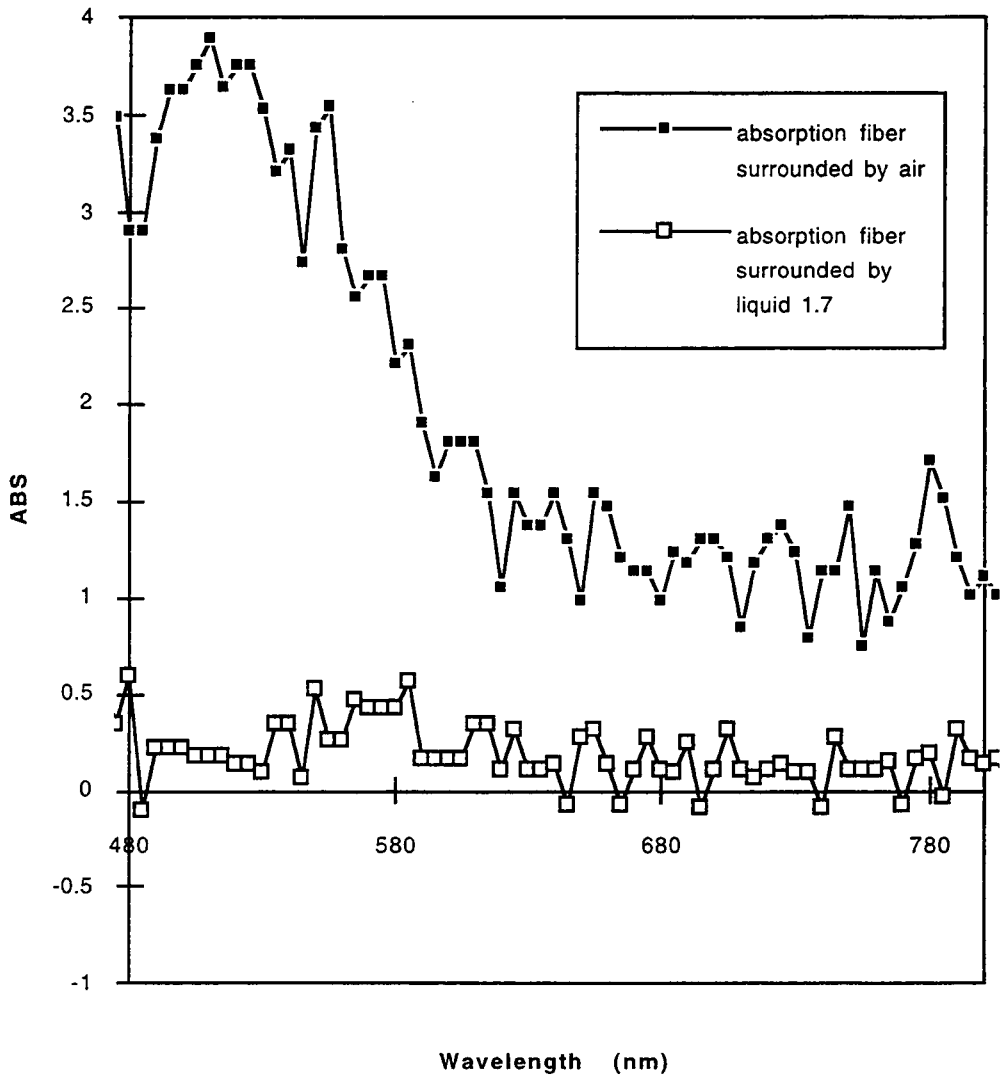

Figure IV.15. Calculated ABS for n_S=1.700 E. Sample was annealed at 800°C for 4 minutes. The data was not normalized, or smoothed; data was taken every 5 nm. The absorption peak centered at approximately 500 nm is evidently removed with the application of the n=1.700 liquid.

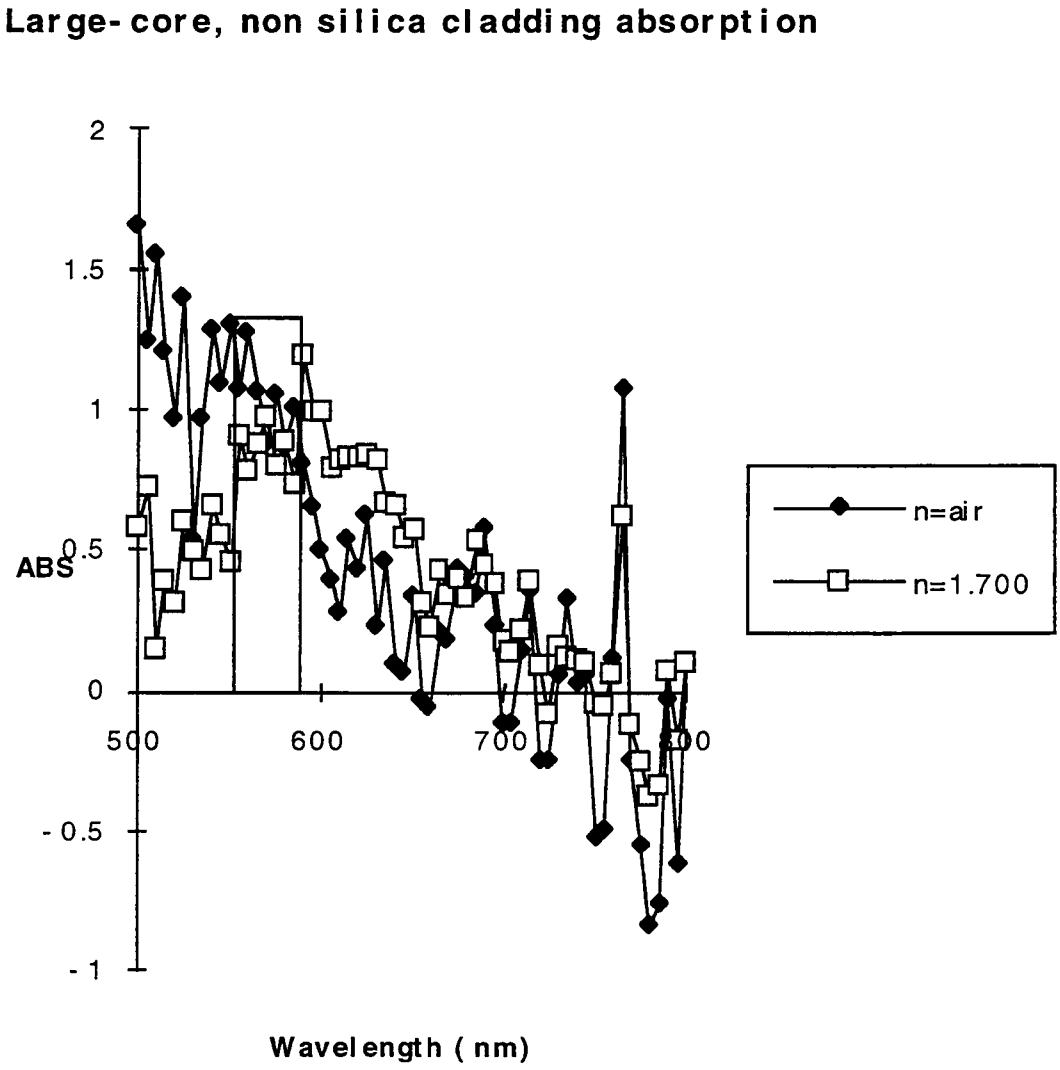

Figure IV.16. Calculated ABS for n_S=1.700 F. Sample was annealed at 800°C for 4 minutes. The data was normalized at 775 nm and smoothed with a width of 10 nm; data was taken every 5 nm. High absorption for the region below 550 nm for the n=air data is caused by the smoothing function acting on rapidly changing data; the absorption peak is assumed to occur at 550 nm. A shift of approximately 35 nm occurs with the application of the n=1.700 liquid.

The paper chart recordings were scanned into Photoshop PICT files and were then digitized using FlexiTrace. Below are **Figure IV.17.** through **Figure IV.21.**, which show comparisons between heated samples with and without an optical fluid covering the islands. Comparing **Figure IV.18.** and **Figure IV.19.**, which both had the n=1.35 liquid applied, very different shift amounts occured. These samples were created during separate evaporations and were tested within two hours of removal from the evaporation chamber. We attribute the different shift amounts to the creation of two different R distributions on these samples.

F. Extra cladding results

We have made initial investigations of the effect of adding an extra evaporation layer of MgF_2 on top of the annealed gold islands. MgF_2 has an index or refraction that is less than the index of the core, and will confine the light inside the fiber. We assume that this layer will act as a cladding layer that will completely surround the islands, and should allow for absorption shift measurements for n=1.500 and higher liquids if the correct amount of MgF_2 is deposited. **Figure IV.22.** shows the results for a large core fiber that had 60 nm of MgF_2 applied on top of high temperature annealed islands, while **Figure IV.23.** shows data for 40 nm of MgF_2. The inconclusive shift result in **Figure IV.22.** could be caused by the moving average acting on rapidly changing data. **Figure IV.23.** demonstrates that approximately 40 nm of MgF_2 forms an extra cladding layer that both disallows mode changes at the core to cladding interface, while allowing the surrounding medium to be tested.

We have also made preliminary investigations of the effect of adding an extra evaporation layer of gold on top of the annealed gold islands. We assume that this extra unheated gold will almost completely surround the islands, and should allow for absorption shift measurements

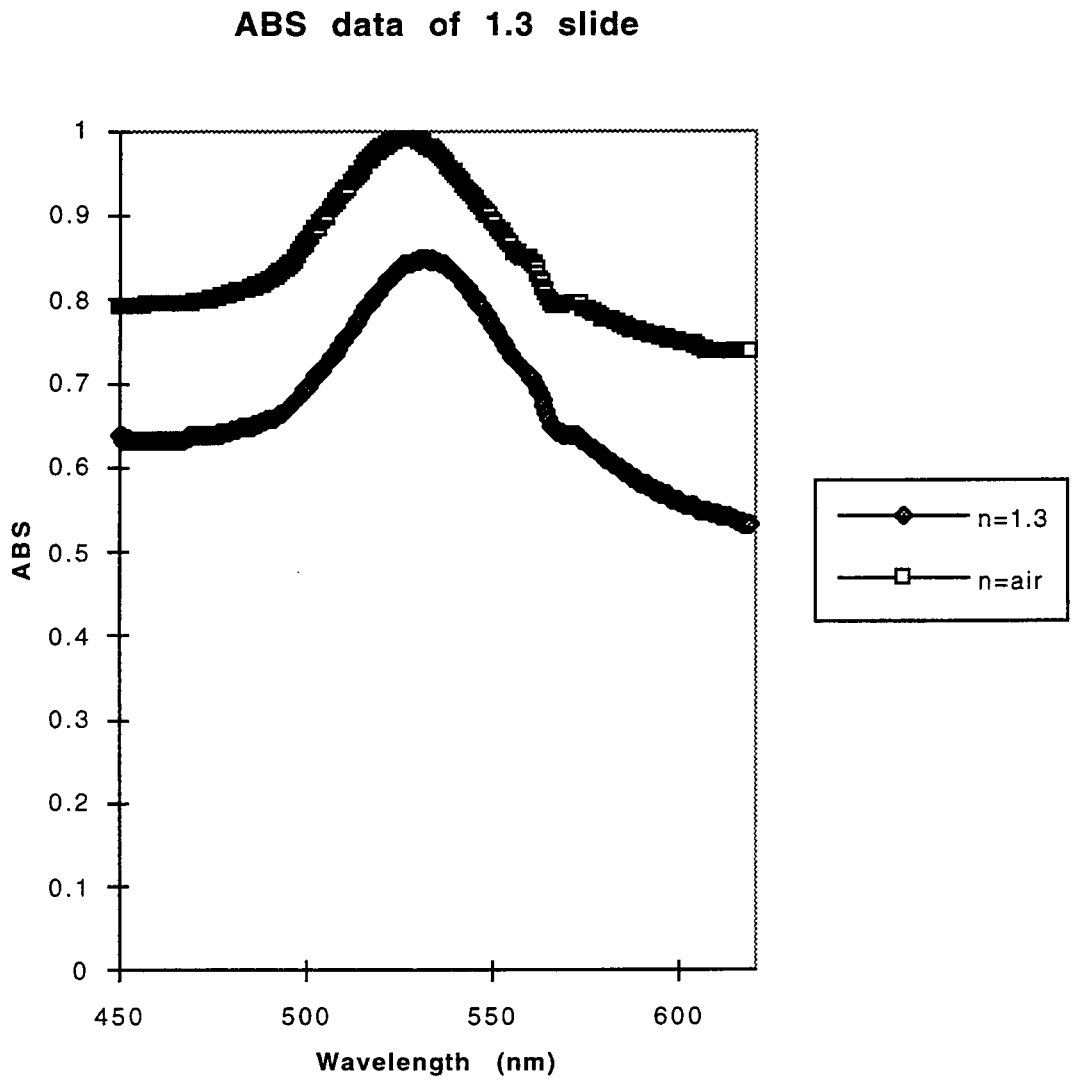

Figure IV.17. Graph of ABS data for n=1.3 slide. Sample was annealed at 800°C for 4 minutes. A shift of 7 nm is created by the liquid.

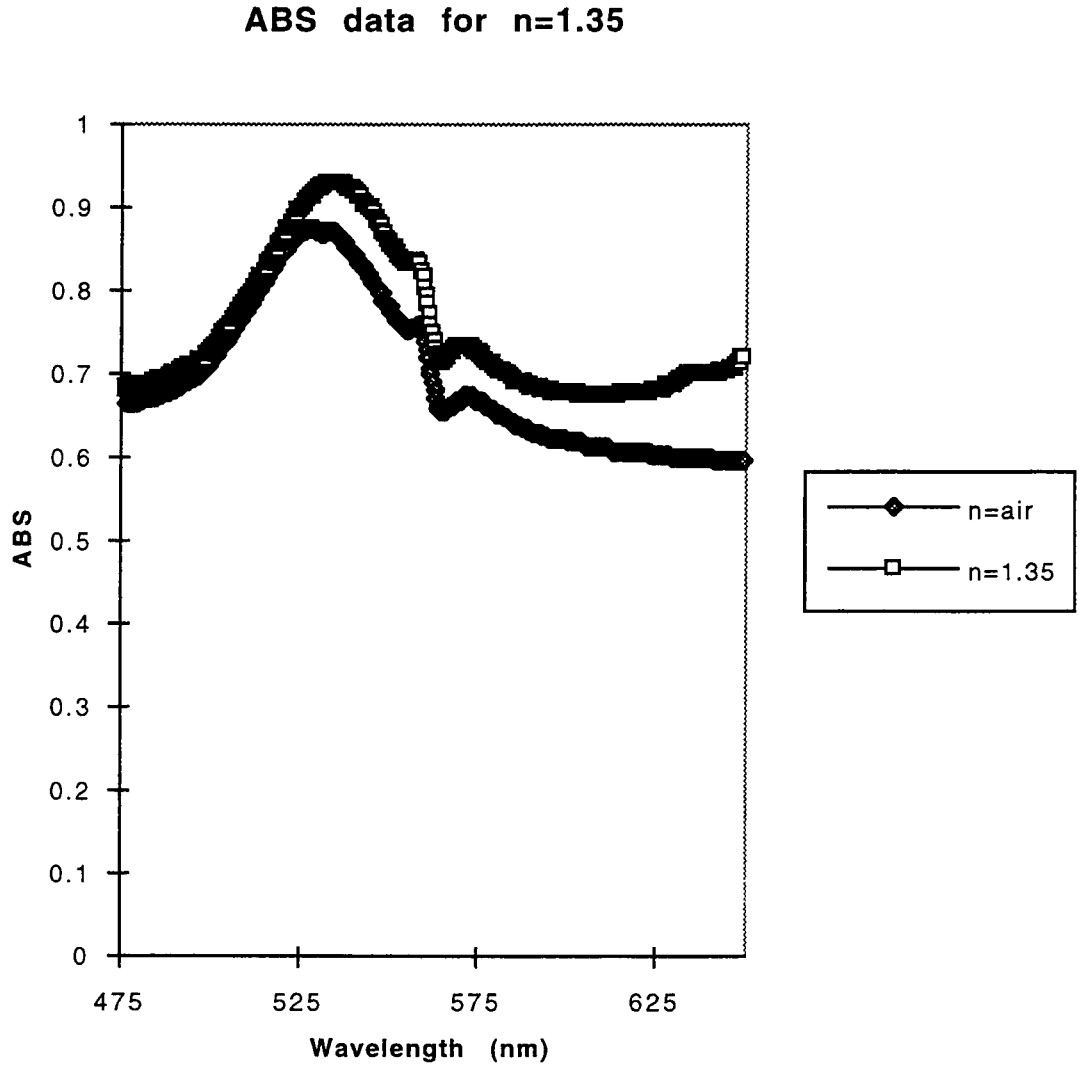

Figure IV.18. Graph of ABS data for n=1.35 slide A. A shift of 9 nm is created by the liquid.

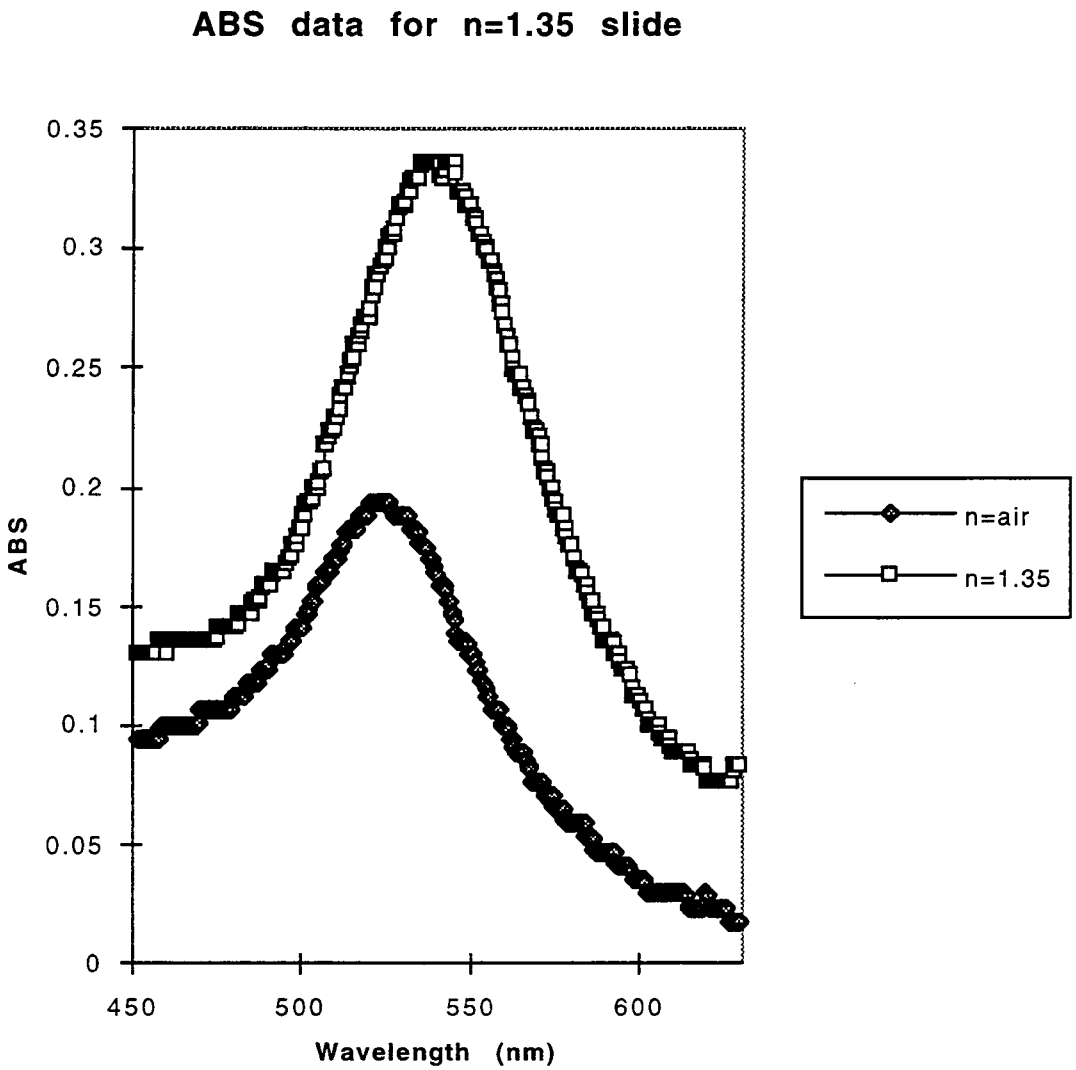

Figure IV.19. Graph of ABS data for n=1.35 slide B. A shift of 16 nm is created by the liquid.

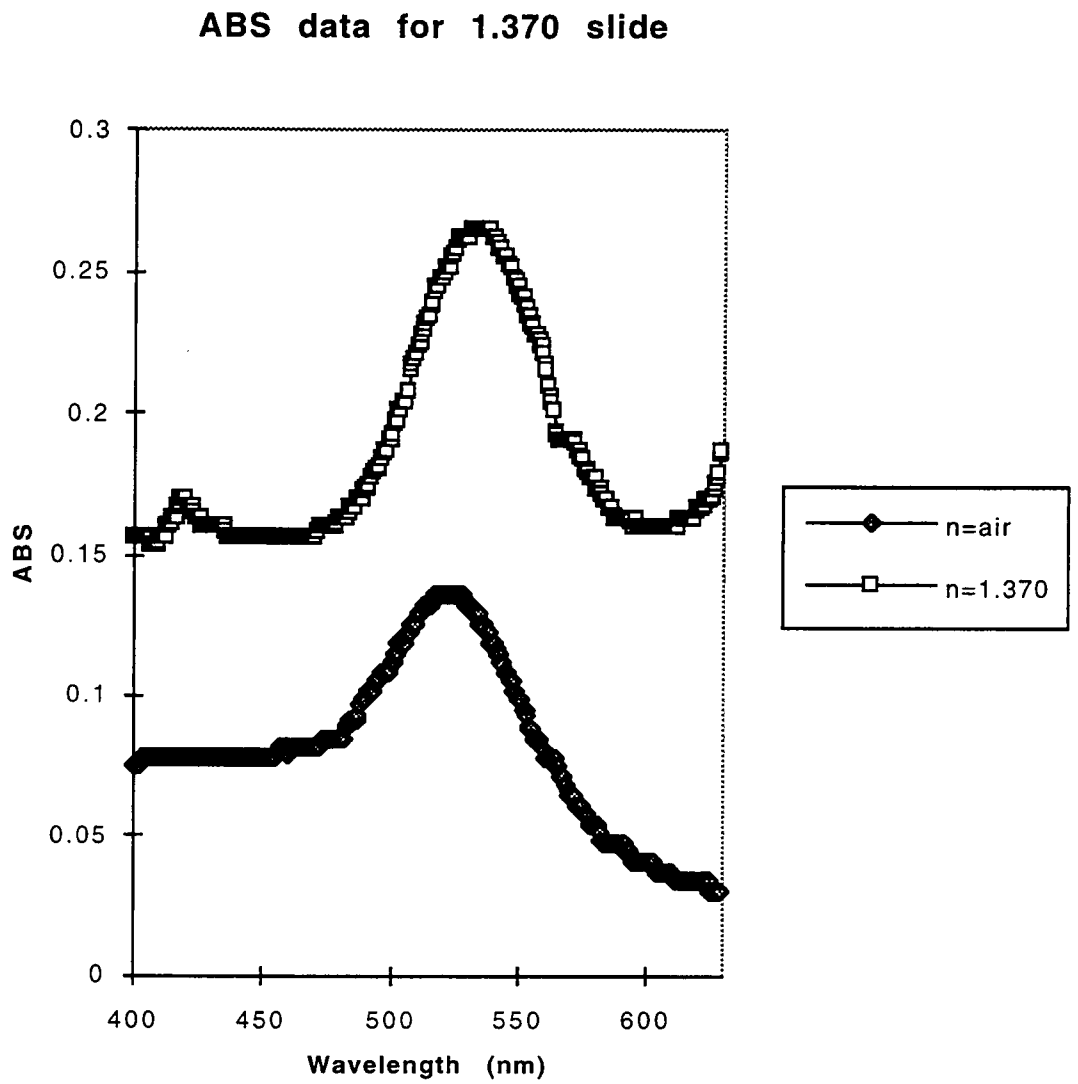

Figure IV.20. Graph of ABS data for n=1.370 slide. A shift of 14 nm is created by the liquid.

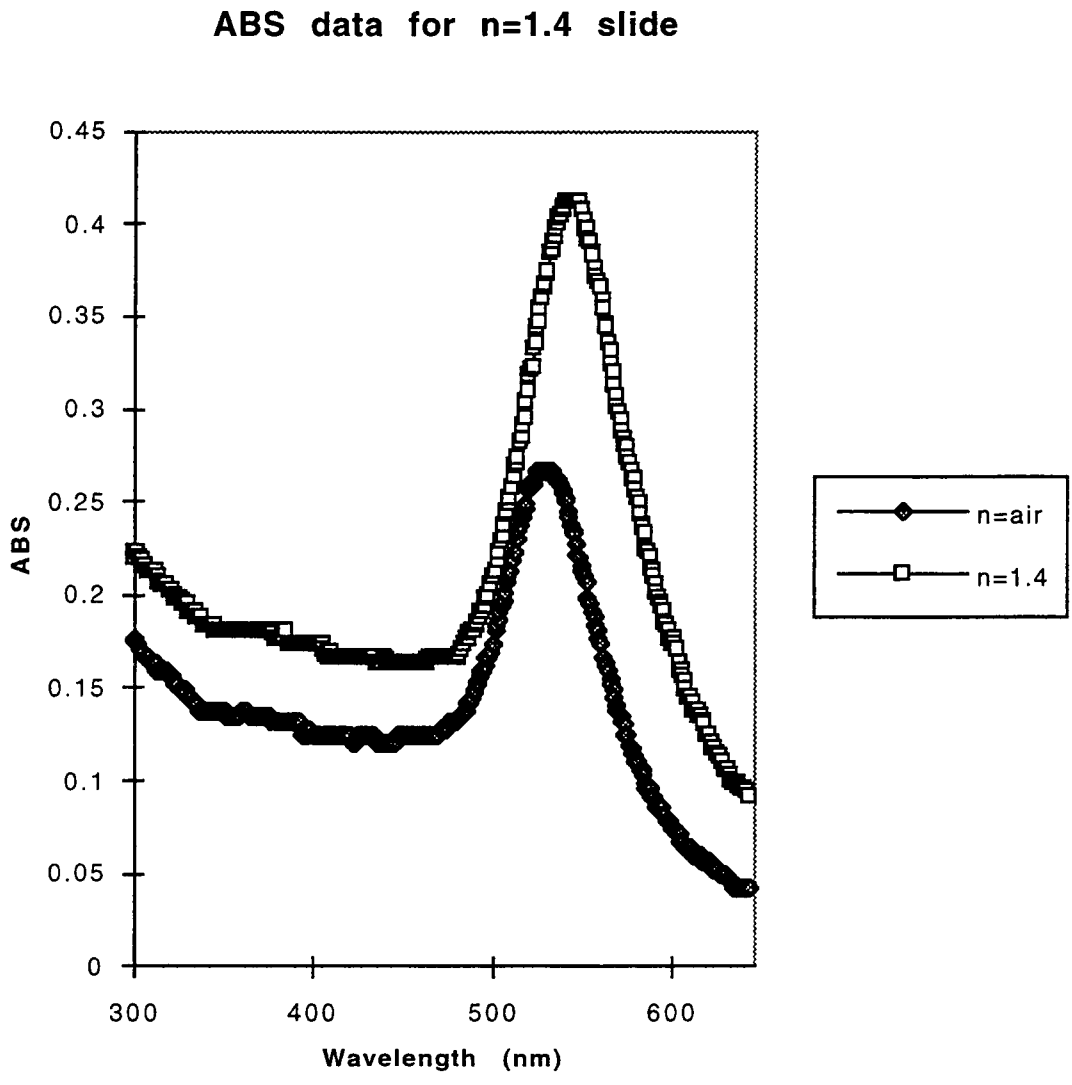

Figure IV.21. Graph of ABS data for n=1.4 slide. A shift of 16 nm is created by the liquid.

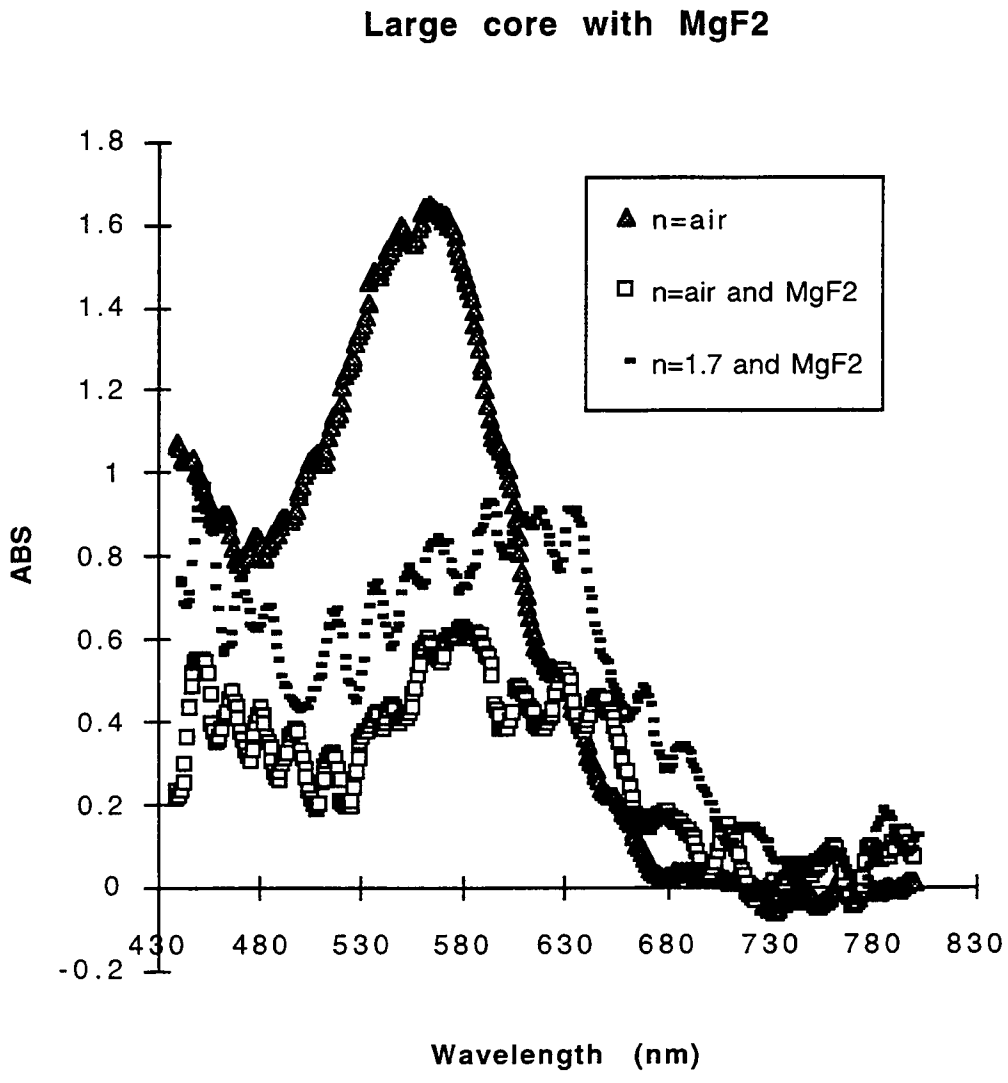

Figure IV.22. MgF_2 cladded large-core fiber results for n=1.7. Data was smoothed with a moving average of width=10 nm and normalized at 775 nm. 60 nm of MgF_2 evaporated on top of the islands; annealed at 800°C for 4 minutes. A shift is observable with the application of the MgF_2 layer, from 564 nm to 580 nm, and the addition of the n=1.700 liquid yields an extra peak position shift to 591 nm.

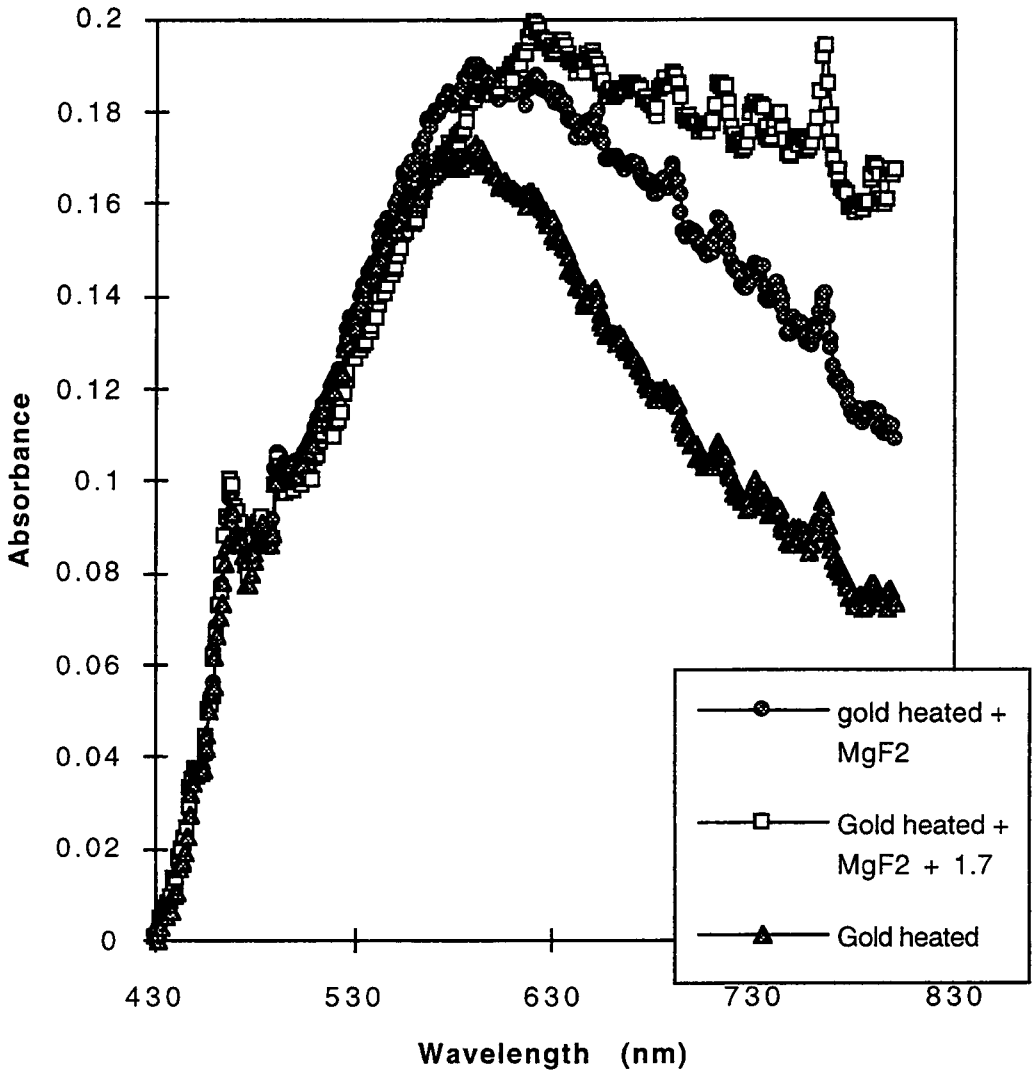

Figure IV.23. Another MgF_2 cladded large-core fiber result. 40 nm of MgF_2 applied. This sample shows that the extra coating of the MgF_2 does act as a cladding layer and allows for detection of optical liquids with indices greater than the fiber sample core.

for n=1.500 and higher liquids. At the very least, the extra layer of gold will form a film of small gold islands that fill in the separations between the larger islands.

Figure IV.24. shows the results of this double evaporation procedure. While an absorption peak exists for the annealed single gold layer sample, when the second layer was applied this peak disappeared. We then heated this double layer sample and found a shifted absorption peak. We believe the second annealing caused the first and second layers to be combined into one, with different sized islands with a smaller major to minor axis ratio. This moved the n=air resonance peak to a higher wavelength. We attribute this move to a change of R from about R=0.6 to R=0.35 The application of the n=1.700 liquid on the annealed double layer sample caused the absorption to disappear.

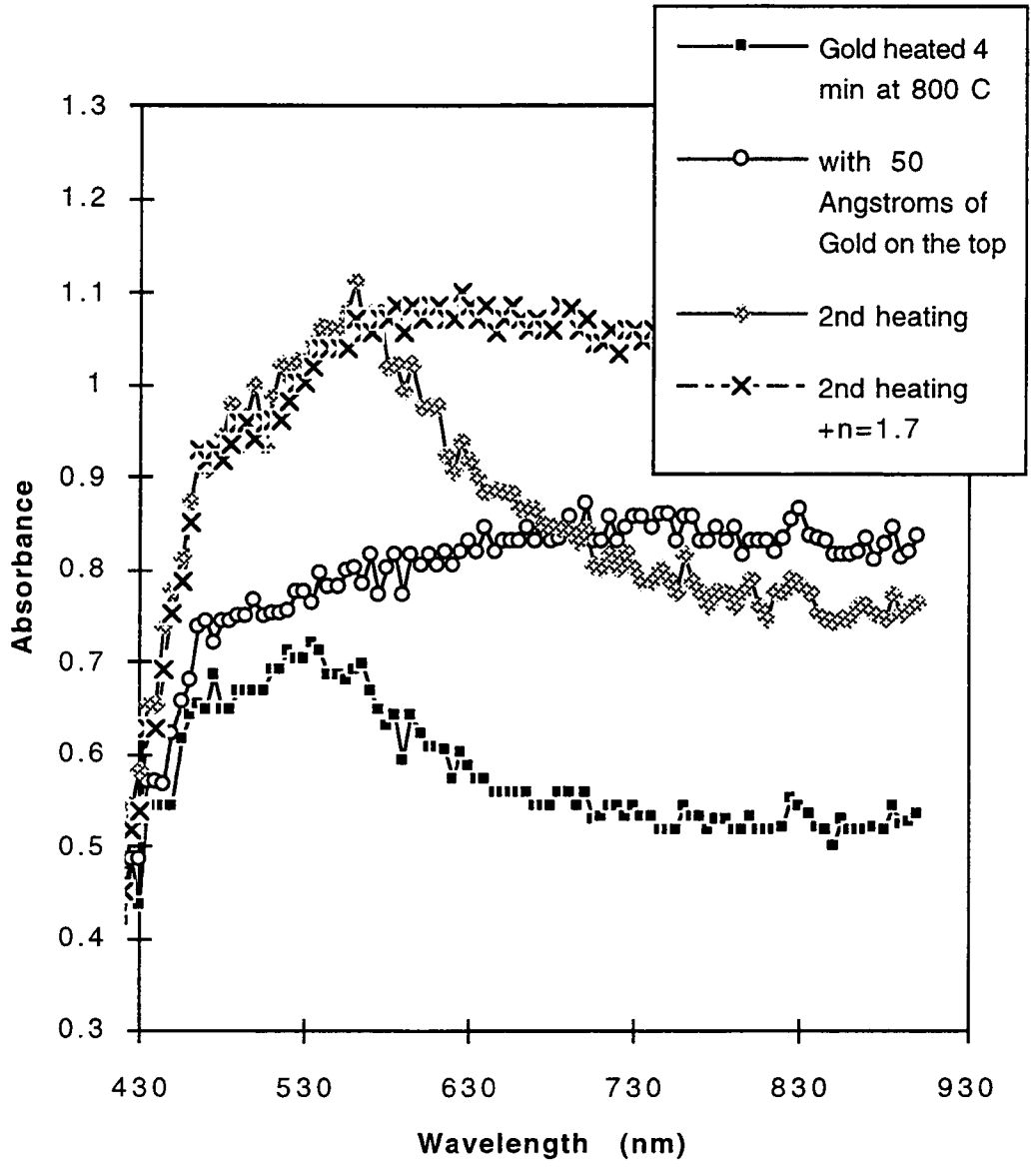

Figure IV.24. Extra Au layer, large-core fiber results. A slight shift is observable with the application of the extra gold layer, but the addition of the n=1.700 liquid yields an inconclusive peak position result.

Chapter V

Conclusions

We measured the absorption of light passing through an optical fiber that has a coating of annealed gold islands surrounding a decladded portion of the fiber. The excitation of surface plasmons on the gold islands was assumed to produce the absorption. We found that 100 Å of gold evaporated at a rate of approximately 4Å/sec, when the sample was rotating slowly, was an adequate amount to produce good absorption results.

A variable temperature annealing process that was used to form different sized islands was verified by microphotographs of island covered slide samples prepared directly adjacent to fiber samples. Based on our concurrent experiments[68] with these quartz slides with applied gold island thin films, we have shown that heating the sample at a temperature of 700 to 800 ^{o}C for 4 minutes produces the narrowest resonance curve and highest amount of absorption with the resonance peak centered around 550 nm. As both the AFM and SEM images presented above show, the amount of surface area of the substrate that is not in contact with the gold islands increases as the islands coalesce into larger islands with higher annealing temperature.

We applied optical liquids with known refractive indices over the islands, and recorded a shift in the position of the peak of the resonance. We were able to produce absorption shift measurements for high temperature annealed samples for optical liquids with an index less than the fused silica core (n=1.47), with small resonance peak shifts of 10 to 20 nm. However, due to the large gaps that occur between islands in high temperature annealing, the introduction of an optical liquid of n=1.500 or higher lead to many cases of the disappearance of the absorption peak entirely. Low temperature annealed samples showed much less occurrence of this effect. In fact, for low temperature annealed samples, we obtained absorption shift measurements with the application of

optical liquids with index of refraction's ranging from 1.300 to 1.700, with approximately 45 nm peak shifts for the n=1.700 samples.

Figure V.1. provides a summary of the peak shift results that we have obtained, and compares them with theoretical predictions for three different R values. This graph provides evidence of agreement between our data and the theory since the peak positions predicted by the theory for the largest and smallest values of R used are similar to those found in the experiment for low and high temperature annealed samples. The peak shifts for the experimental measurements are close to the shifts from the theory, considering the accuracy limits of our equipment.

We attributed the disappearance of the absorption to a change in the eigenmode supported by the core-cladding interface in the gaps between islands, and to losses attributed to the transmitted component that is created with the application of liquids that have an index higher than the sample core index. The application of the optical liquid forms a cladding layer that is discontinuous at the metal-islands. When the optical liquid has an index of refraction that is different from the initial cladding material, this changes the possible modes of propagation of the light through the fiber. When the mode change was large enough, it moved the system away from resonance. Understanding this mode change may prove to be particularly useful, if harnessed correctly. It may be important to use different optical fiber that has a cladding layer with an index of refraction higher than the optical liquid to be tested in future investigations.

We found reproducibility to be a problem, whereas several fiber samples prepared together had different peak shifts with the same applied index. Typically, we saw as much as 10-15 nm differences. We also observed irreproducible peak shifts in our normal incidence, slide-only experiments. These experiments utilized a commercial spectrophotometer to record the absorbance curves, and should lead to greater precision. Because of this, we believe that both the characteristics of any set of samples prepared at the same time are not quite exact and change during testing time.

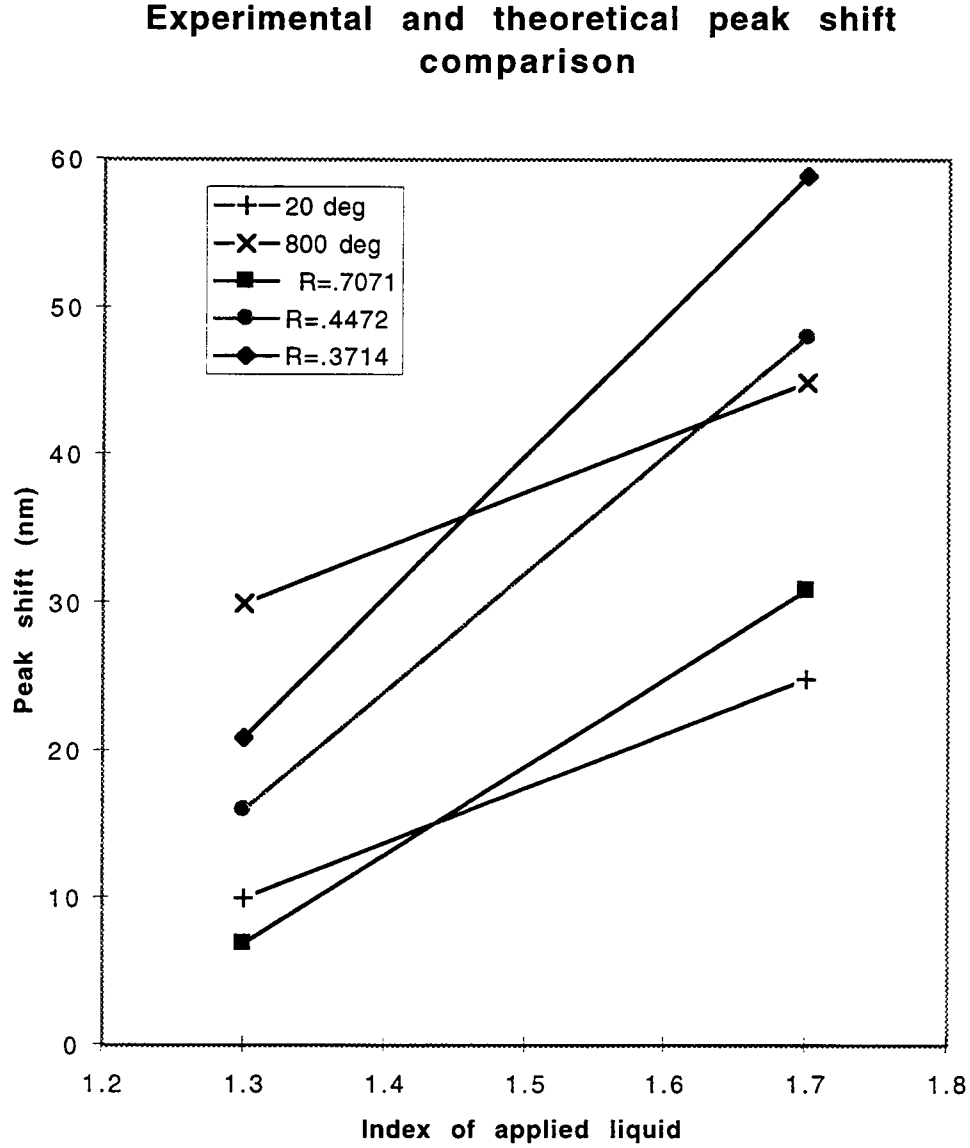

Figure V.1. Comparison of experimental and theoretical shifts. Peak shift values for room temperature and high temperature samples, 20 deg and 800 deg respectively, for n=1.3 and n=1.7 are compared to the peak shifts predicted by the theory for three different minor to major axis R values and the same two n values.

The different results for our experimental measurements and our theoretical calculations can, in part, be explained by the inaccurate experimental measurements of the optical constants for gold that we used in compiling a set values to use in our calculations. When the real part of the complex dielectric function for gold is in error, that error manifests itself in an incorrect wavelength for the location of the resonance peak position. When the imaginary part is in error, the height of the peak is incorrect. Since we are concerned here with peak shifts specified by two different wavelengths, we attribute, in part, our differences in the experimental data and the theoretical calculations for peak positions to error in the values for the real part in the bulk optical data for gold. Also, the wider absorption peaks can be attributed to two differences between our calculations in Chapter II and our actual data. As previously stated, is the inclusion a Gaussian distribution of the ratio R, instead of a single value. Changing the ratio R has been shown[69] to change the position and strength of the peak. Including a distribution will widen the ABS curve because each R value will contribute to the resonance curve at a different wavelength.

In comparisons of data for samples annealed at room temperature for 24 hours and samples annealed at higher temperatures for a few minutes, several important observations are seen. First, the broadening of the absorption curve can be attributed to a Gaussian distribution of sizes of the islands. Our measurements of room and high temperature annealed samples showed that the higher temperature sample pictures have a wider distribution. The widths of the ABS curves for high temperature samples should be wider. The high temperature annealed samples have ABS peak maximums for n=air at higher wavelengths than the room temperature samples. The peak shifts are greater for the high temperature samples, and extend to higher wavelengths. These observations may be improtant when the effect is implemented in a usable sensing device.

Our theoretical calculations led to the peak shift caused by the n=1.700 optical liquid being approximately three times the peak shift for the n=1.300 liquid. We found similar numbers in our experimental studies. We consider this the first step in calibration of the effect so that

it may be applied to sensing of an unknown index material. However, care must be taken when using our experimentally obtained numbers, since they include shifts obtained from different temperature anneals and, therefore, different island sizes and R ratios.

Both of the extra evaporation step procedures, presented above in chapter IV. will be investigated further in the future. It is important to note that the theoretical developments may have to account for an additional Gaussian distribution of small particles, in the case of the extra unheated gold coating. Alternatively, if the extra gold layer is thick enough and forms a continuous film between the annealed island, then a roughened[70], or dimpled continuous thin film calculation may be more useful. We will also endeavor to modify the amount of gold added in the second coating, and to immediately test a double-coated sample after the second evaporation step.

Another experimental aspect that may provide interesting results, and will be investigated in the future, is polarization dependant absorbance studies. A broad-band, linear polarizing sheet may inserted between the objective and the entrance face of the fiber to control the polarization of the light that propagates through the fiber. This polarizing sheet could be rotated and changes in the amount of absorbance could be measured. This may provide a method of maximizing the absorbance, since a certain polarization could provide the largest component of the field along an axis of the islands and thereby increase the surface plasmon amplitude and absorbance. It obviously would be important to have the specific linear polarization state that is launched into the fiber sample not be randomized while it travels through a fiber. Since we are using lengths of optical fiber of approximately 10 cm., the amount of polarization randomization that occurs is minimal, but possibly quite significant. Polarization preserving optical cable exists, but is only found in single-mode form. Single-mode fiber has a very small core diameter (5 microns or less) and may prove very hard to etch the surrounding 100 or more microns of cladding without also etching the core, although it may be possible to stabilize the fiber and monitor the etching rate and amount.

During our investigations presented here, we also performed an analysis of changes in the slope of the absorption curve. We performed this analysis to determine if slope changes are a valid method of characterizing the peak shift effect of the applied liquid. Our normal incidence, slide-based experiments showed an increase in the slope of the ABS curve for samples with an applied index, when the slopes were compared at the point of maximum absorbance for n=air. These slide experiments also showed only changes in the intercept of the slope of the two graphs, not in the overall slope of the curve for a complete wavelength range. We attempted to make the same slope analysis with our fiber sample experiments. However, our results showed changes in both the intercept and slope for the two curves. We investigated the effect of different sets of baseline intensity data on the slope measurements and found none. For these reasons, our results are not presented here.

In terms of other procedures that may be helpful in future investigations, a previous paper[71] has emphasised the use of an argon atmosphere in the annealing oven in order to disallow the formation of unwanted non-metal layers on the surface of the metal-islands, particularly silver sulfide on silver islands. This procedure was not followed in our work here, but may prove to be useful for future work.

We also consider the effect of humidity changes in the laboratory environment to, possibly, be important. Our samples were protected from overhead debris falling and attaching to the islands or mixing with the surrounding liquid, but were not isolated from humidity changes. It is also important to remember that a complete experimental test for both n=air and n=other-index ran for more than an hour. Therefore, several samples that were prepared at the same time could not be tested at the same time. This waiting time could lead to island size/shape changes, while exposed to room temperature annealing. Humidity changes could lead to a layer of water forming on the islands, and when the sample is tested with a liquid could lead to measurements of the resonance shift caused by the water and not by the liquid.

Other ideas to be investigated soon include the use of a dual crucible evaporation system that would allow the application of two

materials, specifically gold and MgF_2, without exposure to the environment. All of these ideas, and invariably others, shall further our efforts to produce a well defined calibration curve of peak shift versus applied index to be utilized in fiber optic sensors that are based on absorption peak shifts caused by island plasmon excitation.

List of References

List of References

[1]K. Estermann, Z. Phys. Chem. **106**, 403 (1923); Z. Phys. **33**, 320 (1925); O.Heavens, Optical Properties of Thin Solid Films (Dover, New York, 1965).

[2]R.J. Warmack and S. L. Humphrey, Phys. Rev. B **34**, 2246 (1986).

[3]P. Royer, J. L. Bijeon, J. P. Goudonnet, T. Inagaki, and E. T. Arakawa, Surface Science **217** (1989)

[4]J. W. Little, T. L. Ferrell, T. A. Callcott, and E. T. Arakawa, Phys. Rev B **26**, 5953(1982).

[5]J. W. Little, T. A. Callcott, T. L. Ferrell, and E. T. Arakawa, Phys. Rev B **29**, 1606(1984).

[6]S. W. Kennerly, J. W. Little, R. J. Warmack, and T. L. Ferrell, Phys. Rev B **29**, 2926 (1984).

[7]R. H. Ritchie, Phys. Rev. **106**, 874 (1957).

[8]R. H. Ritchie, J. C. Ashley, and T. L. Ferrell, in *Electromagnetic Surface Modes*, edited by A. D. Boardman (Wiley, Chichester, England, 1982), p. 119.

[9]Development of a Fiber Optic Biosensor based on Surface Plasmon Resonance, R. D. Clapsadle, M. C. Buncick , T. R. Downey, T. L. Ferrell, Oral Presentation, American Physical Society, Southeastern Section Fall Meeting, Nov. 1997.

[10]A. Otto, Z. Phys. **216**, 398 (1968).

[11]E. Ktetschmann, H. Raether, Z. Naturforsch. A **23**, 2135 (1968).

[12]E. Kretschmann, Z. Physik, **241**, 313 (1971).

[13]P.Royer, J. P. Goudonnet, R. J. Warmack, and T. L. Ferrell, Phys. Rev B **35**, 3753(1987).

[14]E. Kretschmann, Z. Physik, **241**, 313 (1971).

[15]K. M. Shakesheff, X. Chen, M. C. Davies, A. Domb, C.J. Roberts, S.J.B. Tendler, P.M. Williams, Langmuir, **11**, 3921-3927 (1995). Bio.

[16]H. Kano, S. Kawata, Applied optics, Vol **33**, N 22, 5166 (1994).

[17]A. Otto, Z. Physik **216**, 398-410, (1968).

[18]The Use of Metal Island Films to Support Radiative Surface Plasmons as a Method of Transducing Interfacial Events, pages 329-336, in *Biosensor Technology, Fundamentals and Applications*, ed. R. P. Buck et al. 1990.

[19]Development of a Fiber Optic Biosensor based on Surface Plasmon Resonance, R. D. Clapsadle, M. C. Buncick , T. R. Downey, T. L. Ferrell, Oral Presentation, American Physical Society, Southeastern Section Fall Meeting, Nov. 1997.

[20]J.L. Bigeon, P. Royer, J.P. Goudonnet, R.J. Warmack and T. L. Ferrell, Thin Solid Films, **155**,(1987), L1-L3.

[21]J.P. Goudonnet, J.L. Bigeon, R.J. Warmack, J. Appl. Phys **67** (6), 3093 (1990).

[22]A. Abdelghani, J.M. Chovelon, N. Jaffrezic-Renault, C. Ronot-Trioli, C. Veillas, H. Gagnaire, Sensors and Actuators, B **38-39**, 407-410 (1997).

[23]C. Ronot-Trioli, A. Trouillet, C. Veillas, A. El-Shaikh, H. Gagnaire, Analytica Chemica Acta, 121-127 (1996).

[24]R. C. Jorgenson, S.S. Yee, Sensors and Actuators, B **12**, 213-220, (1993).

[25]Refractive Index Liquids Technical Bulletin, RI-TCCP-T-263, R.P. Cargille Laboratories Inc., 55 Commerce Rd. Cedar Grove, NJ, 07009-1289.

[26]Ph.D. Dissertation, Milan Buncick, The University of Tennessee, Knoxville, 1987.

[27]S. W. Kennerly, J. W. Little, R. J. Warmack, and T. L. Ferrell, Phys. Rev B **29**, 2926 (1984).

[28]Chipmunk Basic program AUMATCH.BAS, Thomas L. Ferrell, Oak Ridge National Laboratory.

[29]Physik Daten (Physics Data), Optical Properties of Metals, Part 1, J.H. Weaver, C.G. Olson and D.W. Lynch, 1981.

[30]S. W. Kennerly, J. W. Little, R. J. Warmack, and T. L. Ferrell, Phys. Rev B **29**, 2926(1984); P.Royer, J. P. Goudonnet, R. J. Warmack, and T. L. Ferrell, Phys. Rev B **35**, 3753(1987).

[31]P.Royer, J. P. Goudonnet, R. J. Warmack, and T. L. Ferrell, Phys. Rev B **35**, 3753(1987).

[32]Part number 16-0200-HAS-C22, General Fiber Optics, Inc., 1 Washington Ave., Fairfield, NJ 07004. Silica/silica fiber, core/cladding/buffer = 200/220/280 microns, NA=0.22.

[33]Stock #NN254, Spindler a& Hoyer, Inc., 459 Fortune Blvd., Milford, MA, 01757-1745

[34]Catalog number 21312, Norland Products, Inc., 695 Joyce Kilmer Ave., N. Brunswick, NJ 08902.

[35]Branson Cleaning Equipment, Parrot Drive, Shelton, CN, 06484.

[36]The Use of Metal Island Films to Support Radiative Surface Plasmons as a Method of Transducing Interfacial Events, pages 329-336, in *Biosensor Technology, Fundamentals and Applications*, ed. R. P. Buck et al. 1990.

[37]P.Royer, J. P. Goudonnet, R. J. Warmack, and T. L. Ferrell, Phys. Rev B **35**, 3753(1987).

[38]P.Royer, J. P. Goudonnet, R. J. Warmack, and T. L. Ferrell, Phys. Rev B **35**, 3753(1987).

[39]R.J. Warmack and S. L. Humphrey, Phys. Rev. B **34**, 2246 (1986).

[40]P.Royer, J. P. Goudonnet, R. J. Warmack, and T. L. Ferrell, Phys. Rev B **35**, 3753(1987).

[41]F. Meriaudeau, T.R. Downey, A. Passian, P.I. Oden, A. Wig, P. Crilly, T.L. Ferrell, submitted to SPIE/ICAPT'98.

[42]Model UV-250, Shimadzu Scientific Instruments, Inc., Columbia, MD.

[43]R.J. Warmack and S. L. Humphrey, Phys. Rev. B **34**, 2246 (1986).

[44]Model: XBO75W-2, Oriel Corp., 250 Long Beach Blvd., Stratford CT, 06497.

[45]Model HR 640, Instruments SA, Inc. Div. Jobin Yvon, 16, 18 rue du Canal, B.P. 118, 91160 Longjumeau, France.

[46]1994 products catalog, vol. II, Oriel Corp., 250 Long Beach Blvd., Stratford CT, 06497.

[47]Model 68805, Oriel Corp., 250 Long Beach Blvd., Stratford CT, 06497.

[48]60000 Series Q, Oriel Corp., 250 Long Beach Blvd., Stratford CT, 06497.

[49]Model M304, Photochemical Research Associated Inc., 45 Meg drive, London, Ontario, Canada, N6E 2V2.

[50]Model ALH215, Photochemical Research Associated Inc., 45 Meg d rive, London, Ontario, Canada, N6E 2V2.

[51]Model number 13610, Oriel Corp., 250 Long Beach Blvd., Stratford CT, 06497.

[52]Part number 81-0100-2001, General Fiber Optics, Inc., 1 Washington Ave., Fairfield, NJ 07004

[53]Part number 906-122-5000, 144 micron SMA and part number 698-DSC-0250, 250 micron SMA., Newark Electronics, 4801 N. Ravenswood Ave., Chicago IL, 60640-4496.

[54]Newport Corp, 1791 Deere Ave., Irvine, CA, Photonics Catalog 1997-1998.

[55]Model number 73000019A, Instruments SA, Inc. Div. Jobin Yvon, 16, 18 rue du Canal, B.P. 118, 91160 Longjumeau, France.

[56]Part number 750250381, General Fiber Optics, Inc., 1 Washington Ave., Fairfield, NJ 07004, 25mm silica lens collimator with SMA connector.

[57]Model F-915T, Newport Corp., 1791 Deere Ave., Irvine, CA 92606

[58]Model 425-1, Newport Corp., 1791 Deere Ave., Irvine, CA 92606

[59]Model VPT-4, Newport Corp., 1791 Deere Ave., Irvine, CA 92606

[60]Model 110, Newport Corp., 1791 Deere Ave., Irvine, CA 92606

[61]Catalog number 22-168, Radio Shack, Fort Worth, TX 76102

[62]Board # CIO-DAS08-AOM, Computer Boards, Inc., 125 High Street, Mansfield, MA 02048.

[63]J.M. Senior, *Optical Fiber Communications, Principles and Practice* (Prentice Hall, 1985), pages 21-45.

[64]Item # FG-1.0-UAT, ThorLabs Inc., 435 Route 206, PO Box 366, Newton, NJ 07860-0366; 0.16 NA silica/silica multimode fiber, core/cladding/buffer of 1000/1250/1850 microns.

[65]Item # 11050A, ThorLabs Inc., 435 Route 206, PO Box 366, Newton, NJ 07860-0366. 1.05 mm. SMA connector.

[66]Item # FG-1.0-EMT, ThorLabs Inc., 435 Route 206, PO Box 366, Newton, NJ 07860-0366. 0.39 NA silica/TECS multimode fiber, core/cladding/buffer of 1000/1035/1400 microns.

[67]Esco Products Inc., 171 Oak Ridge Road, Oak Ridge, NJ 07438.

[68]F. Meriaudeau, T.R. Downey, A. Passian, P.I. Oden, A. Wig, P. Crilly, T.L. Ferrell, .

[69]P. Royer, J. L. Bijeon, J. P. Goudonnet, T. Inagaki, and E. T. Arakawa, Surface Science **217** (1989)

[70]Proposed in personal correspondence from Dr. Milan Buncick, The University of Memphis, Memphis TN, 38152.

[71]P.Royer, J. P. Goudonnet, R. J. Warmack, and T. L. Ferrell, Phys. Rev B **35**, 3753(1987).

Appendices

Appendix A

Sensor device prototypes

We present here a prototype device that will use our gold island surface plasmon absorption of the light passing through an optical fiber effect to sense changes in the index of refraction of the medium surrounding the islands. Several versions of this device are proposed.

This device contains four light emitting diodes (LED) that provide different wavelengths of source light. The four LEDs will be chosen to have peak output intensity wavelengths (λ_1, λ_2, λ_3, λ_4) that correspond to the positions shown in **Figure A.1.** below.

In our 4-LED/4-fiber version of this device, the light from these LEDs will each enter a different optical fiber. These four fibers will be prepared together, utilizing the technique discussed above in Chapter II. Each fiber will have a silicon photodiode that will provide voltage data before and after immersion of the devices active area into the surrounding medium to be analyzed. Data analysis will consist of fitting a parabola to the four pre-immersion data points, and also to the four post-immersion voltage data points.

When working properly the voltages created by λ_1, and λ_2, should decrease after immersion when the absorption curve shifts to higher wavelengths, while the voltages created by λ_3 and λ_4 should increase. The shapes of the two fitted curves (pre and post-immersion) and the changes in the pre and post-immersion voltages attained from testing our optical liquids could be used to produce a calibration curve to accurately analyze unknown liquids.

Figure A.2. shows an overview of the proposed 4-LED/4-fiber device. The lens collects most of the forward emitted light from the LED and launches it into the fiber. A very short focal length microball lens attached to the end of LED has been tested and served this purpose well. The active areas (AA) of the fibers would be immersed in the medium to be tested.

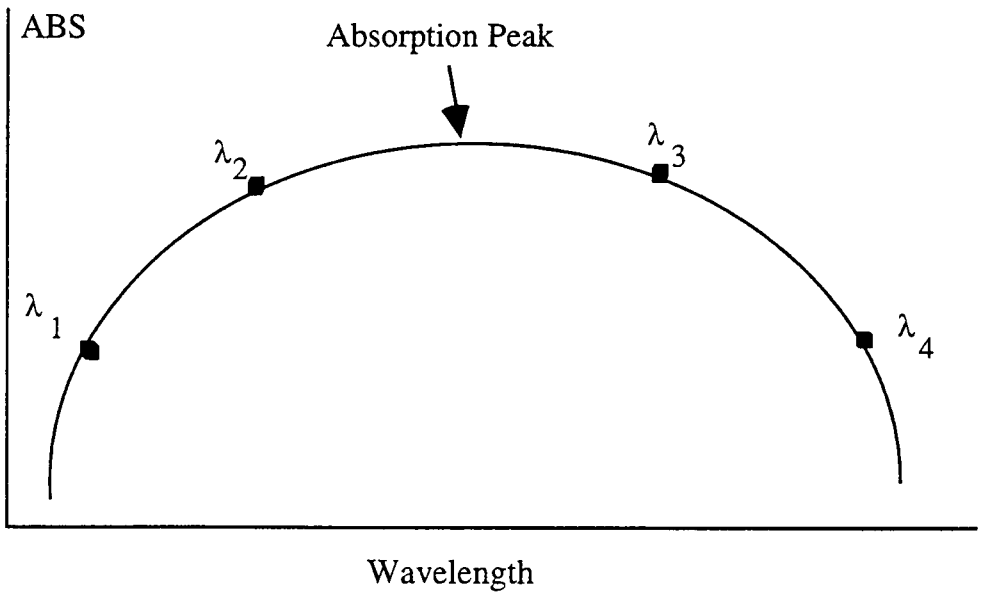

Figure A.1. Positions of λ_1, λ_2, λ_3 and λ_4.

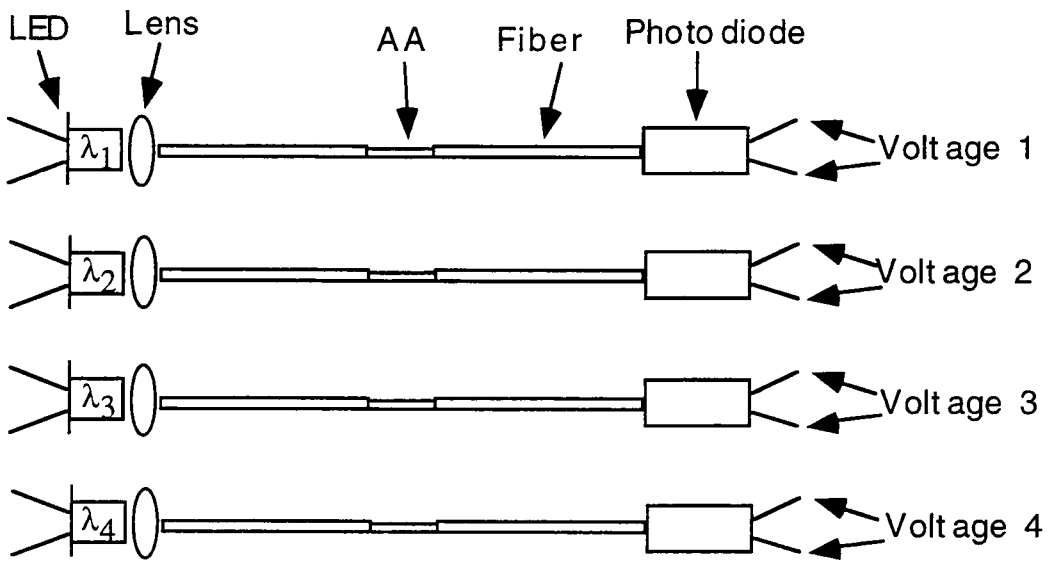

Figure A.2. Proposed 4-LED/4-fiber device. AA refers to the decladded portion of the fiber that has been coated with gold islands and annealed.

We also recognize the possibility of several more different wavelength LEDs being used to provide more data points for analysis; therefore a N-LED/N-fiber device could be more accurate, with N being greater than 4. Care should be used when choosing N, since LEDs emit a broad range of wavelengths and overlap of the light emitted from LEDs that have peak wavelengths λ_i and λ_{i+1} that are too closely spaced could be considerable and render the extra LEDs insignificant. Optical bandpass filters could be used to reduce this overlap, but may reduce intensity.

Careful examination of the data that we have presented above shows that these wavelength positions should be at λ_1= 525 nm, λ_2= 545 nm, λ_3= 565 nm and λ_4= 585 nm. We used the n=air curves for fiber samples #139 and #140, shown in chapter IV, as a basis for these numbers. However, this depends entirely on the n=air peak position and the width of absorption peak curve, and, therefore, the major to minor axis ratio R distribution for the islands that are created. A different set of LED wavelengths should be chosen for a different R distribution.

The 4-LED/1-fiber version of this device simply uses one gold island coated optical fiber and one silicon photodiode. This single fiber has the light from one of the 4 LEDs launched into it and its voltage is recorded, followed by a source switching routine that would produce the 4 needed voltage values. The sensor would then be immersed in the medium and the four post-immersion voltages collected. Data analysis would be the same as the 4 fiber device. This prototype would protect against the possibility of differences existing between the distribution of the R values for the islands created on the different fibers in the 4-LED/4-fiber version, but would be complicated by the source switching mechanism. Again, a N-LED/1-fiber configuration should increase the accuracy of the sensor, if N is chosen correctly.

LEDs are not necessarily available for any λ chosen. This may hamper the use of various values of a certain R distribution that is created. In fact, the relative availability for blue LEDs, at different wavelengths, is low, although improving. Because of this, we may need to utilize sample preparation techniques that shift the n=air resonance peak close to, or beyond, 600 nm. Also, several 2 color LED lamps exist and

may reduce a N-LED/N-fiber implementation to (N/2)-LED/(N/2)-fiber. All of these implementations are in the process of being developed.

Appendix B

Computer Program Listings

The following three listings of FORM1AU2.BAS, FORM3.BAS and MODL1AUX.BAS form the complete written code for the Visual Basic for Windows program PLASMON.EXE that controlled the experimental measurement and data-logging for the fiber samples. A listing for the Visual Basic forms that composed the visual part of the program is not listed here.

FILE: FORM1AU2.BAS

```
---------------------------------------------------------------
Function Calculate_ISB (Pos, MSB_Sub)
    Calculate_ISB = Int((Pos * 1000 - MSB_Sub * 65536) / 256)
End Function

Function Calculate_LSB (Pos, MSB_Sub, ISB_Sub)
    Calculate_LSB = Int(1000 * Pos - MSB_Sub * 65536 - ISB_Sub * 256)
End Function

Function Calculate_MSB (Pos)
    Calculate_MSB = Int(Pos * 1000 / 65536)
   Form2.Text1.Text = Pos
End Function

Sub Command1_Click ()
     beginwave = Val(Text1.Text)
     endingwave = Val(Text2.Text)
     increment = Val(Text3.Text)
    Start_Pos = Val(Text5.Text)
    backwave = Val(Text6.Text)
   File1 = Text4.Text & ".XLS"
    If (beginwave < 300 Or beginwave > 900)
   Then
           reply = MsgBox("Beginning Wavelength should be between 300 and
900                    nm -  continue?", 292, "")
       If reply = 7 Then
   End
   End If
    If (endingwave < 300 Or endingwave > 900) Then
      reply = MsgBox("Ending Wavelength should be between 300 and
900 nm - Continue?", 292, "")
       If reply = 7 Then End
   End If
    If (Start_Pos < 300 Or Star_Pos > 900) Then
```

```
      reply = MsgBox("Starting Position should be between 300 and 900
nm - Continue?", 292, "")
      If reply = 7 Then End
   End If
    If (backwave < 300 Or backwave > 900) Then
      reply = MsgBox("Back Wavelength should be between 300 and 900
nm - Continue?", 292, "")
      If reply = 7 Then End
   End If


   Comm1.CommPort = 1                    'Serial Port #1 for voltmeter connection
   Comm1.Settings = "1200,N,7,2"         'baud rate, no parity, 7 data bits, 2 stop
bit
   Comm1.InputLen = 0                    '
   Comm1.PortOpen = True

   Comm2.CommPort = 2                    'Serial Port #2 for motor connection
   Comm2.Settings = "9600,N,8,1"         'baud rate, no parity, 8 data bits, 1 stop
bit
   Comm2.InputLen = 0                    '
   Comm2.PortOpen = True

   MSB = Calculate_MSB(Start_Pos)
   ISB = Calculate_ISB(Start_Pos, MSB)
   LSB = Calculate_LSB(Start_Pos, MSB, ISB)
   Form2.Text3.Text = "Loading Absolute Position"
   Call Load_Absolute_Position(MSB, ISB, LSB)

   If Start_Pos <> beginwave Then Call Move_From_To(Start_Pos,
beginwave)

    Wavelength$ = Str$(beginwave)

   If endingwave <> beginwave Then

      Form2.Show
      Form2.Text4.Text = "Voltage (mV)"
      Form2.Text5.Text = "Wavelength (nm)"
      Form2.Text1.Text = "XX.XX"
      Form2.Text2.Text = "XXX"
      Form2.Text3.Text = "Initializing"

      Open File1 For Output As #1

      For counter = 0 To Abs(endingwave - beginwave) Step increment

          Wavelength$ = Str$(beginwave + counter)
          Wave_Save = beginwave + counter - increment
          Wavelen = beginwave + counter

        If counter <> 0 Then
```

```
            Call  Move_From_To(Wave_Save,  Wavelen)

          End If

voltmeter:
           Form2.Text3.Text = "Connecting To Voltmeter"
          Start = Timer
          Comm1.Output = "D"                    'tell voltmeter to send data
           Comm1.InputLen = 14
         Do
          Loop Until (Comm1.InBufferCount = 14 Or Timer >= Start + 3)
          If Comm1.InBufferCount < 14 Then
              reply = MsgBox("Please check the connection between the
PC and                                    the Voltmeter", 48, "")
              GoTo voltmeter
          End If

          Volt$ = Comm1.Input        'Input is the complete set of data for 1
reading
          Volt$ = Right$(Volt$, 10)
          Volt$ = Left$(Volt$, 5)
           Wavelength$ = Left$(Wavelength$, 4)
           Wavelength$ = Right$(Wavelength$, 3)
          Total$ = Wavelength$ & Chr$(9) & Volt$
          Print #1, Total$
          Form2.Text1.Text = Volt$
          Form2.Text2.Text = Wavelength$


      Next  counter
```

The above voltmeter code was changed to allow the use of the A/D board by inserting the following lines:

```
Const BoardNum% = 0              ' Board number
Start = Timer
   Do
          Loop Until (Timer >= (Start + 3))
         Gain% = BIP5VOLTS              ' set the gain
          Chan% = 0  ' set input channel
          For counter2 = 1 To 100
                 ULStat% = cbAIn%(BoardNum%, Chan%, Gain%, DataValue%)
               If ULStat% = 30 Then MsgBox "Change the Gain% argument to
one
                                                  supported by this board.", 0,
                                                "Unsupported Gain"
            If ULStat% <> 0 Then Stop

              ULStat% = cbToEngUnits(BoardNum%, Gain%, DataValue%,
                                     EngUnits!)
```

```
            If ULStat% <> 0 Then Stop
              voltavg! = voltavg! + EngUnits!
          Next counter2

          voltavg! = voltavg! / 100
          Volt$ = Format$(voltavg!, "0.0000000")          ' print the voltage

          Volt$ = Right$(Volt$, 10)
          ...
------------------------- continue with unchanged code here

       Close #1
       Unload Form2

   End If

    If endingwave <> backwave Then Call Move_From_To(endingwave,
backwave)

    Form3.Show
    Form3.SetFocus

End Sub

Sub Command2_Click ()

    Unload Form1
   End

End Sub

Sub Go_To_Target ()


       Start = Timer
       Comm2.Output = Chr$(58)
       Do
       Loop Until (Comm2.InBufferCount >= 1 Or Timer >= Start + 5)
       If Comm2.InBufferCount = 0 Then
            reply = MsgBox("Please check the connection between the PC
and the                          Monochromator - Program Terminated",
16, "")
          End
       End If
       Echo$ = Comm2.Input
       Form2.Text1.Text = Asc(Echo$)
'----------
       Comm2.Output = Chr$(3)
       Do
       Loop Until (Comm2.InBufferCount >= 1 Or Timer >= Start + 5)
       If Comm2.InBufferCount = 0 Then
```

```
            reply = MsgBox("Please check the connection between the PC
and the                         Monochromator - Program Terminated",
16, "")
         End
      End If
      Echo$ = Comm2.Input
      Form2.Text1.Text = Asc(Echo$)
'------------
      Comm2.Output = Chr$(71)    'Go
      Do
      Loop Until (Comm2.InBufferCount >= 1 Or Timer >= Start + 5)
      If Comm2.InBufferCount = 0 Then
            reply = MsgBox("Please check the connection between the PC
and the                         Monochromator - Program Terminated",
16, "")
         End
      End If
      Echo$ = Comm2.Input
      Form2.Text1.Text = Asc(Echo$)

      Comm2.Output = Chr$(0)
      Do
      Loop Until (Comm2.InBufferCount >= 1 Or Timer >= Start + 5)
      If Comm2.InBufferCount = 0 Then
            reply = MsgBox("Please check the connection between the PC
and the                         Monochromator - Program Terminated",
16, "")
         End
      End If
      Echo$ = Comm2.Input
      Form2.Text1.Text = Asc(Echo$)

      Comm2.Output = Chr$(58)
      Do
      Loop Until (Comm2.InBufferCount >= 1 Or Timer >= Start + 5)
      If Comm2.InBufferCount = 0 Then
            reply = MsgBox("Please check the connection between the PC
and the                         Monochromator - Program Terminated",
16, "")
         End
      End If
      Echo$ = Comm2.Input
      Form2.Text1.Text = Asc(Echo$)


End Sub

Sub Load_Absolute_Position (MSB_Sub, ISB_Sub, LSB_Sub)

      Start = Timer
      Comm2.Output = Chr$(58)
      Do
```

```
        Loop Until (Comm2.InBufferCount >= 1 Or Timer >= Start + 5)
        If Comm2.InBufferCount = 0 Then
            reply = MsgBox("Please check the connection between the PC
and the                         Monochromator - Program Terminated",
16, "")
            End
        End If
        Echo$ = Comm2.Input
        Form2.Text1.Text = Asc(Echo$)
        Comm2.Output = Chr$(3)
        Do
        Loop Until (Comm2.InBufferCount >= 1 Or Timer >= Start + 5)
        If Comm2.InBufferCount = 0 Then
            reply = MsgBox("Please check the connection between the PC
and the                         Monochromator - Program Terminated",
16, "")
            End
        End If
        Echo$ = Comm2.Input
        Form2.Text1.Text = Asc(Echo$)
        Comm2.Output = Chr$(65)
        Do
        Loop Until (Comm2.InBufferCount >= 1 Or Timer >= Start + 5)
        If Comm2.InBufferCount = 0 Then
            reply = MsgBox("Please check the connection between the PC
and the                         Monochromator - Program Terminated",
16, "")
            End
        End If
        Echo$ = Comm2.Input
        Form2.Text1.Text = Asc(Echo$)
        Comm2.Output = Chr$(3)
        Do
        Loop Until (Comm2.InBufferCount >= 1 Or Timer >= Start + 5)
        If Comm2.InBufferCount = 0 Then
            reply = MsgBox("Please check the connection between the PC
and the                         Monochromator - Program Terminated",
16, "")
            End
        End If
        Echo$ = Comm2.Input
        Form2.Text1.Text = Asc(Echo$)
        Comm2.Output = Chr$(LSB_Sub)            'LSB
        Do
        Loop Until (Comm2.InBufferCount >= 1 Or Timer >= Start + 5)
        If Comm2.InBufferCount = 0 Then
            reply = MsgBox("Please check the connection between the PC
and the                         Monochromator - Program Terminated",
16, "")
            End
        End If
        Echo$ = Comm2.Input
```

```
        Form2.Text1.Text = Asc(Echo$)
        Comm2.Output = Chr$(ISB_Sub)            'ISB
        Do
        Loop Until (Comm2.InBufferCount >= 1 Or Timer >= Start + 5)
        If Comm2.InBufferCount = 0 Then
             reply = MsgBox("Please check the connection between the PC
and the                          Monochromator - Program Terminated",
16, "")
           End
        End If
        Echo$ = Comm2.Input
        Form2.Text1.Text = Asc(Echo$)
        Comm2.Output = Chr$(MSB_Sub)            'MSB
        Do
        Loop Until (Comm2.InBufferCount >= 1 Or Timer >= Start + 5)
        If Comm2.InBufferCount = 0 Then
             reply = MsgBox("Please check the connection between the PC
and the                          Monochromator - Program Terminated",
16, "")
           End
        End If
        Echo$ = Comm2.Input
        Form2.Text1.Text = Asc(Echo$)
        Comm2.Output = Chr$(58)
        Do
        Loop Until (Comm2.InBufferCount >= 1 Or Timer >= Start + 5)
        If Comm2.InBufferCount = 0 Then
             reply = MsgBox("Please check the connection between the PC
and the                          Monochromator - Program Terminated",
16, "")
           End
        End If
        Echo$ = Comm2.Input
        Form2.Text1.Text = Asc(Echo$)

End Sub

Sub Load_Speed (Speed)

        Start = Timer
        Comm2.Output = Chr$(58)
        Do
        Loop Until (Comm2.InBufferCount >= 1 Or Timer >= Start + 5)
        If Comm2.InBufferCount = 0 Then
             reply = MsgBox("Please check the connection between the PC
and the                          Monochromator - Program Terminated",
16, "")
           End
        End If
        Echo$ = Comm2.Input
        Form2.Text1.Text = Asc(Echo$)
'----------
```

```
        Comm2.Output = Chr$(3)
        Do
        Loop Until (Comm2.InBufferCount >= 1 Or Timer >= Start + 5)
         If Comm2.InBufferCount = 0 Then
              reply = MsgBox("Please check the connection between the PC
and the                          Monochromator - Program Terminated",
16, "")
           End
        End If
        Echo$ = Comm2.Input
        Form2.Text1.Text = Asc(Echo$)
'-----------
        Comm2.Output = Chr$(83) 'Load Speed
        Do
        Loop Until (Comm2.InBufferCount >= 1 Or Timer >= Start + 5)
        If Comm2.InBufferCount = 0 Then
              reply = MsgBox("Please check the connection between the PC
and the                          Monochromator - Program Terminated",
16, "")
           End
        End If
        Echo$ = Comm2.Input
        Form2.Text1.Text = Asc(Echo$)
'----------
        Comm2.Output = Chr$(2)
        Do
        Loop Until (Comm2.InBufferCount >= 1 Or Timer >= Start + 5)
         If Comm2.InBufferCount = 0 Then
              reply = MsgBox("Please check the connection between the PC
and the                          Monochromator - Program Terminated",
16, "")
           End
        End If
        Echo$ = Comm2.Input
        Form2.Text1.Text = Asc(Echo$)
'----------
        Comm2.Output = Chr$(Speed)      'Speed  1=Fast   65536=Slow
        Do
        Loop Until (Comm2.InBufferCount >= 1 Or Timer >= Start + 5)
        If Comm2.InBufferCount = 0 Then
              reply = MsgBox("Please check the connection between the PC
and the                          Monochromator - Program Terminated",
16, "")
           End
        End If
        Echo$ = Comm2.Input
        Form2.Text1.Text = Asc(Echo$)
'----------
        Comm2.Output = Chr$(0)
        Do
        Loop Until (Comm2.InBufferCount >= 1 Or Timer >= Start + 5)
        If Comm2.InBufferCount = 0 Then
```

```
            reply = MsgBox("Please check the connection between the PC
and the                         Monochromator - Program Terminated",
16, "")
          End
        End If
        Echo$ = Comm2.Input
        Form2.Text1.Text = Asc(Echo$)
'----------
        Comm2.Output = Chr$(58)
        Do
        Loop Until (Comm2.InBufferCount >= 1 Or Timer >= Start + 5)
        If Comm2.InBufferCount = 0 Then
            reply = MsgBox("Please check the connection between the PC
and the                         Monochromator - Program Terminated",
16, "")
          End
        End If
        Echo$ = Comm2.Input
        Form2.Text1.Text = Asc(Echo$)
        'Do
        'Loop Until Comm2.InBufferCount = 1
        'Echo$ = Comm2.Input
         'Form2.Text1.Text = Asc(Echo$)
End Sub

Sub Load_Target (MSB_Sub, ISB_Sub, LSB_Sub)


        Start = Timer
        Comm2.Output = Chr$(58)
        Do
        Loop Until (Comm2.InBufferCount >= 1 Or Timer >= Start + 5)
        If Comm2.InBufferCount = 0 Then
            reply = MsgBox("Please check the connection between the PC
and the                         Monochromator - Program Terminated",
16, "")
          End
        End If
        Echo$ = Comm2.Input
          Form2.Text1.Text = Asc(Echo$)

        Comm2.Output = Chr$(3)
        Do
         Loop Until (Comm2.InBufferCount >= 1 Or Timer >= Start + 5)
        If Comm2.InBufferCount = 0 Then
            reply = MsgBox("Please check the connection between the PC
and the                         Monochromator - Program Terminated",
16, "")
          End
        End If
        Echo$ = Comm2.Input
          Form2.Text1.Text = Asc(Echo$)
```

```
        Comm2.Output = Chr$(84)          'Load Target Position
        Do
        Loop Until (Comm2.InBufferCount >= 1 Or Timer >= Start + 5)
        If Comm2.InBufferCount = 0 Then
             reply = MsgBox("Please check the connection between the PC
and the                          Monochromator - Program Terminated",
16, "")
           End
        End If
        Echo$ = Comm2.Input
           Form2.Text1.Text = Asc(Echo$)

        Comm2.Output = Chr$(3)
        Do
        Loop Until (Comm2.InBufferCount >= 1 Or Timer >= Start + 5)
        If Comm2.InBufferCount = 0 Then
             reply = MsgBox("Please check the connection between the PC
and the                          Monochromator - Program Terminated",
16, "")
           End
        End If
        Echo$ = Comm2.Input
           Form2.Text1.Text = Asc(Echo$)

        Comm2.Output = Chr$(LSB_Sub)             'LSB
        Do
        Loop Until (Comm2.InBufferCount >= 1 Or Timer >= Start + 5)
        If Comm2.InBufferCount = 0 Then
             reply = MsgBox("Please check the connection between the PC
and the                          Monochromator - Program Terminated",
16, "")
           End
        End If
        Echo$ = Comm2.Input
           Form2.Text1.Text = Asc(Echo$)

        Comm2.Output = Chr$(ISB_Sub)             'ISB
        Do
        Loop Until (Comm2.InBufferCount >= 1 Or Timer >= Start + 5)
        If Comm2.InBufferCount = 0 Then
             reply = MsgBox("Please check the connection between the PC
and the                          Monochromator - Program Terminated",
16, "")
           End
        End If
        Echo$ = Comm2.Input
           Form2.Text1.Text = Asc(Echo$)

        Comm2.Output = Chr$(MSB_Sub)             'MSB
        Do
        Loop Until (Comm2.InBufferCount >= 1 Or Timer >= Start + 5)
```

```
        If Comm2.InBufferCount = 0 Then
            reply = MsgBox("Please check the connection between the PC
and the                          Monochromator - Program Terminated",
16, "")
          End
        End If
        Echo$ = Comm2.Input
           Form2.Text1.Text = Asc(Echo$)

        Comm2.Output = Chr$(58)
        Do
        Loop Until (Comm2.InBufferCount >= 1 Or Timer >= Start + 5)
        If Comm2.InBufferCount = 0 Then
            reply = MsgBox("Please check the connection between the PC
and the                          Monochromator - Program Terminated",
16, "")
          End
        End If
        Echo$ = Comm2.Input
        Form2.Text1.Text = Asc(Echo$)

End Sub

Sub Move_From_To (Beginwave_Sub, Endingwave_Sub)

     If Abs(Endingwave_Sub - Beginwave_Sub) < 20 Then Speed_Sub =
                                                          10
     If Abs(Endingwave_Sub - Beginwave_Sub) >= 20 Then Speed_Sub = 1
   'Speed_Sub = 2
      Time_Wait = Abs(Endingwave_Sub - Beginwave_Sub) * Speed_Sub

     MSB = Calculate_MSB(Endingwave_Sub)
     ISB = Calculate_ISB(Endingwave_Sub, MSB)
     LSB = Calculate_LSB(Endingwave_Sub, MSB, ISB)

     Form2.Text3.Text = "Loading Speed"
     Call Load_Speed(Speed_Sub)

     Form2.Text3.Text = "Loading Target Position"
    Call Load_Target(MSB, ISB, LSB)

     Form2.Text3.Text = "Going To Target Position"
    Call Go_To_Target

     Form2.Text3.Text = "Waiting"
    Start = Timer
   Do
    Loop Until Timer >= Start + Int(Time_Wait * .2 + 3.5)

End Sub
```

```
---------------------------
FILE: FORM3.BAS
---------------------------------------------------------------
Sub Command1_Click ()

Restart_Excel:
    On Error GoTo Restart_Excel
    Chart_Title = Form3.Text4.Text
   Ref_File = Form3.Text2.Text & ".XLS"
   Cur_File = Form1.Text4.Text & ".XLS"
     beginwave = Val(Form1.Text1.Text)
     Endingwave = Val(Form1.Text2.Text)
     Increment = Val(Form1.Text3.Text)
      Selection = Int((Endingwave - beginwave) / Increment)

   Start_Excel = False
    Start_Excel = test(Ref_File, Cur_File)
    If Start_Excel = True Then
      Form3.Hide
         Call Excel(Selection, Chart_Title, Ref_File, Cur_File)
     End
   End If

End Sub

Sub Command2_Click ()
  End
End Sub

Sub Excel (Selection, Chart_Title, Ref_File_Sub, Cur_File_Sub)
    'This subroutine performs the conversion of the raw data into excell
format
    'and places the converted data into the appropriately named excell file
via a
   'series of SendKeys and DoEvents commands that are not listed here.
End Sub

Function test (Ref_File_Fct, Cur_File_Fct)

    Open Ref_File_Fct For Input As #1
    Open Cur_File_Fct For Input As #2

     Line Input #1, Ref_Beginning
     Line Input #2, Cur_Beginning
     Ref_Beginning = Left$(Ref_Beginning, 3)        'read reference file first
                                                    'wavelength
      Cur_Beginning = Left$(Cur_Beginning, 3)
  j = 0
   Start_Excel = False
     If Val(Ref_Beginning) = Val(Cur_Beginning) Then
     Test_Excel = 0
   End If
```

```
    If Val(Ref_Beginning) > Val(Cur_Beginning) Then 'Excel must have a
                                                    'reference
       reply = MsgBox("Reference file starts after " & beginwave & ". Please
                       change the Reference File", 48, "")
  End If
    If Val(Ref_Beginning) < Val(Cur_Beginning) Then      'reference file
starts                                                    'after current
file
     If EOF(1) = False Then
      Do
            Line Input #1, Ref_Beginning
             Ref_Beginning = Left$(Ref_Beginning, 3)   'find common
                                                      'starting
                                                      'wavelength
       j = j + 1
        Loop Until ((EOF(1) = True) Or (Val(Ref_Beginning) =
                                          Val(Cur_Beginning)))'
    End If
  End If

    If (Val(Ref_Beginning) = Val(Cur_Beginning)) Then
   Do
         Line Input #1, Ref_Wavelength
         Line Input #2, Cur_Wavelength
          Ref_Wavelength = Left$(Ref_Wavelength, 3)
          Cur_Wavelength = Left$(Cur_Wavelength, 3)
    Loop Until ((EOF(1) = True) Or (EOF(2) = True) Or
     (Val(Ref_Wavelength) <> Val(Cur_Wavelength)))
  End If

    If ((Val(Ref_Beginning) <> Val(Cur_Beginning)) Or
            (Val(Ref_Wavelength) <> Val(Cur_Wavelength))) Then
       reply = MsgBox("Reference and current file don't have enough
     common  wavelengths. Please change the Reference File
     or Quit the Plasmon Program", 48, "")
  End If

  If EOF(2) = False Then
       reply = MsgBox("Reference file isn't long enough. Please change the
                    Reference File or Quit the Plasmon Program", 48, "")
  End If
    If ((EOF(2) = True) And (Val(Ref_Wavelength) = Val(Cur_Wavelength)))
  Then
     Start_Excel = True
    Test_Excel = j
  End If
  test = Start_Excel
  Close #1
  Close #2
End  Function
---------------------------
```

```
---------------------------------------------------------------
FILE: MODL1AUX.BAS
---------------------------------------------------------------
Global Start_Pos, MSB, ISB, LSB
Global Increment, Beginwave, Endingwave, AVoltage, AWavelength
Dim Shared Voltage(2000)
Dim Shared Wavelength(2000)
---------------------------------------------------------------
---------------------------------------------------------------
```

The following program fragment listing was used to provide the slope at each available wavelength for the curves that were fitted to the data in Sigma-Plot. The filenames, wavelength ranges and coefficients changed respective to the different datasets analyzed, but the basic program structure remained the same for all of datasets.

```
---------------------------------------------------------------
FILE: SPBSSLO9.BAS
---------------------------------------------------------------
COMMON SHARED b1 AS DOUBLE, b2 AS DOUBLE, b3 AS DOUBLE, b4 AS
DOUBLE, b5 AS DOUBLE, b6 AS DOUBLE
COMMON SHARED b7 AS DOUBLE, b8 AS DOUBLE, b9 AS DOUBLE, x AS
DOUBLE, fofx1 AS DOUBLE, fofx2 AS DOUBLE, fofx3 AS DOUBLE
COMMON SHARED file AS STRING, liner AS STRING
COMMON SHARED counter AS INTEGER
DIM SHARED b(10) AS DOUBLE

OPEN "c:\todd\01083_56.slp" FOR OUTPUT AS #1
PRINT #1, "Filename: "; file
PRINT #1, "Curve # 1"
b(1) = .0086537921053#
b(2) = -.0000069503141127#
FOR counter = 500 TO 650
    x = counter
    fofx1 = b(1) + (2 * b(2) * x)
    PRINT #1, "slope is "; fofx1; " at x= "; counter
NEXT counter
PRINT #1,
PRINT #1,
PRINT #1,
PRINT #1,
PRINT #1, "Curve # 2"
PRINT #1,
b(1) = .0181786641#
b(2) = -.000015892907195#
FOR counter = 500 TO 650
    x = counter
    fofx1 = b(1) + (2 * b(2) * x)
    PRINT #1, "slope is "; fofx1; " at x= "; counter
NEXT counter
PRINT "Slope analysis completed."
PRINT
PRINT
PRINT
PRINT
PRINT
CLOSE #1
```

Vita

Todd Richard Downey was born on November 13, 1964 in Endicott, New York to Mr. Robert-Todd Downey and Mrs. Virginia Marion Downey. He graduated from Vestal Central Senior High School in Vestal, New York in 1982. He received a B. S. in Mathematical Physics from Binghamton University in 1988. He worked as a computer operator/programmer until 1994, when he enrolled in the Graduate School of the University of Tennessee, Knoxville until he received his Master of Science degree in May, 1998.